Molecular Profiling of Clear Cell Renal Cell Carcinoma and Targeted Therapy Response

---

Dissertation

Zur Erlangung der naturwissenschaftlichen Doktorwürde

(Dr. sc. nat.)

vorgelegt der

Mathematisch-naturwissenschaftlichen Fakultät

der Universität Zürich

von

Caroline Fanja Razafinjatovo

aus Frankreich

Promotionskomitee

Prof. Ulrich Hübscher (Vorsitz)

Prof. Holger Moch (Leitung der Dissertation)

PD Dr. Peter Schraml

Prof. Roland Wenger

Prof. Niko Beerenwinkel

Zürich, 2016

… à ma Famille

Contents

List of abbreviations

BAP1	BRCA1 associated protein-1
BSA	Bovine Serum Albumine
CAIX	Carbonic anhydrase IX
ccRCC	Clear cell renal-cell carcinoma
CCT-ζ-2	Chaperonin Containing TCP1, Subunit 6B (Zeta 2)
Co-IP	Co-immunoprecipitation
CPT	Camptothecin
CXCR4	Chemokine (C-X-C Motif) Receptor 4
DMEM	Dulbecco's Modified Eagle Medium
DMSO	Dimethyl-sulfoxyde
EEF1A1	Eukaryotic Translation Elongation Factor 1 Alpha 1
EPO	Erythropoïetin
FFPE	Formalin-fixed, paraffin-embedded
HIF	Hypoxia-inducible factor
HRE	Hypoxia-responsive elements
IP	Immunoprecipitation
LOF	Loss-of-function
MDM2	Mouse double minute 2 homolog
mTOR	Mammalian target of rapamycin
MTT	Methyl-thiazolyl-tetrazolium
NF-κB	Nuclear factor-kappa B
NGS	Next-Generation sequencing

PBRM1	Protein polybromo-1
PCR	Polymerase chain reaction
PDGF/R	Platelet-derived growth factor /receptor
PHD	prolyl hydroxylase
PTEN	Phosphatase and tensin homolog
pVHL	Von Hippel-Lindau protein
qPCR	Quantitative polymerase chain reaction
RCC	Renal cell carcinoma
RPB1	RNA Polymerase II Subunit B1
RT-PCR	Retro-transcription polymerase chain reaction
SETD2	SET Domain Containing 2
SPR	Surface plasmon resonance
TBST	Tris-Buffered Saline and Tween 20 buffer
TKI	Tyrosine kinase inhibitor
TMA	Tissue micro-array
VDU1/2	pVHL-interacting deubiquitinating enzyme-1
VEGF/R	Vascular endothelial growth factor /receptor
VHL	Von Hippel-Lindau gene
WT	Wild-type

Summary

Clear-cell subtype is the most frequent and aggressive form of renal cell carcinoma and is highly metastatic, leaving the patients with a very poor prognosis. Metastatic ccRCC is mainly treated with small molecules therapies with anti-angiogenic properties. Despite recent advances in that matter, ccRCC seems to be intrinsically resistant or acquire resistance to these treatments. Von-Hippel Lindau tumor-suppressor gene (*VHL*) inactivation occurring in almost 90% of the ccRCC cases has been proven to be a critical and early event in tumor initiation. This high rate of alteration led researchers to focus on this gene to unravel its implication in ccRCC development and to evaluate its potential as a prognostic or predictive biomarker. Most of the current research tend to concentrate on *VHL* protein's (pVHL) best studied function: the downregulation of the hypoxia inducible factor (HIF). However, as a multiadaptor protein, pVHL is also involved in many other oncogenic processes. The overall goal of my PhD thesis was to investigate i. *VHL* mutations, and especially missense mutations; ii. the pathways that could be affected and iii. the way those mutations can influence cell behavior with or without treatment. We found that some of pVHL binding domains were preferentially altered by missense mutations: HIF1AN, BCL2L11, HIF1/2α, RPB1, PRKCZ, aPKC-λ/ι, EEF1A1, CCT-ζ-2, and Cullin2 binding regions were indeed more frequently affected by missense mutations than what is expected by chance. Those interactors and the pathways in which they are involved may represent interesting new therapeutic targets. One potential binding protein of pVHL is the tumor suppressor p53 whose gene is rarely mutated in ccRCC but downregulated in most of the tumors. We studied the different effects of particular *VHL* missense mutations on p53 signaling pathway and found that all mutations influenced more or less p53 transactivation, which in turn differently attenuated apoptosis of the mutated cells. The use of a p53-mediated pro-apoptotic drug, Camptothecin, may therefore be a promising way of treating ccRCC. Since *VHL* inactivation alone cannot explain

ccRCC development and treatment resistance, we attempted to unravel variants clusters among 400 cancer-related genes that could be related to the response to current treatments of ccRCC patients using next-generation sequencing. Of the genes known to be important in ccRCC, *VHL*, *PBRM1*, *SETD2*, *MTOR* and *PDGFRA* were the most frequently altered ones in our cohort. Responder patients were presenting in general more variants than non-responders in the genes *PBRM1*, *BAP1*, *CARD11* and *HIF1α*.

Zusammenfassung

Der klarzellige Subtyp ist die häufigste und zugleich aggressivste Form des Nierenzellkarzinoms (NZK), hat hohes Meatastasierungspotenzial und geht einher mit einer schlechten Prognose. Metastasierte klarzellige NZK werden mit kleinen Molekülen behandelt, welche die Blutgefässneubildung hemmen. Trotz erzielter Fortschritte mit dieser Therapie, scheint das klarzellige NZK oft gegen diese Behandlung resistent zu sein beziehungsweise resistent zu werden. Das Von-Hippel Lindau Tumorsuppressorgen (*VHL*) ist in fast 90% der klarzelligen NZK inaktiviert und stellt ein kritisches und frühes Ereignis bei der Tumorentstehung dar. Die hohe Mutationsrate führte Forscher dazu dieses Gen näher zu betrachten, um seine Beteiligung an der Entwicklung des klarzelligen NZK sowie sein Potenzial als prognostischer oder prädiktiver Biomarker zu untersuchen. Die gegenwärtige Forschung fokussiert sich hauptsächlich auf die am besten untersuchte Funktion des VHL Proteins: die negative Regulation des Hypoxie-induzierbaren Faktors. pVHL ist jedoch als Multiadaptor Protein noch in vielen anderen Tumorprozessen involviert. Das Hauptziel meiner Doktorarbeit war die Untersuchung von *VHL* Mutationen, insbesondere Missense Mutationen, die durch sie betroffenen molekularen Signalwege sowie die Art und Weise, wie diese Mutationen Zelleigenschaften mit oder ohne Behandlung beeinflussen. Wir fanden heraus, dass einige der pVHL Bindungsdomänen bevorzugt von Missense Mutationen betroffen sind: Die Bindungsregionen von HIF1AN, BCL2L11, HIF1/2α, RPB1, PRKCZ, aPKC-λ/ι, EEF1A1, CCT-ζ-2 und Cullin2 waren in der Tat häufiger mutiert als zufällig erwartet. Diese pVHL Bindungspartner und die molekularen Signalwege, an welchen sie beteiligt sind, könnten somit interessante neue Therapieziele repräsentieren. Ein potenzielles Bindungsprotein von pVHL ist auch der Tumorsuppressor p53, dessen Gen in klarzelligen NZK kaum mutiert ist, aber in den meisten Fällen nicht exprimiert ist. Wir analysierten die unterschiedlichen Effekte bestimmter *VHL* Missense Mutationen auf den

p53 Signalweg und fanden, dass alle Mutationen mehr oder weniger die p53 Transaktivierung beeinflussten und somit unterschiedlich die Apoptose von Zellen abschwächten. Die Anwendung des p53 aktivierenden, Apoptose fördernden Medikaments Camptothecin könnte daher ein vielversprechender Weg sein, klarzellige NZK zu behandeln. Da die Inaktivierung von *VHL* alleine nicht ausreicht, um die NZK-Entstehung und die Behandlungsresistenz zu erklären, wurde mittels Next-Generation-Sequencing versucht, Mutationsmuster unter 400 krebsrelevanten Genen zu finden, die mit dem Ansprechen von klarzelligen NZK Patienten auf gegenwärtig durchgeführte Behandlungen korrelieren. Von den bekannten NZK-relevanten Genen waren *VHL*, *PBRM1*, *SETD2*, *MTOR* und *PDGFRA* die am häufigsten mutierten in unserer Kohorte. Patienten, die auf die Therapie ansprachen, wiesen generell mehr Varianten in den Genen *PBRM1*, *BAP1*, *CARD11* and *HIF1α* auf als solche, die nicht ansprachen.

Résumé

Le carcinome du rein à cellules claires est la forme la plus fréquente et la plus agressive de cancer du rein et est fortement métastatique. Il est ainsi associé à un très mauvais pronostic de survie pour les malades. Lorsqu'il est métastatique, ce cancer est principalement traité avec des médicaments à visée anti-angiogénique. Malgré les récents progrès dans ce domaine, le carcinome du rein à cellules claires semble être intrinsèquement résistant ou acquérir une résistance à ces traitements. L'inactivation du gène suppresseur de tumeur Von Hippel-Lindau (*VHL*) survenant dans près de 90% des cas a été démontrée comme étant une étape majeure dans l'initiation de la tumeur. Cette fréquence élevée d'inactivation du gène *VHL* a conduit les chercheurs à se concentrer sur ce gène afin d'évaluer son implication dans le développement du carcinome du rein à cellules claires ainsi que son potentiel en tant que biomarqueur pronostique ou prédictif. La plupart des recherches actuelles sont axées sur la fonction la plus étudiée de la protéine VHL (pVHL): la baisse d'expression des facteurs induits par l'hypoxie (HIF). Cependant, étant une protéine à multiples fonctions, pVHL est également impliquée dans de nombreux autres processus oncogéniques. L'objectif général de ma thèse a été d'étudier i. les mutations de *VHL* et en particulier les mutations faux-sens, ii. les voies de signalisation qui pourraient être altérées et iii. le rôle de ces mutations sur le comportement des cellules avec ou sans traitement. Nous avons mis en évidence que certains des domaines de liaison de pVHL sont préférentiellement touchés par les mutations faux-sens: les domaines de liaison de HIF1AN, BCL2L11, HIF1 / 2a, RPB1, PRKCZ, aPKC-λ / ι, EEF1A1, CCT-ζ-2, et Cullin2. Ces derniers ont montré en effet une fréquence de mutations faux-sens significative. Les protéines de liaison et les voies de signalisation associées à ces domaines peuvent représenter de nouvelles cibles thérapeutiques potentielles. Une protéine de liaison candidate de pVHL est p53, une potéine suppresseur de tumeur dont le gène est rarement muté dans le carcinome du rein à cellules claires

mais est sous-exprimé dans la plupart des cas. Nous avons étudié les effets de mutations faux-sens spécifiques de la voie de signalisation de p53 et avons trouvé que toutes les mutations ont un effet plus ou moins important sur la transactivation de p53, ce qui se traduit par une apoptose plus ou moins diminuée des cellules mutées. L'utilisation d'un médicament pro-apoptotique dépendant de l'activation de p53, la camptothécine, peut donc être un moyen prometteur de traiter le carcinome du rein à cellules claires. Puisque la seule inactivation de *VHL* ne peut pas expliquer le développement du carcinome du rein à cellules claires et du fait de la résistance au traitement de ce carcinome, nous avons tenté d'identifier des groupes de mutations qui pourraient être liés à la réponse aux traitements actuels des patients parmi plus de 400 gènes liés au cancer en utilisant le séquençage de nouvelle génération. Parmi les gènes connus pour être importants dans le développement du carcinome du rein à cellules claires *VHL*, *PBRM1*, *SETD2*, *MTOR* et *PDGFRA* étaient les plus fréquemment mutés chez les patients répondeurs au traitement de notre cohorte. Ces derniers présentaient de manière générale plus de mutations dans les gènes *PBRM1*, *BAP1*, *CARD11* et *HIF1α* que les patients non-répondeurs.

I. Introduction

A. Epidemiology of Renal Cell Carcinoma

Renal Cell carcinoma (RCC) represents more than 3% of all the cancer types and is the ninth most common cancer worldwide [1-3]. In the USA, more than 61'000 new cases and more than 14000 RCC related deaths have been predicted in 2015. The number of new cases has continuously increased over the years, whereas the number of deaths remains stable. The five year survival rate has greatly increased in the last 30 years, reaching today 73%. RCC is mainly asymptomatic and is usually incidentally diagnosed by computed tomography. The common symptoms of RCC are blood in the urine, lump in the abdomen, pain in the side, loss of appetite, weight loss, and anemia. The three main risk factors are smoking, obesity, and high blood pressure. The median age at time of diagnosis is 64 years (Figure 1) [4].

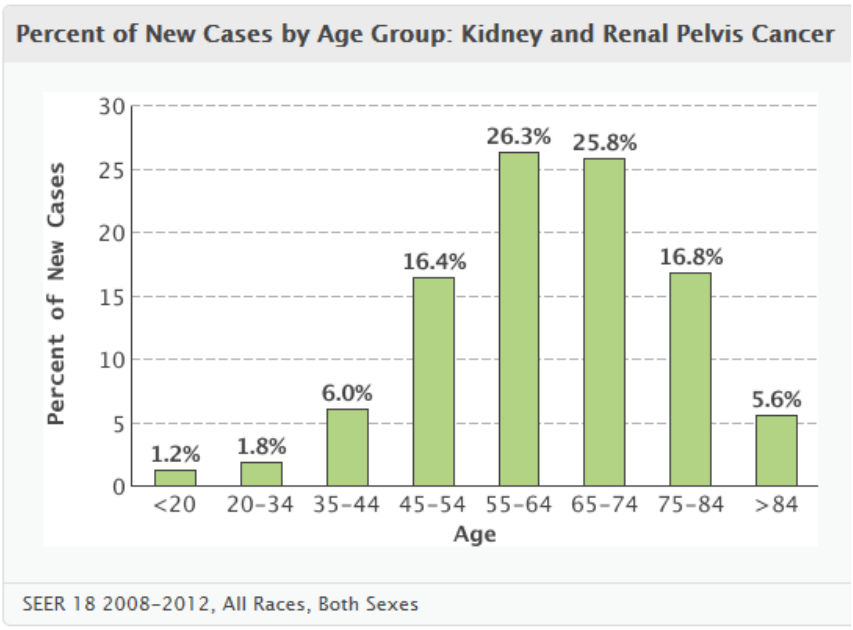

Figure 1: Percent of new cases by age group [4].

While patients with localized disease have a good prognosis, patients with distant metastasis have a five year survival rate of less than 12% (Figure 2). Metastasizing RCC, either present at time of

diagnosis (up to 20%) or progressing (20-40%), remain the most challenging feature of patient's disease management after surgical resection of the tumor [5, 6].

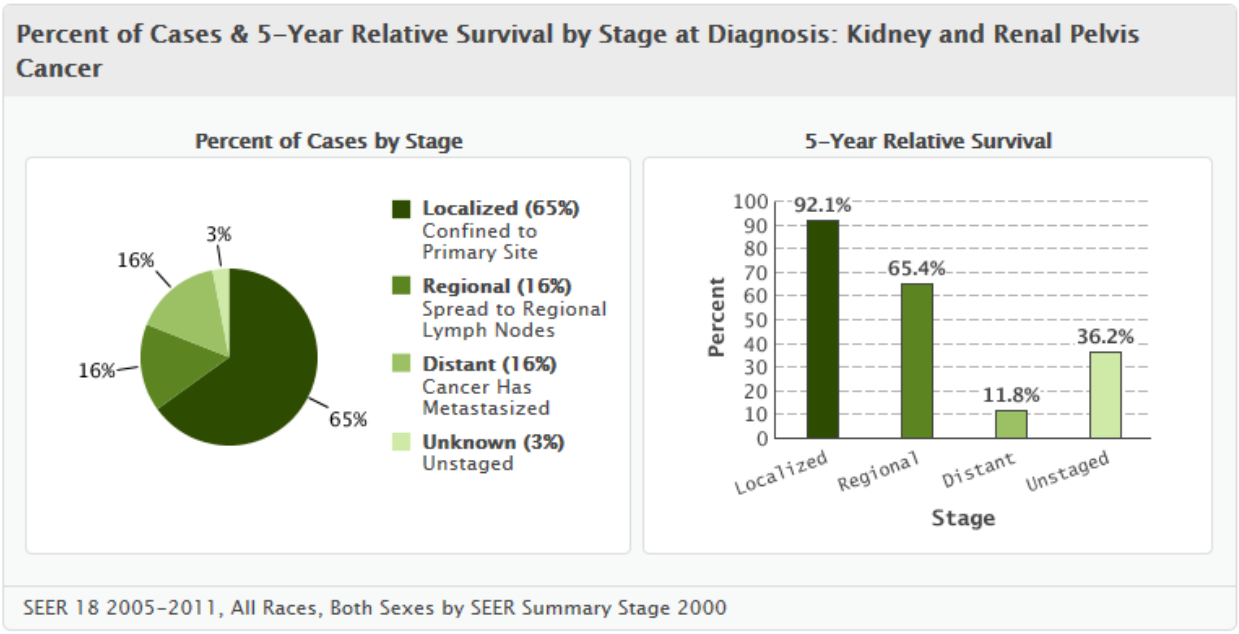

Figure 2 Cases by stage of the disease and related 5-year survival rate [4].

B. RCC prognostic parameters

a. TNM staging

The TNM staging is a classification system of tumor characterization using 3 categories: "T" stands for the description of size and extension of the primary tumor, "N" stands for the regional lymph node involvement and "M" for the presence or absence of distant metastatic sites (Table 1). TNM staging can be divided in two categories: cTNM is based on clinical examination and is used for the choice of treatment, and pTNM pathological classification is based on additional evidences acquired from surgery and pathological examination providing insights on prognosis [7, 8]. Although TNM staging is a good prognostic tool for RCC, it is not suitable for predicting the long term evolution of the disease [8].

Table 1: TNM staging of RCC.

Staging	Classification	Tumor size and extension
Localized RCC	T1	Tumor ≤7.0 cm, limited to kidney
	T1α	Tumor ≤4 cm, limited to kidney
	T1b	Tumor >4 cm and ≤7 cm, limited to kidney
	T2	Tumor >7 cm, limited to kidney
Locally advanced RCC	T3	Tumor extends into major veins or invades adrenal or perinephric tissues but not? beyond
	T3a	Perinephric or sinus fat or adrenal extension
	T3b	Renal vein or vena cava involvement below diaphragm
	T3c-T4b	Vena cava involvement above diaphragm
Regional lymph nodes	Nx	Regional lymph node cannot be assessed
	N0	No regional lymph node metatases
	N1	Metastases in one regional lymph node
	N2	Metastases in more than one regional lymph node
	N3	Metastasis in one lymph node >5 cm
Distant metastases	Mx	Distant metastases cannot be assessed
	M0	No distant metastases
	M1	Distant metastases

b. Fuhrman grade

Microscopic differentiation grading of RCC is based on the nuclear morphology of the neoplasm with hematoxylin and eosin staining. The most widely used system is the 4-tiered Fuhrman grading, scored 1 to 4, going along with increasing nuclear size and irregularity as well as nucleolar prominence (Table 2). According to Fuhrman et al. [9], nuclear grading is the most significant prognostic tool for outcome prediction of stage I renal cell carcinoma.

Table 2: Fuhrman grading system. Adapted from Sun et al. [10] and Fuhrman et al. [9]

	Nuclear diameter	Nuclear shape	Nucleoli
Grade I	Small, 10uM	Round, uniform	Absent, inconspicuous
Grade II	Larger, 15uM	Irregularities in outline	Visible at 400x
Grade III	Even larger, 20uM	Obvious irregular outline	Prominent at 100x
Grade IV			Bizarre multi-lobed with spindles

C. RCC subtypes

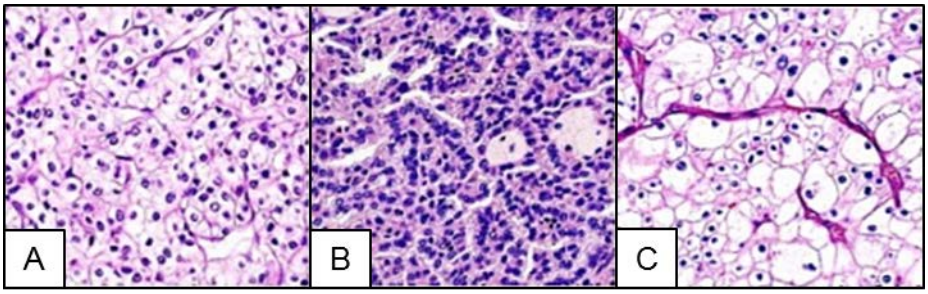

Figure 3: Histology of the major RCC subtypes (stained with hematoxylin and eosin). A: clear-cell renal cell carcinoma; B: Papillary renal-cell carcinoma; C: chromophobe renal cell carcinoma. Adapted from Ficarra et al. [11]

Three major histological subtypes of RCC exist (Figure 3): clear cell subtype (ccRCC) (more than 75% of the cases), known to be related with inactivation of the Von Hippel-Lindau gene (*VHL*), papillary RCC (10-15% of RCC cases, associated with *cMet* alterations in its hereditary form), and chromophobe RCC (5%, associated with *FLCN* mutations in Birt-Hogg-Dubé syndrome) (Table 3) [12].

Table 3: Characteristics of RCC subtypes and associated hereditary syndromes. Adapted from Pavlovich et al. [13].

Histological type	Cell of origin	Genes implicated	Associated hereditary syndromes
Clear-cell renal cell carcinoma	Proximal renal tubule	*VHL, FLCN*	Von Hippel-Lindau constitutional chromosome 3 translocation Birt-Hogg-Dubé
Papillary renal-cell carcinoma	Proximal renal tubule	*MET, FH, HRPT2*	Hereditary papillary renal carcinoma hereditary leiomyomatosis renal-cell cancer hyperparathyroïdism-jaw tumor familial papillary thyroid cancer
Chromophobe renal-cell carcinoma	Intercalated cell of renal collecting duct	*FLCN*	Birt-Hogg-Dubé

The clear cell subtype, which is the focus of this thesis, is the most common RCC subtype and is also the most aggressive form of RCC. The average size of the primary tumor is 7cm diameter and forms globular mass protruding from the renal cortex, presenting a "pushing margins" phenotype with a pseudocapsule. ccRCC appears macroscopically as a golden yellow mass due to its rich lipid content.

D. The von-Hippel Lindau gene and protein

a. Gene, function and pathway

The *VHL* gene, located at the 3p25.3 locus in the human genome, is a tumor suppressor gene of 639 coding nucleotides divided in three exons [14]. The VHL protein (pVHL) can be produced as 3 different isoforms due to alternative splicing of *VHL* RNA. Isoform 1 is a 30kDa protein located mainly in the cytoplasm. This isoform is composed of 213 amino acids and is the major form of pVHL. Isoform 2 differs from isoform 1 by missing amino-acids 114 to 154 that normally form exon 2. Isoform 3 comes from the initiation of translation at the Methionine amino acid at position 54 and leads to the expression of a 19kDa protein located in the cytoplasm and in the nucleus of the cells. pVHL is formed by two tightly coupled domains, α and β. The β-domain consists of seven strands arranged in two β-sheets in sandwich with a α-helix, and it has the properties of a substrate docking site. The α-domain consists of three α-helices and is known to bind Elongin C [15]. pVHL is known to act as substrate recognition in an E3 ubiquitin protein ligase complex, called the VBC complex, to target other proteins for proteasomal degradation [16, 17]. Additionally to pVHL, this complex is formed by Elongin B and C, Cullin2 and Rbx-1.

b. The pVHL-HIF axis

Among its targets for ubiquitination and subsequent degradation are the hypoxia-inducible factors 1α and 2α (HIF1α and HIF2α), which are involved in the cell response to low oxygen. Under

normoxic conditions, HIF1α and 2α are hydroxylated by prolyl hydroxylase 1, 2 and 3 (PHD). Prolyl-hydroxylated HIFα is recognized by the VBC complex via the core of the HIFα oxygen-dependent degradation domain and is targeted for ubiquitination and subsequent proteasomal degradation. PHD1, PHD2 and PHD3 are inactive in hypoxic conditions, causing dihydroxylation of HIFα and impairing the formation of VBC complex. HIFα then forms a complex with HIFβ units that binds hypoxia-response elements (HRE) (Figure 4), leading to upregulation of many genes, such as *VEGF*, *PDGF*, *EPO*, *CAIX* and *CXCR4*, which proteins are known to be important in angiogenesis and other metastatic processes [18, 19]. In ccRCC, pVHL deficiency impairs the VBC complex assembly, HIFα is then stabilized, its accumulation reflects pseudo-hypoxic conditions and triggers the activation of several pro-oncogenic genes involved in angiogenesis, pH regulation, glucose transport, invasion, metastasis and glycolysis, in turn leading to the "Warburg effect" [20, 21].

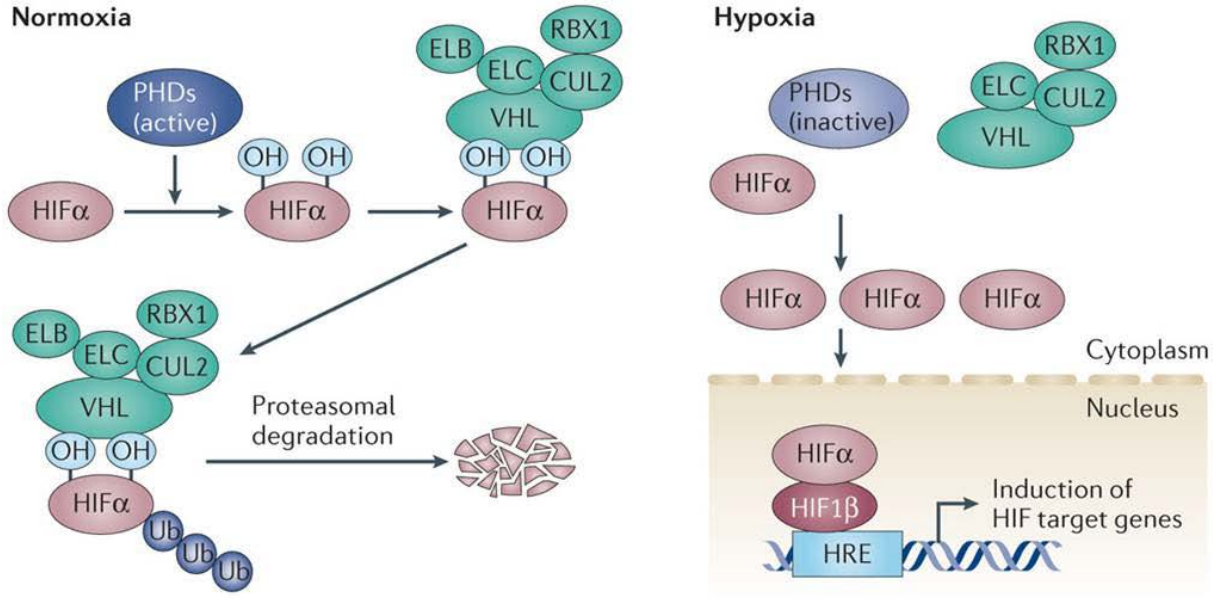

Figure 4: pVHL pathway in normoxic and hypoxic conditions (Gossage et al. [15]).

Although HIF1α and HIF2α share many transcriptional targets, recent evidences showed that HIF1α rather has tumor suppression properties, and HIF2α is considered as an oncoprotein [18].

Loss of chromosomal arm 14q, where *HIF1α* is located, was shown to be associated with worse outcome in ccRCC patients compared to loss of 3p, where *VHL* is located [22, 23]. In xenograft experiments, HIF2α promoted tumor growth whereas HIF1α attenuated tumor growth [24].

c. *VHL* as prognostic and predictive factor

To date, no consensus exists regarding the use of *VHL* as a prognostic or predictive biomarker in ccRCC [25-30]. Generally, no correlation was found between presence/absence or type of *VHL* mutations and pathological parameters, overall and disease-free survival. Some studies reported that the alteration of *VHL* (mutation or hypermethylation) is even associated with a better outcome [31].

d. *VHL* inactivation and mutation classification

VHL has been shown to be affected in more than 90% of the ccRCC cases, either by allelic deletion, promoter methylation (20%), or mutations (70-80%) [29, 32]. The inactivation of *VHL* has been found to be a critical point in the initiation of tumor formation and is the major aspect of this study in the context of ccRCC [33-35]. In the particular case of VHL disease, a syndrome caused by genetic mutations of *VHL*, individuals inherit a defective allele of *VHL* and the remaining wild-type allele becomes inactivated or lost [36]. This disease is characterized by the formation of multiple tumors and cysts such as hemangioblastomas, pheochromocytomas and ccRCC. In this disease, mutations are classified depending on their type: frameshift and nonsense mutations that most likely abrogate pVHL functions (type 1 disease), and missense mutations whose effects can range from no or little impact to high destabilization of pVHL (type 2 disease). Type 2 VHL disease can be further divided into type 2A with a low risk of developing ccRCC, type 2B with a high risk of ccRCC and type 2C with an increased risk of pheochromocytoma [37].

e. *VHL* missense mutations

Although it has been shown that patients presenting loss-of-function (LOF) mutations in *VHL* may have a poorer prognosis compared to wild-type or missense [30], little is known about the effects of missense mutations on pVHL functions. Evidence of mutant *VHL* expression at the RNA level [38, 39] as well as at the protein level [40, 41] were described in other studies. Although pVHL mutant forms tend to rapidly degrade, they still may exhibit partial function [42]. In sporadic ccRCC, Rechsteiner et al. proposed a functional classification of missense mutations in three groups: A: mutations leading to a severe destabilization of pVHL; B: mutations with no destabilizing effects on pVHL but impaired interaction with HIF1α, elongin B, and elongin C; and C: mutations leading to protein behaving like the wild-type (WT) protein [43]. *VHL* LOF mutations (frameshift, nonsense and splice site mutations) highly likely abrogate pVHL function, whereas the consequences of missense mutations on pVHL stability and interactors binding ability are rather unclear. Indeed, missense mutations may provoke diverse effects on pVHL interactions with binding partners, thus exerting different impact on pathways normally regulated by pVHL. This was shown for HIF1α and HIF2α degradation [43] as well as for other pVHL binding partners including Jade1, RPB1, VDU1, EEF1α1 and CCT-ζ-2 for which loss of binding capability upon missense mutations was demonstrated [44-49]. One part of this project was a detailed analysis of the *VHL* missense mutation spectrum, their effects on pVHL stability and the potential pVHL interactor binding domains affected.

f. pVHL acts as a multiadaptor protein

The pVHL structure is divided in two major binding regions. The β-sheet is known to bare the HIF1/2α binding domains and the α-helical domain is responsible for EloB/C interaction. Additionally, pVHL has been identified as a multiadaptor protein and Leonardi et al. reviewed 35

experimentally verified proteins interacting with pVHL with their putative binding regions (Figure 5) [50-53]. In addition to HIF1/2α degradation, pVHL is also involved in the recruitment of many effector proteins to regulate a variety of cellular processes including microtubule stability, activation of p53, neuronal apoptosis, cellular senescence and aneuploidy, ubiquitination of RNA polymerase II and regulation of NF-κB activity [54].

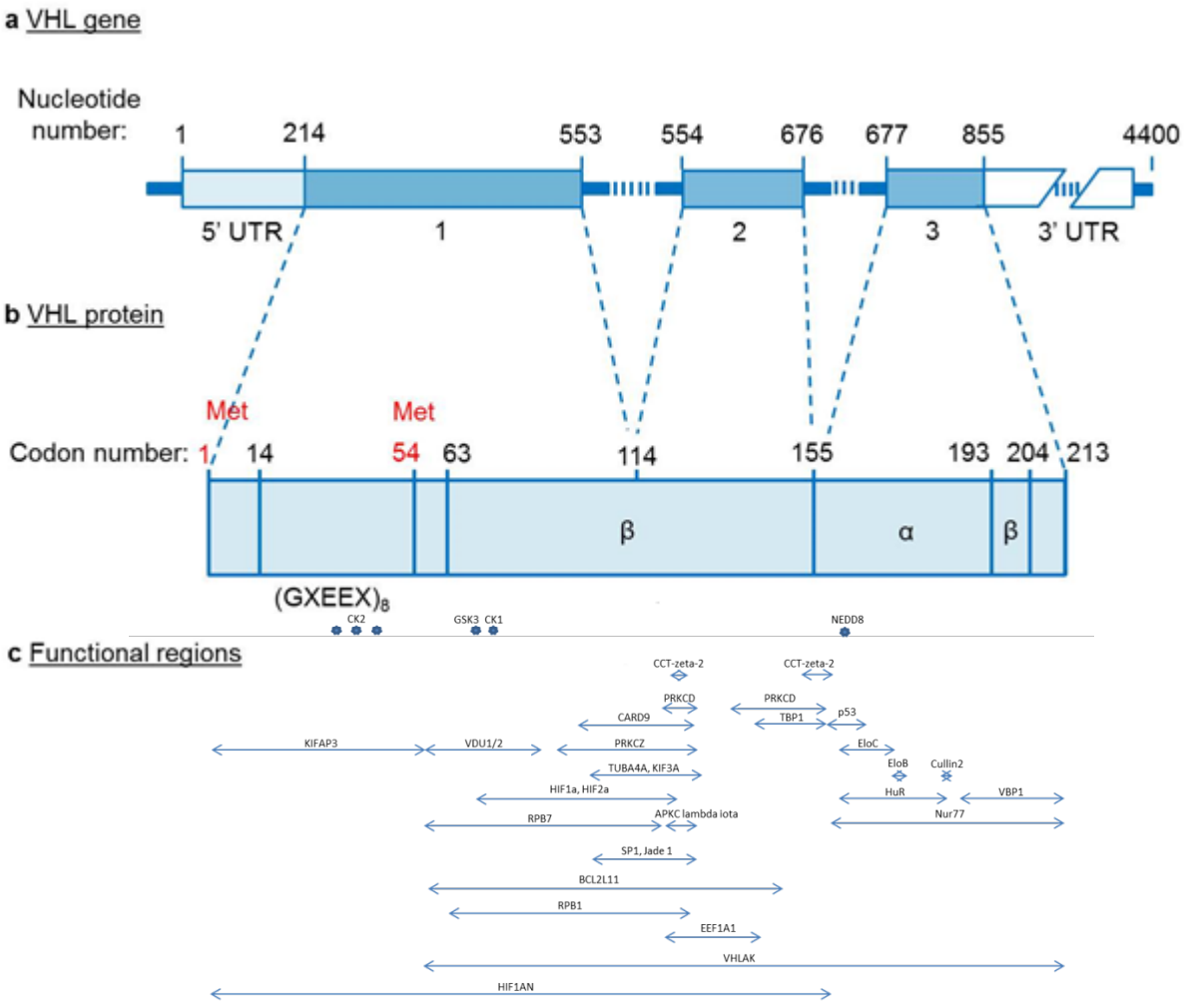

Figure 5: *VHL* gene and pVHL structure, and protein-protein interaction sites Adapted from Richards et al. [55] and Leonardi et al. [50]

E. ccRCC treatment strategies

The different treatments strategies for ccRCC are partial or total nephrectomy, radiation and chemotherapy (which is rather unusual because ccRCC is often resistant to these therapies), and targeted therapy. Treatments currently used in the clinics for metastatic disease are mostly anti-angiogenic tyrosine-kinase inhibitors that target VEGFR and PDGFR to counter the upregulation of HIFs caused by inactivation of *VHL*, and drugs targeting the mTOR pathway which is a critical regulator of cell growth. Those treatments are currently the gold standard for treating ccRCC but despite all the recent efforts towards finding efficient therapies they remain suboptimal for most metastatic ccRCC [1]. Sunitinib is the most often used drug with only 31% of mainly partial response [56].

F. p53

a. Gene, function, pathways

The human tumor suppressor protein p53 is encoded by the *TP53* gene located at the locus 17p13.1 in the genome. This protein contains domains for transcriptional activation, DNA binding, and oligomerization, as the protein can associate in tetramers. p53 activation leads to cell cycle arrest, DNA repair and apoptosis. p53 degradation is mediated by a ubiquitin ligase, Mdm2, that binds and targets p53 for its proteasomal degradation. p53 activation and stabilization is very complex and is driven by several mechanisms (reviewed by Lavin et al. [57]). Post-translational modifications such as phosphorylation (i.e. by ATM, AMPK and JNK), acetylation (i.e. by p300), methylation, ubiquitination and sumoylation occur in more than 20 different sites of p53, leading to its activation. Cellular stresses such as UV light, DNA damage, hypoxia or response to cytokine stimulation, cell-cell contact, viruses and other metabolic changes also activate p53. Other pathways of p53 activation involve the inhibition of Mdm2 (i.e. through PTEN or p19).

p53 stabilization and activation leads to transactivation of its downstream target genes such as *p21*, *Bax* and *Noxa* (Figure 6) [58]. The transcriptional activation of these downstream targets can induce cell cycle arrest, apoptosis, senescence, DNA repair, or metabolic changes. In contrast, p53 inactivation promotes tumor progression. Many human cancers have mutations in *p53* which is the most frequently mutated gene in cancer [59-61].

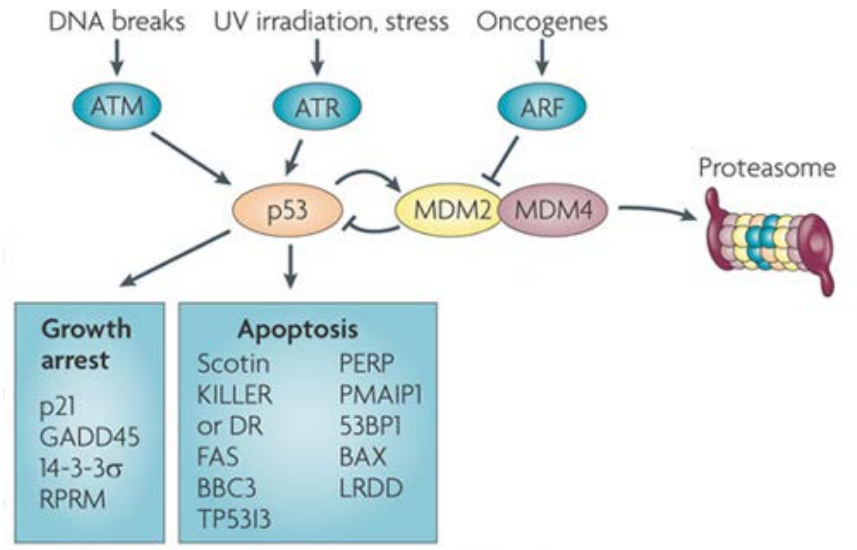

Figure 6: p53 pathway. Adapted from Brown et al. [62]

b. p53, pVHL and HIF

The role of p53 in ccRCC and its relation to pVHL is yet unclear. Whereas one research group concluded that p53 expression was not pVHL-dependent [63], others showed that pVHL can associate directly to p53, leading to p53 stabilization and enhancement of its transcriptional activity [64-66]. As an indirect stabilizing effect , Roe et al. suggested the suppression of Mdm2-mediated ubiquitination of p53 by pVHL [67]. pVHL inactivation in RCC cells have been proven to lead to decreased apoptosis [67], which may be explained in part by the lack of phosphorylation of pVHL by checkpoint-kinase 2, impairing the recruitment of p53 coactivators (such as p300 and Tip60) [65]. The loss of *VHL* has also been demonstrated to lead to p53

inactivation through progerin expression [68]. Moreover, recent findings suggest complex regulation between p53 and HIFs. Indeed, p53 has been described to bind HIF1α [69] which will affect its stability and activity [70]. Since p300 is a co-activator of both p53 and HIF1α [71], p53 may regulate HIF1α by a competition mechanism leading to a downregulation of HIF1α signaling [72]. Additionally, HIF2α accumulation could lead to p53 suppression [73] and its inhibition to p53 activity enhancement [74].

c. p53 in ccRCC

Previous studies showed that p53 was immunohistochemically 4 to 5 times less expressed in ccRCC than in other RCC subtypes [75]. Seventy percent of papillary, 27% of chromophobe, and only 12% of ccRCC cases overexpressed p53. There was no association with stage and grade of the tumor [76]. In a previous study, p53 overexpression in 50 clear cell RCC cases was associated with rapid proliferation and was linked to poor prognosis [77]. In contrast to many other cancer types where p53 is one of the most frequently mutated genes [78], p53 mutations are rare in ccRCC [79-81]. Like tumors with p53 mutations, ccRCC is also known to be associated with chemoresistance [82]. Gurova et al. suggested that p53 signaling in this tumor type might be repressed by some other mechanisms independent of p53 mutations [83], such as constitutive activation of NF-kB [84]. More recently, the multi-domain ubiquitin E3 ligase UHRF1 has been proposed as a suppressor of p53 pathway activation and p53-dependent apoptosis in ccRCC [85]. The downregulation of TRIM8, another E3 ubiquitin ligase, has also been shown to suppress p53 activity in ccRCC [86] but there is to date no consensus on p53 signaling downregulation in ccRCC. Interestingly, p21, a p53 downstream target responsible of cell-cycle arrest, has been shown to be a possible prognostic factor for ccRCC patients for localized disease, its overexpression leading to a decreased risk of death due to ccRCC [87, 88].

d. p53 and therapy

Cancer cell resistance is often related to p53 pathway. Although p53 in ccRCC is wild-type in the vast majority of the cases, ccRCC is resistant to chemotherapy and can be intrinsically resistant or acquire resistance to anti-angiogenic therapies [89].

Recently, it has also been shown that Sunitinib can increase p53 activity through inhibition of NF-κB for cell senescence in metastatic RCC [90] and that loss of p53 lead to a decrease of anti-angiogenic therapy efficiency in colorectal cancer [91].

Camptothecin (CPT), a specific inhibitor of DNA topoisomerase I that activates p53 for apoptosis through DNA damage, has been shown in other studies to trigger enhanced apoptosis in the presence of pVHL. CPT has been tested in preclinical and clinical trials in breast cancer and ovarian cancer with promising effects by enhancing apoptosis and downregulating HIF1/2α, alone or in combination with bevacizumab. This drug is currently studied in clinical trial phase II for metastatic RCC [92-94].

G. Other genes frequently mutated in ccRCC

Although *VHL* alterations are by far the most prominent ones in ccRCC, impaired pVHL functions are not always sufficient for tumor formation and proliferation and *VHL* inactivation alone cannot explain ccRCC development [95, 96]. Several other frequently mutated genes have been identified in this disease, such as *PBRM1*, *BAP1* and *SETD2* [97, 98]. All 3 genes are located on the short arm of chromosome 3, which is frequently lost in ccRCC, and have chromatin-remodeling functions. PBRM1 protein is functionally regulated by p53-induced protein degradation in renal cell carcinomas and *PBRM1* showed truncating mutations in more than 30% of ccRCC cases in previous studies [97, 99, 100]. SETD2 is required for DNA double-strand break repair and activation of p53 and a 15% mutation rate of its encoding gene was

reported [97, 101, 102]. BAP1 is a protein involved in chromatin remodeling and transcriptional regulation and has been found mutated in up to 15% of the cases [97, 103, 104]. Other genes involved in chromatin modification and MTOR pathway such as *KDM5C*, *KDM6A*, *MTOR*, *TSC1* and *PTEN* are also altered in about 20% of ccRCCs [105, 106].

This intratumoral heterogeneity in ccRCC can lead to different treatment responses from different cell populations [107]. This feature is particularly important and a proper mutation landscape overview of these genes could be used for selecting appropriate targeted therapies [54]. A recent review published by Wei et al. proposed a “river model” for illustrating the events leading to tumor formation in ccRCC. In this model, *VHL* is considered as a first hit initiating the tumor, *PBRM1* alteration as a second hit, and *SETD2* and *TSC1* mutations would appear in a later stage. This group also described a “window of opportunity” when the hallmarks of cancer are already acquired and after which targeted therapies could have a limited efficiency due to treatment resistance caused by additional genetic alterations (Figure 7) [108].

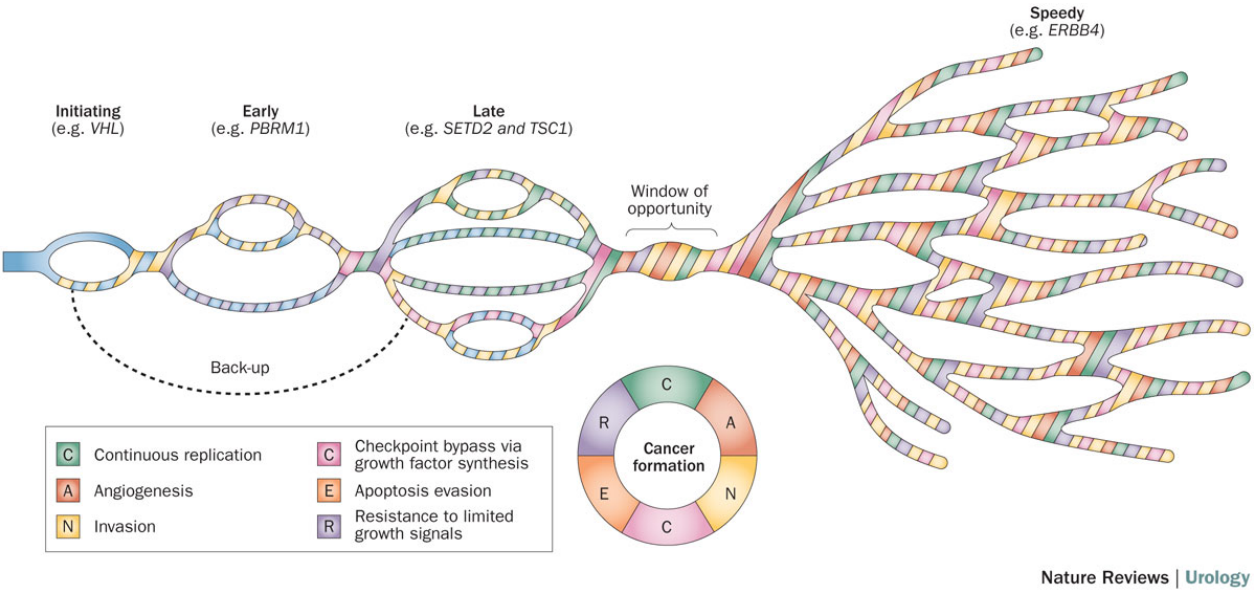

Figure 7: The braided river model of convergent cancer evolution from Wei et al. [108]

II. Objectives

In this thesis, we intended to investigate more closely the *VHL* missense mutations spectrum to determine the most frequently affected binding domains of pVHL, and their potential impact on pVHL function and on response to treatment. We hypothesized that missense mutations exert different impact on the binding capability of pVHL targets and its pathways which may lead to diverse tumor aggressiveness.

In the first part of the project, we investigated the *VHL* mutation status in a cohort of 360 patients with sporadic ccRCC. We particularly focused on missense mutations and their potential biological effects on the pathways regulated by pVHL's interactors and studied their association with clinical follow-up of 30 patients treated with tyrosine-kinase inhibitors (TKI).

In the second part, we specifically focused on the *VHL* missense mutations occurring in the p53/EloC binding domain region and their functional effects on protein stability, HIF degradation, p53 signaling and cell behavior towards proliferation and apoptosis. We hypothesized that *VHL* missense mutations occurring in the p53 binding domain of pVHL can lead to a deficiency in p53 transactivation and/or promote HIF1α and HIF2α accumulation, thus impacting tumor development and possibly therapy efficiency. In this study, we investigated 4 different missense mutations located in the p53 binding site (codons 154-163), which is overlapping with the ElonginC binding domain (codons 157-171). Due to this overlap, the missense mutations investigated could have an impact on p53 signaling and/or on HIF degradation through an altered binding to ElonginC. We also investigated their influence on cells behavior under treatment with chemotherapy or TKI.

Finally, we used next-generation sequencing on DNA samples from the 30 ccRCC patients with follow-up data after treatment. The goal was to unravel possible variant clusters that could be

associated with tumor regression among more than 400 cancer-related genes. We focused particularly on a set of 18 genes: *VHL*, *BAP1*, *HIF1a*, *PDGFRA*, *PDGF(R)B*, *TP53*, *CARD11*, *NFkB*, *TSC1*, *MTOR*, *EGFR*, *PBRM1*, *SETD2*, *KDM5C*, *KDM6A*, *PTEN* and *PIK3CA*, all of which have been reported to be mutated in ccRCC.

III. Characterization of *VHL* missense mutations in sporadic clear cell renal cell carcinoma: hotspots, affected binding domains, functional impact on pVHL and therapeutic relevance

In the following part, we studied the distribution and impact of the 89 missense mutations found in our cohort of 360 ccRCC cases and determined the pathways potentially affected by the resulting protein alterations.

A. Abstract

Background: The VHL protein (pVHL) is a multiadaptor protein that interacts with more than 30 different binding partners involved in many oncogenic processes. About 70% of clear cell renal cell carcinoma (ccRCC) have *VHL* mutations with varying impact on pVHL function. Loss of pVHL function leads to the accumulation of Hypoxia Inducible Factor (HIF), which is targeted by current targeted treatments. In contrast to nonsense and frameshift mutations that highly likely nullify pVHL multipurpose functions, missense mutations may rather specifically influence the binding capability of pVHL to its partners. The affected pathways may offer predictive clues to therapy and response to treatment. In this study, we focused on the *VHL* missense mutation pattern in ccRCC, and studied their potential effects on pVHL protein stability and binding partners and discussed treatment options.

Methods: We sequenced *VHL* in 360 sporadic ccRCC FFPE samples and compared observed and expected frequency of missense mutations in 32 different binding domains. The prediction of the impact of those mutations on protein stability and function was assessed *in silico*. The response to HIF-related, anti-angiogenic treatment of 30 patients with known *VHL* mutation status was also investigated.

Results: We identified 254 *VHL* mutations (68.3% of the cases) including 89 missense mutations (35%). Codons Ser65, Asn78, Ser80, Trp117 and Leu184 represented hotspots and missense mutations in Trp117 and Leu 184 were predicted to highly destabilize pVHL. About 40% of *VHL* missense mutations were predicted to cause severe protein malfunction. The pVHL binding domains for HIF1αN, BCL2L11, HIF1/2α, RPB1, PRKCZ, aPKC-λ/ι, EEF1α1, CCT-ζ-2, and Cullin2 were preferentially affected. These binding partners are mainly acting in transcriptional regulation, apoptosis and ubiquitin ligation. There was no correlation between *VHL* mutation status and response to treatment.

Conclusions: *VHL* missense mutations may exert mild, moderate or strong impact on pVHL stability. Besides the HIF binding domain, other pVHL binding sites seem to be non-randomly altered by missense mutations. In contrast to LOF mutations that affect all the different pathways normally controlled by pVHL, missense mutations may be rather appropriate for designing tailor-made treatment strategies for ccRCC.

Keywords: clear cell renal cell carcinoma, *VHL*, missense mutations, binding domains, pVHL stability, therapy

B. Results

a. *VHL* mutation types, mutation sites, tumor stage and grade distribution

Two hundred forty-six of 360 (68.3%) sequenced ccRCC were mutated. Eight of these tumors had two mutations. The frequencies of the *VHL* mutation types are illustrated in Figure 8.

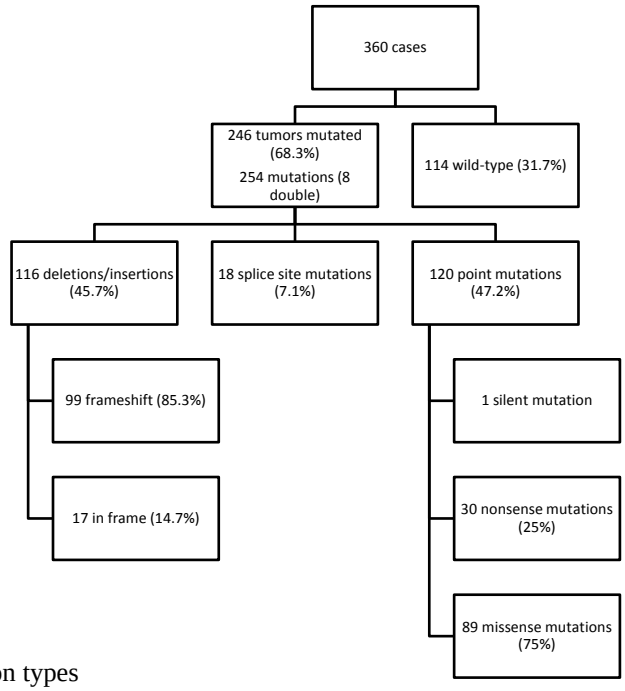

Figure 8: *VHL* mutation types

Since deletions, insertions, splice site mutations and nonsense mutations most likely abrogate most if not all pVHL functions, they were referred to as loss of function (LOF) mutations. An overview of *VHL* LOF and missense mutation sites in the pVHL sequence and the affected binding domains of pVHL's interactors are shown in Figure 9.

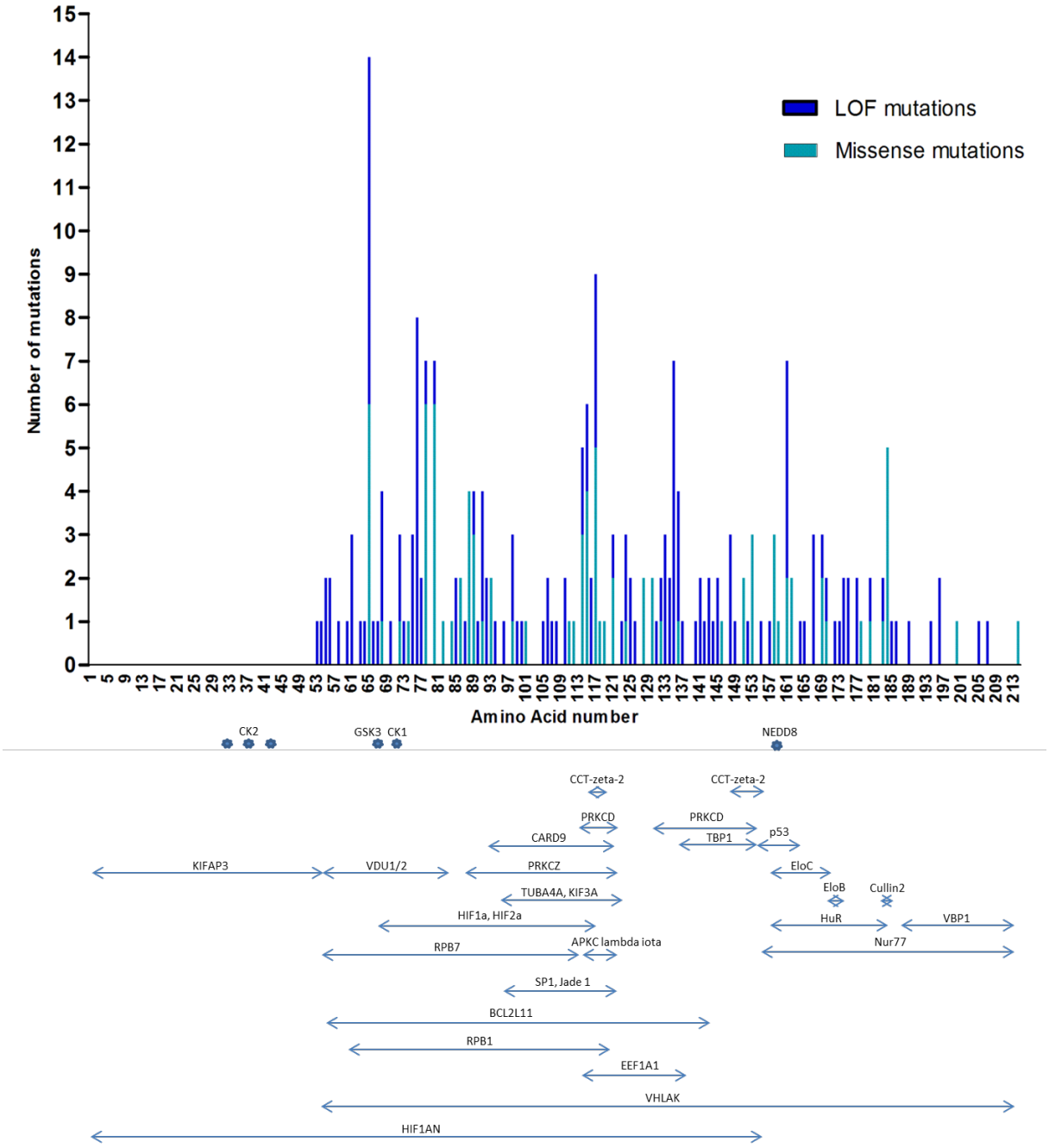

Figure 9: *VHL* mutations sites

VHL mutation frequencies were similar in organ-confined pT1/2 and metastasizing pT3/4 ccRCC. There was no correlation between the number of mutations and stage or grade (Table 4).

Table 4: Tumor stage, Fuhrman grade and type of *VHL* mutations in 346 ccRCC patients.

	Fuhrman n (%)		Tumor stage (pT) n (%)	
VHL status	*1+2*	*3+4*	*1+2*	*3+4*
Nonsense	6 (21.4)	22 (78.6)	15 (53.6)	13 (46.4)
Frame shift	43 (44.8)	53 (55.2)	51 (53.1)	45 (46.9)
Missense	21 (26.9)	57 (73.1)	45 (56.3)	35 (43.8)
In frame	6 (35.3)	11 (64.7)	6 (37.5)	10 (62.5)
Splice site	3 (20)	12 (80)	9 (56.3)	7 (43.8)
Wild-type	37 (33)	75 (67)	52 (47.3)	58 (52.7)

Tumor stage or grade information was not available for 14 patients.

Detailed information of the 256 mutations is given in supplementary table 1 (see Annex).

b. *VHL* mutation hotspots

A closer look at the mutation sites within the protein revealed that some codons were more frequently mutated than others. Fourteen mutations (5.5%) were located at Ser65, nine (3.5%) at Trp117, 8 (3.1%) at Phe76, 7 (2.8% each) at Asn78, Ser80, Leu135, and Arg161, 6 (2.4%) at His115, and 5 mutations were at Gly114 and Leu184 (2% each).

The codons that were most often affected by missense mutations were Ser65, Asn78, Ser80 (six mutations each, 6.7%), Trp117 and Leu184 (five mutations each, 5.6%). Codons Phe76 and Leu135 showed only LOF mutations.

c. Preferentially affected binding domains of pVHL interactors

We next assigned 88 of 89 missense mutations to the putative binding domains of 32 pVHL interactors. One missense mutation in the stop codon was excluded from this analysis. As expected, large binding domains of interacting partners covering more than 60 amino acids of pVHL showed relative high frequencies of mutations. Between 44% and 100% of the missense mutations were located in the VHLAK (100%), HIF1αN (77.3%), BCL2L11 (70.5%), RPB1 (60.2%), and RPB7 (44.3%) binding domains. Notably, about half of the missense mutations

(45/88, 51.1%) resided in the HIF1α and HIF2α (EPAS1) binding domain comprising 51 amino acids.

Between 20-35% of the missense mutations were located in the binding domains of PRKCD, VDU1/2, PRKCZ, EEF1α1, Nur77 and CARD9 (25-60 amino acids). The frequencies of missense mutations found in the smaller binding domains (9-28 amino acids) of JADE1, SP1, KIF3A, TUBA4A, HuR, aPKC-λ/ι, TBP1, CCT-ζ-2, EloC and p53 ranged between 8 and 23%. All interactors, related pathways and binding domains affected by mutations are listed in Table 5. Missense mutations which preferentially affected binding domains were identified by comparing the observed number with the expected number of mutation and by normalizing for each binding domain based on their amino acid length. As the first 54 amino acids of pVHL were not covered by Sanger sequencing, the expected number of missense mutation per codon was 0.55.

We found that the binding domains showing significantly higher rates of missense mutations as expected were for pVHL interactors HIF1αN, BCL2L11, HIF1α, HIF2α, RPB1, PRKCZ, aPKC-λ/ι, EEF1α1, CCT-ζ-2, and Cullin2. pVHL binding partners with involved pathways and the ratio of observed versus expected frequency of missense mutations are shown in Table 5. Additional information on pVHL binding partners is given in supplementary S1 (see Annex).

Table 5: List of interactors and binding domains, number of missense mutations, comparison observed/expected frequency, and pathway affected.

Name of the interactor	pVHL AA involved	Missense mutations count N (%)	Frequency of observed missense mutations compared to expected	p-value	Pathway of the interactor
CK2	S33, S38, S43	0 (0)	lower	ns	Protein amino acid phosphorylation
GSK3	S68	1 (1.1)	1.8X higher	ns	Wnt signaling pathway
CK1	S72	1 (1.1)	1.8X higher	ns	Wnt signaling pathway
NEDD8	K159	1 (1.1)	1.8X higher	ns	Ubl conjugation pathway
KIFAP3	1-54	0 (0)	lower	ns	Microtubule-based movement
HIF1αN	**1-155**	**68 (77.3)**	**1.2X higher**	**	**HIF1α pathway**
VDU1/USP33	54-83	22 (25)	1.3X higher	ns	Ubl conjugation pathway
VDU2/USP20	54-83	22 (25)	1.3X higher	ns	Ubl conjugation pathway
RPB7	54-113	39 (44.3)	1.2X higher	ns	Regulatory RNA pathways
VHLAK	54-213	88 (100)	equal	not applicable	Apoptosis
BCL2L11	**55-143**	**62 (70.5)**	**1.3X higher**	**	**Apoptosis**
HIF1α	**67-117**	**45 (51.1)**	**1.6X higher**	***	**Hif1_tf pathway**
EPAS1 (HIF2α)	**67-117**	**45 (51.1)**	**1.6X higher**	***	**Vegfr1_2 pathway**
RPB1	**60-120**	**53 (60.2)**	**1.6X higher**	***	**Regulatory RNA pathways**
PRKCZ	**87-122**	**30 (34.1)**	**1.5X higher**	**	**Antiapoptosis, intracellular Signaling**
CARD9	92-121	22 (25)	1.3X higher	ns	NFKB and MAPK signalling
TUBA4A	95-123	20 (22.7)	1.3X higher	ns	MT stabilization and dynamic cell polarity
KIF3A	95-123	20 (22.7)	1.3X higher	ns	Hedgehog_gli pathway
SP1	96-122	20 (22.7)	1.3X higher	ns	TGF-beta signaling pathway
JADE1	96-122	20 (22.7)	1.3X higher	ns	Apoptosis
PRKCD	113-122, 130-154	26 (29.5)	1.4X higher	ns	Regulation of receptor activity, senescence
aPKC-λ/ι	**114-122**	**16 (18.2)**	**3.2X higher**	***	**Signalling by NGF**
EEF1α1	**114-138**	**23 (26.1)**	**1.7X higher**	**	**Protein biosynthesis**
CCT-ζ-2	**116-119, 148-155**	**13 (14.8)**	**2X higher**	**	**Chaperone-mediated protein complex assembly**
TBP1	136-154	7 (8)	1.5X lower	ns	Signaling by Wnt, DNA Replication, Apoptosis
p53	154-163	8 (9.1)	1.5X higher	ns	Apoptosis
Nur77	155-213	20 (22.7)	1.6X lower	**	MAPK and NGF signaling pathways
EloC	157-171	11 (12.5)	1.3X higher	ns	Ubl conjugation pathway
HuR (RNA binding protein)	157-184	19 (21.6)	1.2X higher	ns	mRNA stabilization
EloB	170-174	1 (1.1)	2.8X lower	ns	Ubl conjugation pathway
Cullin2	**181-184**	**6 (6.8)**	**2.7X higher**	**	**Ubl conjugation pathway**
VBP1	187-213	1 (1.1)	14.9X lower	***	Morphogenesis

14 splice site mutations and a frameshift mutation for which the position of the affected amino acid cannot be determined and the missense mutation c.642 A>C/ p.X214Cys are excluded from this table. p-value summary: P-value: *<0.05, **<0.01, ***<0.001, ns "not significant"

d. *VHL* missense mutations and pVHL stability

Eighty-eight missense mutations were analyzed *in silico* using the program SDM to determine the protein thermodynamic change (ddG) triggered by those mutations. In this context, ddG is an indicator of pVHL stability and suggests whether or not a missense mutation causes deleterious functional impact and is associated with disease.

A large proportion of the *VHL* missense mutations (60/88, 68%) were predicted to destabilize the resulting protein (ddG<-0.5), eleven mutations (11/88, 12.5%) had a neutral effect (-0.5<ddG<0.5), and seventeen had a stabilizing effect (17/88, 19.3%) on pVHL. Thirty-three of 88 (37.5%) missense mutations were highly destabilizing and only 2 (2.3%), were highly stabilizing, suggesting that about 40% of *VHL* missense mutations were predicted to cause protein malfunction (ddG<-2 and ddG>2 respectively). *VHL* missense mutations and their predicted effects on pVHL stability and association with disease are listed in supplementary table 2 (see Annex).

By focusing on the HIF1/2α binding domain (amino acids 67-117) and the remaining parts of the protein (amino acids 54-66, 118-213) we observed significantly more missense mutations in the HIF1/2α binding domain than expected (43/88 observed, 28/88 expected (p-value <0.0001). However, the frequency of destabilizing mutations (ddG<-0.5) in the HIF1/2α binding domain (32/45, 71.1%) was similar to that seen for the remaining parts of the protein (28/43, 65.1%).

Notably, all of the hotspot missense mutations found in codons Trp117 and Leu184 were destabilizing and 3 out of 5 and 5 out of 5 mutations, respectively, were predicted to cause protein malfunction. In addition, all missense mutations in codon Ser80 destabilize pVHL, codon Ser65 had 3 destabilizing and 3 stabilizing mutations, and codon Ser65 had 2 destabilizing and 4 stabilizing mutations. The sites of all missense mutations are shown together with their stability prediction in Figure 10.

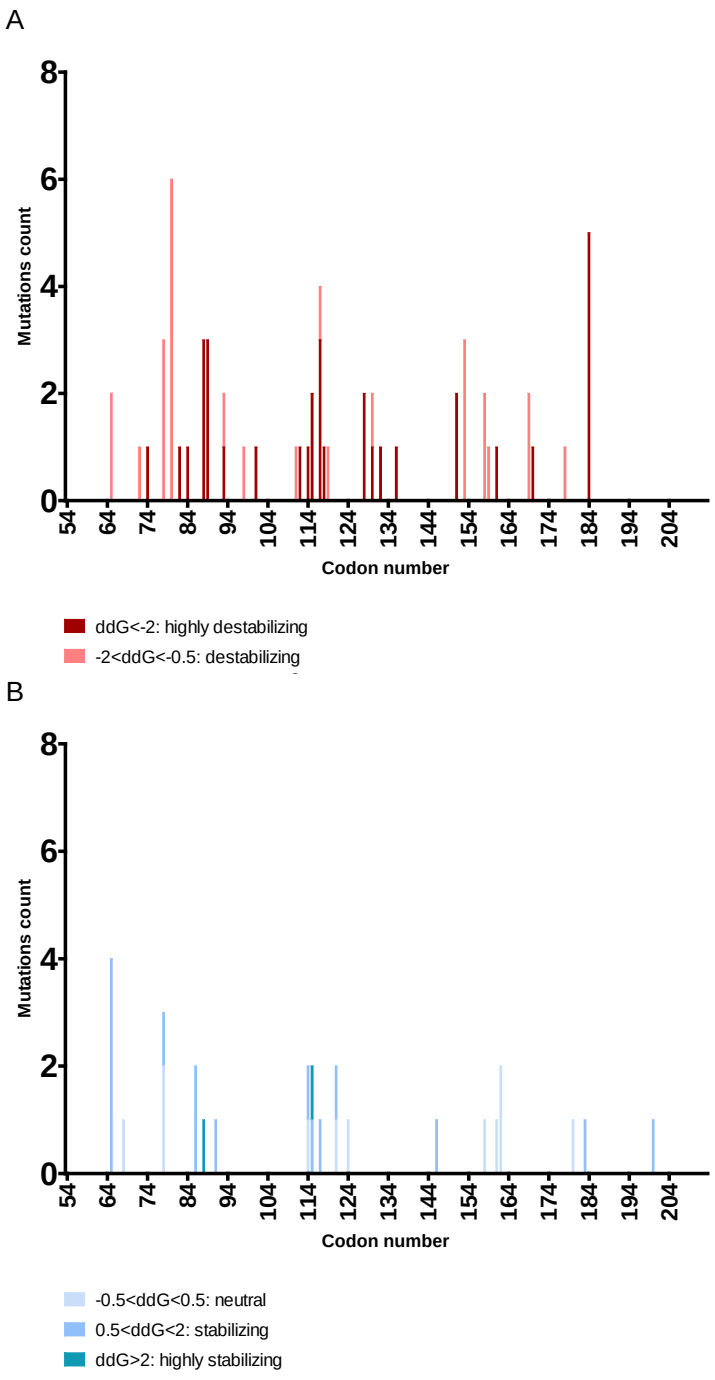

Figure 10: Distribution of *VHL* missense mutations and their predicted stability. A: destabilizing; B: neutral and stabilizing mutations

e. pVHL mutations and treatment response

After surgical resection of the primary tumor, 30 patients from the cohort were treated with anti-angiogenic drugs that are currently used in clinics for patients with metastatic ccRCC. These patients were subdivided into three groups according to response to therapy: progressive, stable and regressive disease. Treatment administered, response, *VHL* mutation status, tumor stage and grade are listed in Table 6. The proportion of responders (stable + regressive disease) was 52.6% for the LOF (10/19), 33.3% for the missense mutations (2/6), and 40% for the wild-type *VHL* (2/5).

There was no correlation between disease progression status, tumor stage, grade and the mutation consequences for the function of pVHL.

Table 6: Treatment, response, and *VHL* mutation status of the patients treated with anti-angiogenic therapies.

Mutation	Mutation consequence	Functionality prediction	Interacting partners	Disease progression status	Treatment	pT stage	Fuhrman grade
c.163delG/p.Glu55ArgfsX11	fs	LOF		PD	Pazopanib>Everolimus	3	3
c172delC/p.Arg58GlyfsX9	fs	LOF		PD	IFNa>Pazopanib		
c.194C>T/p.Ser65Leu	missense	stabilizing	HIF1αN/VDU1/USP33/VDU2/USP20/RPB7/VHLAK/BCL2L11/RPB1	PD	Sunitinib		
c.240T>A/p.Ser80Arg	missense	destabilizing	HIF1αN/VDU1/USP33/VDU2/USP20/RPB7/VHLAK/BCL2L11/HIF1α/EPAS1/RPB1	PD	IFNa>Sorafenib	1	
c. 262T>A/p.Trp88Arg	missense	highly destabilizing	HIF1αN/RPB7/VHLAK/BCL2L11/HIF1α/EPAS1/RPB1/PRKCZ	PD	Sunitinib	3	3
c.268_273del/p.Asn90_Phe91del	in frame	LOF		PD	Sunitinib		3
c.IVS1+1G>A (c.340+1G>A)	splice mut	LOF		PD	Sorafenib>Sunitinib >Everolimus		
c.345_364del/p.Leu116ArgfsX9	fs	LOF		PD	IFNa>Sorafenib		
c.349delT/p.Trp117GlyfsX42	fs	LOF		PD	Sunitinib	3	3
c.484T>C/p.Cys162Arg	missense	neutral	VHLAK/p53/Nur77/EloC/HuR	PD	Sunitinib>Sorafenib >Everolimus>Pazopanib	3	3
c.497_505del9/p.Arg167ValdelSerLeu	in frame	LOF		PD	Sunitinib	3	3
C.580_583delinsAA/p.Val194LysfsX61	fs	LOF		PD	Sunitinib>Sorafenib		
c.586A>T/p.Lys196X	nonsense	LOF		PD	Sunitinib>Sorafenib >Everolimus	1	
	wild-type	wild-type		PD	Pazopanib	3	4
	wild-type	wild-type		PD	Sunitinib>Pazopanib >Sorafenib>Everolimus	4	3
	wild-type	wild-type		PD	Sunitinib	2	3
c.161_162delTG/p.Met54ArgfsX77	fs	LOF		SD	Sunitinib	3	4
c.203C>A/p.Ser68X	nonsense	LOF		SD	Sorafenib>Pazopanib >Everolimus	3	4
c.327insA/p.His110ProfsX22	fs	LOF		SD	Sunitinib>Sorafenib	1	4
c.IVS1+2T>A (c.340+2T>A)	splice mut	LOF		SD	Pazopanib>Axitinib	3	3
c.345insC/p.Leu116ProfsX15	fs	LOF		SD	Bevacizumab>IFNa >Pazopanib	3	4
c.350delG/p.Trp117CysfsX42	fs	LOF		SD	IFNa/Bevacizumab	1	3
c.481C>T/p.Arg161X	nonsense	LOF		SD	Sorafenib	2	2
	wild-type	wild-type		SD	Sunitinib>Sorafenib >Everolimus		
c.167_168delCC/p.Ala56GlyfsX75	fs	LOF		RD	Sorafenib	3	1
c.227_229del3/p.Phe76del	in frame	LOF		RD	Pazopanib>Sunitinib	1	3
c.340G>T/p.Gly114Cys	missense	neutral	HIF1αN/VHLAK/BCL2L11/HIF1α/EPAS1/RPB1/PRKCZ/CARD9/TUBA4A/KIF3A/SP1/JADE1/PRKCD/aPKC-λ/ι/EEF1α1	RD	IFNa>Bevacizumab	2	3
*c.383T>C/p.Leu128Pro **	*missense*	*higly destabilizing*	*HIF1αN/VHLAK/BCL2L11/EEF1α1*	*RD*	*Pazopanib*	*3*	*4*
*c.430G>T/p.Gly144X **	*nonsense*	*LOF*		*RD*	*Pazopanib*	*3*	*4*
c.458T>C/p.Leu153Pro	missense	destabilizing	HIF1αN/VHLAK/PRKCD/CCT-ζ-2/TBP1	RD	Sunitinib	2	3
	wild-type	wild-type		RD	Pazopanib>Everolimus	3	3

PD: progressive disease; SD: Stable disease; RD: Regressive disease; LOF: loss-of-function; fs: frameshift. * one patient with two mutations

C. Discussion

It is widely accepted that in almost all ccRCC both *VHL* alleles are inactivated by chromosome 3p loss, mutation and hypermethylation [15, 29, 32]. In contrast to frameshifts, nonsense codons and alteration of splice sites, which highly likely cause loss of function of pVHL in about 50% of these tumors, the consequences of *VHL* missense mutations present in 25% may significantly vary. A detailed and comprehensive investigation of such mutations in this context can hardly be found in the literature. The goal of our study was therefore to sequence the *VHL* tumor suppressor gene in 360 ccRCC patients and characterize missense mutations by focusing on preferentially affected sites in the gene and their potential consequences on pVHL function and its binding partners.

The frequency of *VHL* mutations found in about 70% of the patients was comparable to previously published data [34, 109]. There was no correlation with *VHL* mutation types and the prognostic parameters tumor stage and grade, which is consistent with previous studies [27, 34, 110]. Although most of the *VHL* mutations were private, we found several hotspot mutations in our cohort. Between 5 and 14 mutations affected codons Ser65, Phe76, Asn78, Ser80, Gly114, His115, Trp117, Leu135, Arg161 and Leu184. Interestingly, approximately one third of the 88 missense mutations occurred at codons Ser65, Asn78, Ser80, Trp117 and Leu184 (5-6 mutations per codon). Those missense mutations have already been described in the *VHL* mutations database-UMD [111] and in the COSMIC database for ccRCC [81] where they represent about 10% of all *VHL* mutations. This frequency is consistent with our finding (28/256, 10.9%) and confirms the quality of the sequencing data obtained from our patient cohort.

In addition to the hotspot missense mutations, we also noticed considerable discrepancies between the expected and observed number of missense mutations which particularly affected the binding domains of 10 of 32 pVHL targets. Significant more missense mutations than expected

were seen in binding domains specific for HIF1αN, BCL2L11, HIF1α, HIF2α, RPB1, PRKCZ, aPKC-λ/ι, EEF1α1, CCT-ζ-2, and Cullin2. Apart from HIFα, most of these proteins are mainly involved in apoptosis (BCL2L11, aPKC-λ/ι), transcriptional regulation (RPB1, PRKCZ) and ubiquitin ligation (CCT-ζ-2, Cullin2). Some of these missense mutations may exert pleiotropic effects on different pathways. This was recently shown with the mutants Phe81Ser and Arg167Gln which cause partial abrogation of VBC complex interactions and fail to downregulate HIF1/2α. Simultaneously, they also lead to enhanced anti-apoptosis signaling and weaken the assembly of RNA Polymerase II complex and protein ubiquitination signaling pathway [112]. Notably, the binding sites for aPKC-λ/ι, CCT-ζ-2, and Cullin2 were the most affected ones and may thus represent potential drug targets alternatively to HIF. For example, disruption of pVHL binding leads to subsequent ubiquitination of aPKC-λ/ι, which in turn deregulates JunB expression and promotes tumor progression in VHL disease-related pheochromocytoma. Uncontrolled expression of JunB may also be important in ccRCC as JunB was found to be upregulated in sporadic, pVHL inactivated, ccRCC [113, 114]. Moreover, *VHL* mutations were shown to impair the interaction with pVHL and CCT-ζ-2 which, consequently, caused improper folding of the VBC complex [49, 115]. Given the function of Cullin2 a default in VBC complex formation may also be expected from disrupted binding of pVHL with this protein. Interestingly, the binding domain for VBP1 located at the 3' end of *VHL* exon 3 seems to be spared from mutations. VBP1 functions as a chaperone protein and may play a role in the transport of pVHL from the perinuclear granules to the nucleus or cytoplasm [116]. The strikingly low frequency of mutations (15 times lower than expected) in this region of *VHL* may reflect the importance of sustaining accurate pVHL trafficking in ccRCC. This is supported by a previous report showing that ccRCC with pVHL expression in both nuclear and cytoplasmic compartments had a better prognosis [40].

The effects of missense mutations on protein stability were determined *in silico* by calculating the thermodynamic change caused by one missense mutation. The tool for determining protein stability was proven powerful with mutations predicted to be highly destabilizing leading to both faster degradation of pVHL and stabilization of HIF1/2α [43]. Based on this observation it is conceivable that those mutations are critical for most if not all binding partners of pVHL.

In addition to their potential influence on pVHL function we also attempted to further characterize the 88 missense mutations with regard to their tumorigenic potential. We used the Symphony classification system that allows subclassifying *VHL* missense mutations in VHL disease patients according to their risk of developing ccRCC [117]. Among the 88 missense mutations, 61 (80%) were classified by Symphony as high risk of developing ccRCC. We conclude that most of the missense mutations, even those with neutral or mild impact on pVHL stability as predicted by SDM, may have strong tumorigenic potential. Notably, only two of the remaining 17 missense mutations were highly destabilizing mutations (Ile151Ser and His115Leu) and classified as low risk of ccRCC.

Current therapeutic strategies for ccRCC focus on Tyrosine Kinase Inhibitors (such as sunitinib, sorafenib, pazopanib, axitinib) or other anti-angiogenic drugs (i.e. bevacizumab) to counteract VEGF/ PDGF upregulation in *VHL* mutated tumors with accumulated HIF1/2α [118]. Treatment with Sunitinib as the most commonly used targeted therapy show mainly partial response in 31% of the patients with metastatic ccRCC [56]. It is tempting to speculate that the response rate of ccRCC patients may be linked to the *VHL* mutation type present in a tumor. We therefore analyzed follow-up data of 30 ccRCC patients with known *VHL* mutation status who were treated with anti-angiogenic drugs. No significant association was seen between *VHL* mutation status and response to treatment in our cohort, although a higher response rate in patients with LOF compared to wild-type or missense mutations has been described in a larger study [30]. Fifty-

three percent of the patients with LOF, 33% with missense mutations, and 40% wild-type responded to the treatment (regressive or stable disease).

D. Conclusions

In summary, our *VHL* sequence analysis of 360 ccRCC revealed pVHL binding sites which are preferentially altered by missense mutations. In contrast to LOF mutations which probably influence most of the pVHL regulated pathways, missense mutations may rather deregulate only single or few of those pathways. Moreover, about 15% of ccRCC patients having missense mutations with no, mild or only moderate impact on pVHL function even may have fully or at least partially functional pVHL. As a consequence, pVHL may retain full ability to degrade HIF1/2α but lose its binding ability to other interactors and vice versa. We therefore hypothesize that the relatively low response rate to anti-angiogenic drugs may be explained by the multipurpose nature of pVHL and the manifold effects on pathways caused by the different mutation types (Figure 11). Patients with *VHL* missense mutation may rather benefit from targeted therapies than patients with LOF mutations. For *VHL* wild-type tumors, other therapy modalities aiming at pVHL non-related pathways controlled by tumor suppressors such as PBRM1, SETD2 or BAP1 may be more appropriate than the common anti-angiogenic treatment [97, 98, 106, 119-124].

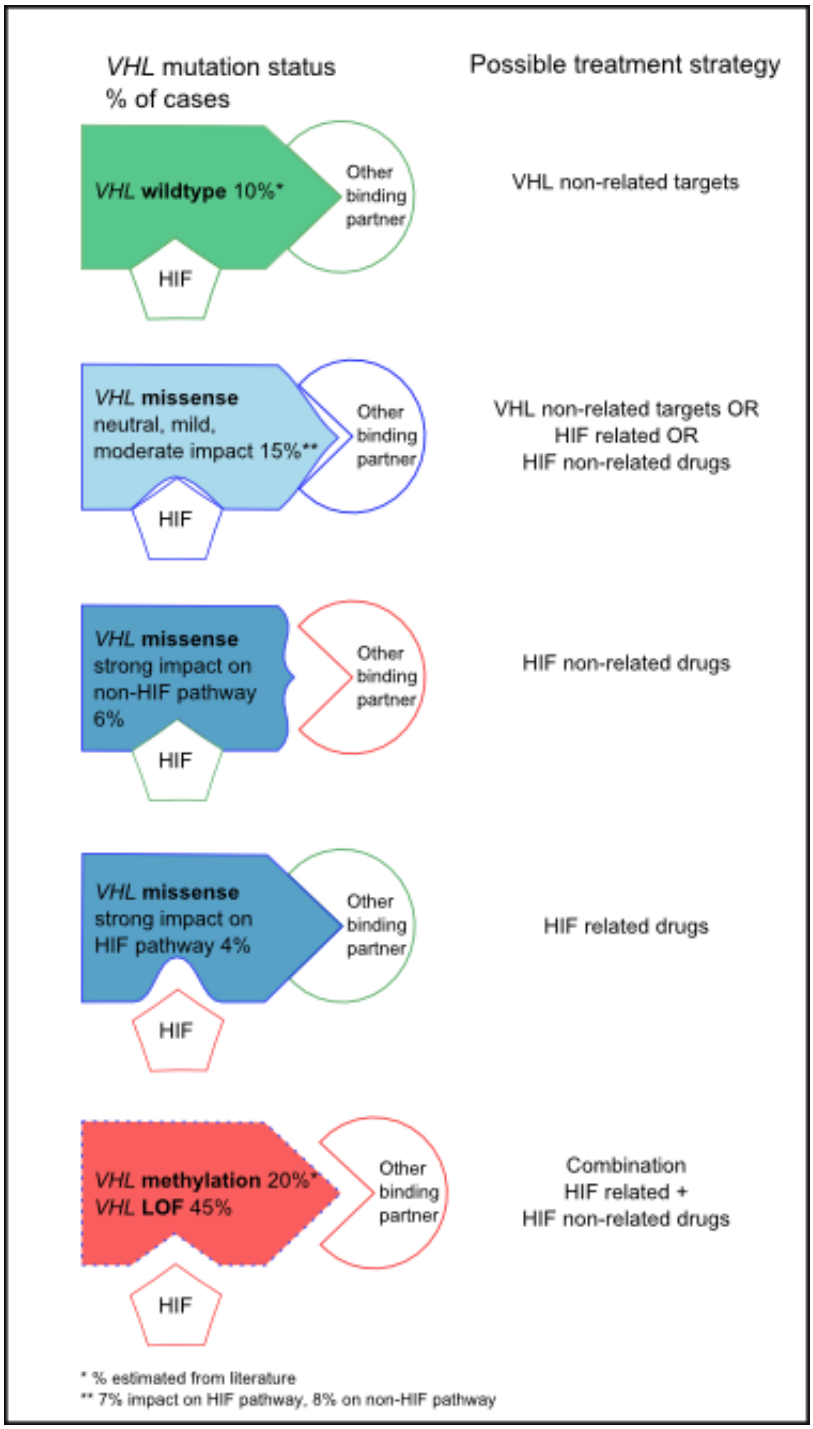

Figure 11: Possible treatment strategies according to *VHL* mutation status

.

IV. Different effects of *VHL* missense mutations on p53 signaling in clear cell renal cell carcinoma

Although the difference between expected and observed missense mutations located in the p53 or in the ElonginC binding domains of pVHL did not reach significance, the overlapping region of these two sites (codons 157 to 163) was 2.1 times more often affected by missense mutations than what would be expected by chance. This overlapping region is then considered as a preferentially affected site. Given the importance of p53 in cancer in general, the low expression of p53 in ccRCC and its relation to chemoresistance, we decided in this next part to focus on 4 missense mutations which were found at this binding site in our cohort of patients.

A. Abstract

Introduction: Clear cell Renal Cell Carcinoma (ccRCC) formation is closely connected to the functional loss of the von Hippel-Lindau (*VHL*) tumor suppressor gene. To date, its best studied interaction partners are the subunits of the hypoxia inducible factor (HIF) HIF1α and HIF2α. However, recent data identified pVHL as a multifunctional adaptor protein involved in a variety of mechanisms, interacting with different binding partners, including p53. p53 is not or low expressed in most ccRCC and, unlike in other cancer types, rarely mutated. As nonsense and frameshift mutations abrogate most if not all pVHL functions, we propose in this study to investigate the impact of *VHL* missense mutations on p53 expression and transactivation as well as the consequences on apoptosis and proliferation with or without treatment.

Methods: A Tissue Microarray containing 262 ccRCC cores was immunohistochemically stained for p53 expression and analyzed regarding their *VHL* mutation status. Seven RCC4 mutant cell lines were engineered, including four missense mutations located in the p53 putative binding domain, two affecting HIF binding domain, and one mutation leading to a truncated pVHL. The

established cell lines were characterized by Western Blot to assess their effect on pVHL expression, HIF degradation and p53 expression as well as by real-time quantitative PCR to verify p53's ability of transactivation on its downstream targets. The cell lines were treated with chemotherapeutic drug (Camptothecin) alone or in combination with an anti-angiogenic treatment (Sunitinib) and their apoptotic and proliferative behavior were investigated.

Results: We found that low and absent p53 expression correlated with *VHL* mutation status and severity of the alteration in ccRCC tissue. As expected, HIFα degradation in cell lines was dependent on the different *VHL* mutants. *p53* mRNA and its effector targets *p21*, *Bax* and *Noxa*, were altered both in cell lines and in tumor tissue. In addition, our results show that *VHL* mutations had an impact on tumor cells' ability to undergo apoptosis, especially when *VHL* is mutated in the p53 binding domain. No effects were seen on cell proliferation. Both drugs were able to efficiently reduce proliferation and Camptothecin additionally increased apoptotic activity of the tumor cells. We found no specific pattern of response to Camptothecin or Sunitinib although the different *VHL* mutant forms showed various intensities of responses. We hypothesize that response rates in ccRCC patients may be improved with p53-mediating drugs which enhance apoptosis.

Conclusion: Improved understanding of the effects of *VHL* mutations on pVHL binding partners may lead to the identification of predictive markers for treatment response and, potentially, to novel therapeutic strategies.

B. Results

a. p53 expression in ccRCC tumors

A Tissue Micro-Array (TMA) containing 262 ccRCC, 48 papillary RCC (24 type I, 24 type II), 22 oncocytoma, 15 chromophobe RCC, 8 from other subtype, and 28 normal tissue cores was immunohistochemically stained for p53 expression. Cores with 5 or less nuclei stained were grouped into "Low content" category and cores showing at least 6 positive nuclei were grouped into "High content". The details of p53 expression scores are shown in Table 7.

Table 7: TMA analysis p53 score details

	Normal tissue	ccRCC	Papillary type I	Papillary type II	Chromophobe	Oncocytoma	Other / undefined
0	17 (60.7)	142 (54.2)	5 (20.8)	4 (16.7)	7 (46.7)	7 (31.8)	2 (25)
+1	8 (28.6)	57 (21.8)	5 (20.8)	5 (20.8)	5 (33.3)	6 (27.3)	3 (37.5)
+2	0 (0)	26 (9.9)	5 (20.8)	5 (20.8)	2 (13.3)	7 (31.8)	1 (12.5)
+3	3 (10.7)	37 (14.1)	9 (37.5)	10 (41.7)	1 (6.7)	2 (9.1)	2 (25)

Nuclear score	*VHL* wt	*VHL* mutant	Mild impact	High impact	LOF
0	35 (43.2)	107 (59.1)	18 (58.1)	16 (57.1)	73 (59.8)
+1	17 (21)	40 (22.1)	2 (6.5)	5 (17.9)	33 (27
+2	13 (16)	13 (7.2)	4 (12.9)	1 (3.6)	8 (6.6)
+3	16 (19.8)	21 (11.6)	7 (22.6)	6 (21.4)	8 (6.6)

High impact on the protein: highly destabilizing + highly stabilizing mutations
Low impact on the protein: Destabilizing + neutral + stabilizing + silent mutations

TMA analysis showed a low p53 expression in ccRCC, oncocytoma, chromophobe and the 8 undefined other subtypes similarly to normal tissue. Papillary type I and II showed significantly higher content of p53 than ccRCC and normal tissue (Figure 12A). By separating the 262 ccRCC in *VHL* wild-type and *VHL* mutated tumors, we observed that p53 expression was less frequent in tumors with *VHL* alterations (p-value: 0.0212) (Figure 12B). We further subdivided mutated tumors into those with mild impact (missense mutations predicted to have a milder effect on the protein stability and silent mutations), high impact (missense mutations predicted to highly destabilize or highly stabilize the protein) and LOF mutations (insertions, deletions, nonsense).

Tumors with wild-type *VHL* or mild impact mutations showed significantly more frequent p53 expression compared to tumors with LOF mutations (Figure 12C) whereas high impact mutations showed a rate in between mild impact and LOF mutations.

A

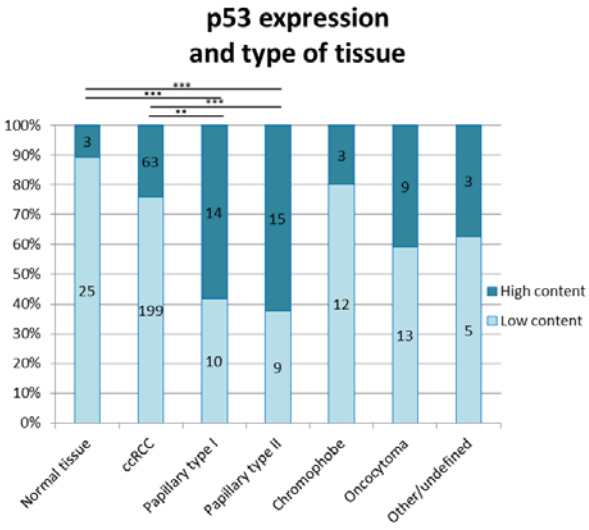

B

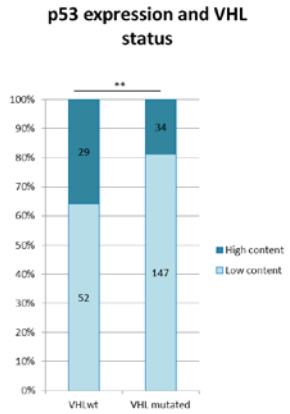

C

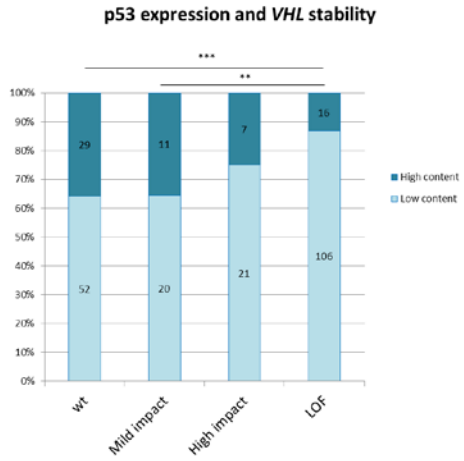

Figure 12: p53 protein expression in A: different tissue types; B: ccRCC according to *VHL* mutation status; and C: ccRCC according to mutation impact on protein stability. Mild impact: Destabilizing + neutral + stabilizing + silent mutations; High impact: highly destabilizing + highly stabilizing mutations; LOF: Insertions/deletions + nonsense mutations p-values: *<0.05, **<0.01, ***<0.001

b. Selection of mutations in the p53/EloC binding domains of pVHL

The binding domains of p53 and EloC are located between codons 154 to 163 and 157 to 171 respectively [34]. Among 254 mutations found in 360 ccRCC tissue specimen, 25 *VHL* mutations resided in these binding domains and 11 were missense mutations which lead to an amino acid change. We used the in silico tool Site Directed Mutator (SDM) (http://mordred.bioc.cam.ac.uk/~sdm/links.php) to predict the thermodynamic change upon missense mutations and their effects on pVHL. Eight missense mutations were predicted to destabilize and 3 missense mutations have no or little impact on pVHL stability.

For this study, we selected 4 out of the 11 missense mutations occurring in the p53/EloC binding domain for further analysis. Three were predicted to have no destabilizing effect on pVHL and to remain functional for the HIF degradation pathway (Leu158Val, Arg161Gln, and Cys162Arg) and one was predicted to highly destabilize pVHL and to fail to downregulate HIF (Arg161Pro). Two other missense mutations occurring in the HIF binding domain, one not affecting and one destabilizing pVHL (Tyr98His, Tyr98Asn), and one nonsense mutation located in p53/EloC binding domain (Arg161X) were predicted to impair HIF degradation pathway and were used as controls. The mutations selected, the binding domain affected and the predicted effect on stability are summarized in Table 8.

Table 8: List of selected mutations

Cell lines stably expressing	Predicted effect	Binding domain affected
Babe (Ser65Trp)	destabilizing and cause protein malfunction and disease	others
VHL30	none	none
Leu158Val	slightly destabilizing and non disease-associated	p53/EloC
Arg161Gln	neutral and non disease-associated	p53/EloC
Cys162Arg	neutral and non-disease-associated	p53/EloC
Arg161Pro	destabilizing and cause protein malfunction and disease	p53/EloC
Tyr98His	neutral and non-disease-associated	HIF1/2α
Tyr98Asn	destabilizing and non-disease-associated	HIF1/2α
Arg161X	LOF	HIF1/2α/p53/EloC

c. Effects of selected *VHL* mutations on HIF and p53

The established stable cell lines were investigated by Western Blot for the effects of the *VHL* missense mutations on HIF degradation and on the two hypoxia markers CAIX and Glut1 (Figure 13A).

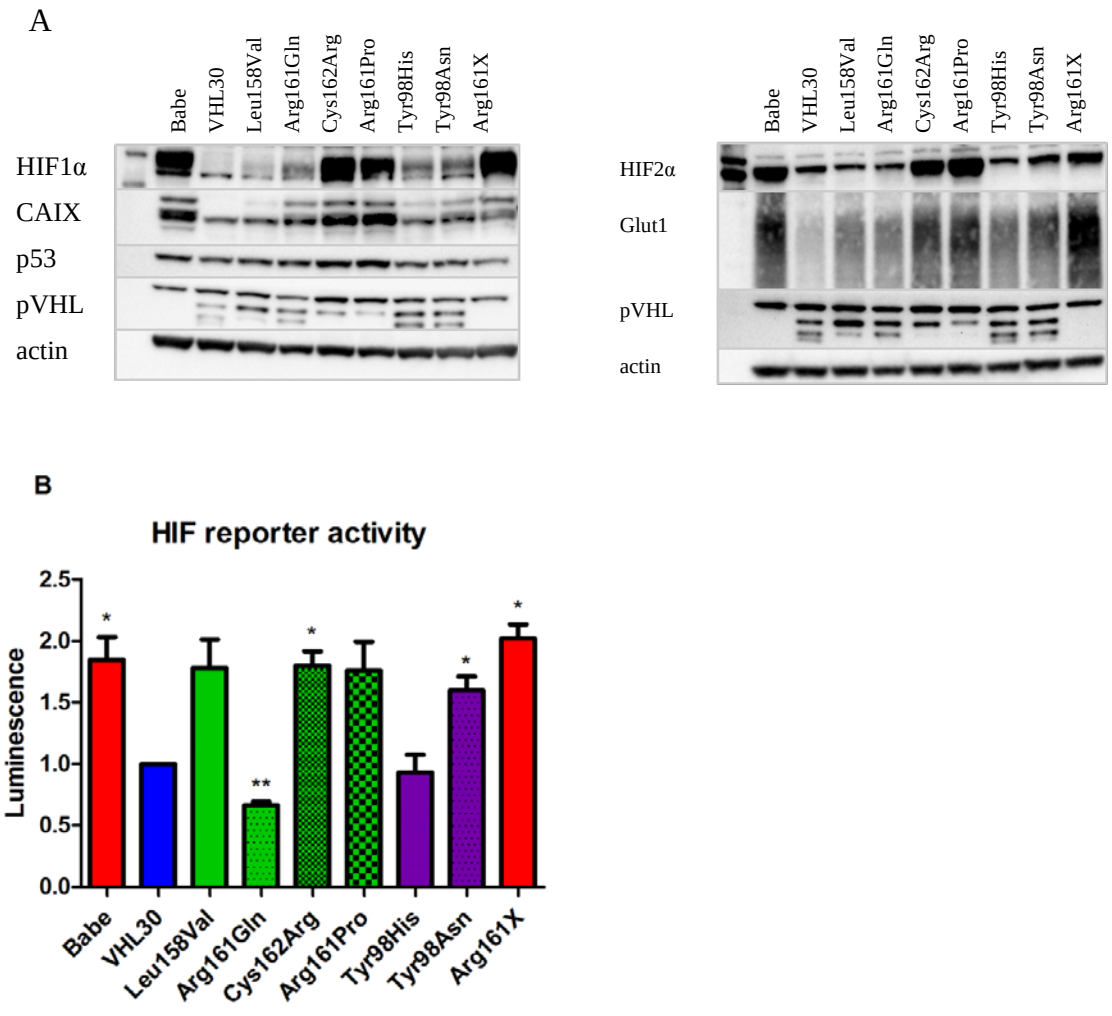

Figure 13: pVHL, p53, HIF1/2α and downstream targets expression in the established stable cell lines expressing the selected mutations A: Western Blot; B: HIF reporter assay, HIF transcriptional activity of each mutant is compared to VHL30. P-value: *<0.05, **<0.01

As expected, pVHL was undetectable in RCC4 Babe and Arg161X. HIF1/2α were upregulated in RCC4 Babe, Arg161Pro and Arg161X and also in Cys162Arg which is predicted to be functional for HIF degradation. RCC4 Arg161Gln, Tyr98His and Tyr98Asn retained partial functionality towards HIF1/2α degradation. The mutant cell line Leu158Val was almost fully functional regarding HIF1α destabilization and presented the same pattern as VHL30. CAIX and Glut1 expression correlated with the HIF1/2α protein levels. No clear difference in p53 expression was seen upon the different mutations.

To further investigate the effect of *VHL* missense mutations on HIF1/2α signal transduction, we performed a HIF reporter assay in the established mutant cell lines.

When wild-type *VHL* is overexpressed in RCC4 (VHL30), it leads to a tremendous downregulation of the HIF signaling pathway compared to Babe (Figure 13B). HIF transcriptional activity is upregulated in Babe, Cys162Arg and Arg161X compared to VHL30 and at least partially downregulated in Arg161Gln, Tyr98His and Tyr98Asn. Except for mutant Leu158Val, results of the HIF reporter assay are comparable to Western Blot analysis.

d. Impact of *VHL* mutations on p53 downstream targets

- In RCC4 stably expressing *VHL* mutants

Previous studies showed that pVHL enhances p53 transcriptional activity and that pVHL with Ser111Arg or Ser111Cys missense mutations led to reduced transcription of p53 downstream targets compared to pVHL wild-type [19, 23]. Here we studied the effects of the *VHL* mutations stably expressed in our RCC4 cell line on the RNA level of *p53* and its effectors *p21*, *Bax* and *Noxa* (Figure 14).

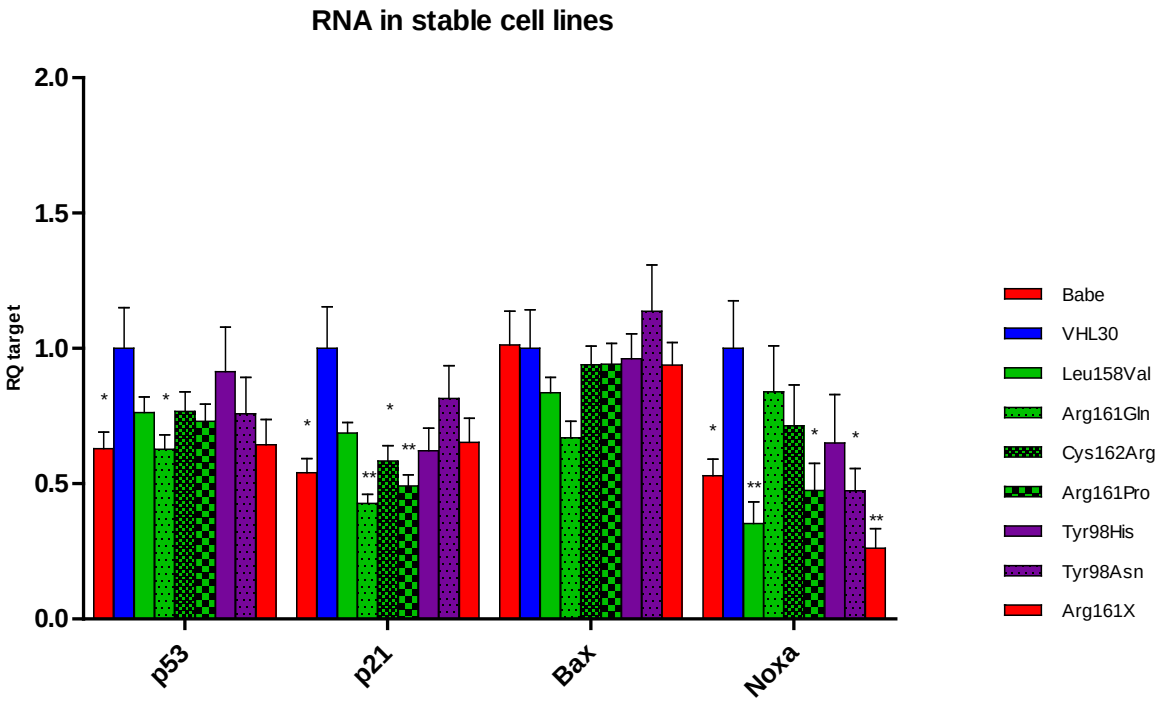

Figure 14: RNA levels of *p53*, *p21*, *Bax*, *Noxa* in the established RCC4 stable cell lines. For each gene the RNA level of the VHL30 sample was used as reference and compared to the RNA levels in the other cell lines; In red, pVHL deficient; in blue, pVHL wild-type; in green, pVHL mutated in p53 binding domain; in purple, pVHL mutated in HIF binding domain. P-value: *<0.05, **<0.01

We saw transcription levels of *p53*, *p21* and *Noxa* in cells expressing the wild-type form of pVHL which were higher than in the different mutant forms. All mutant forms caused a decrease of *p53* RNA level compared to VHL30, although significance was reached only for Babe and Arg161Gln. Transcription level of *p21* was also reduced in the presence of *VHL* mutants compared to RCC4 expressing *VHL* wild-type. This discrepancy was significant for 4 mutant forms (Babe, Arg161Gln, Cys162Arg and Arg161Pro). All mutant forms of *VHL* had lower Noxa RNA levels than VHL30. Significance was found for Babe, Leu158Val, Arg161Pro, Tyr98Asn and the nonsense mutant Arg161X. *Bax* RNA levels were similar in all the stable cell lines,

except for Leu158Val and Arg161Gln showing a lower *Bax* RNA level than VHL30 expressing cells. No significant difference in RNA levels is seen between the 3 mutants in p53 binding domain not destabilizing pVHL and the one with destabilizing effects.

- In ccRCC patients presenting selected *VHL* mutations

Three normal kidney tissues and 9 ccRCC tissues (one *VHL* wild-type, two with mutation Leu158Val (#1, #2), one with Arg161Gln, one with Cys162Arg, one with Arg161Pro, one with Tyr98Asn and two with Arg161X (#1, #2)) were investigated for RNA expression of *VHL*, *TP53* and its downstream targets. First, *VHL* RNA level was assessed in each tissue sample. All but tumor tissue with Arg161Gln expressed *VHL* at least at the same level as the normal tissues (Figure 15A). Second, *p53*, *p21*, *Bax* and *Noxa* RNA levels relative to *VHL* were compared in normal tissues and in *VHL* wild-type ccRCC. Gene expression levels of *p53*, *p21*, *Bax* and *Noxa* in tumor tissue with wild-type *VHL* were similar to the ones seen in normal tissues (Figure 15B).

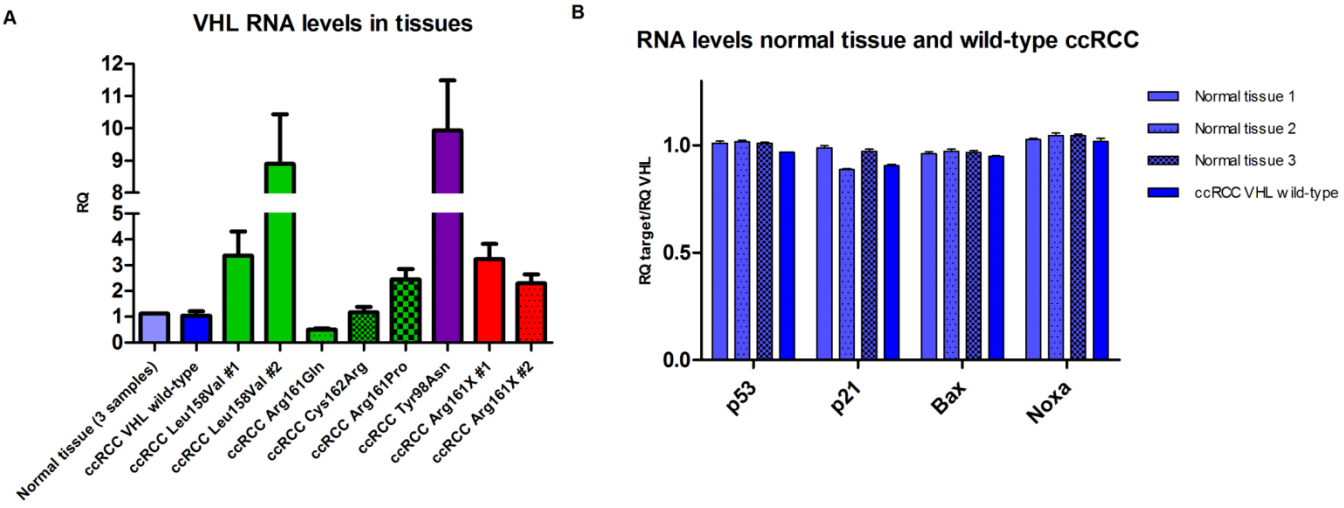

Figure 15: A: *VHL* RNA levels in normal tissue, and in wild type and mutant *VHL* ccRCC; B: RNA levels of *p53*, *p21*, *Bax*, *Noxa* relative to *VHL* transcription levels in normal kidney tissues (3 samples).

Finally, we equalized all *VHL* RNA levels across the samples to present the relative transcription levels of *p53*, *p21*, *Bax* and *Noxa* compared to *VHL*. The RNA levels of *p53* and its downstream targets relative to *VHL* transcription levels were assessed in ccRCC samples expressing the mutant forms of *VHL* (Figure 16).

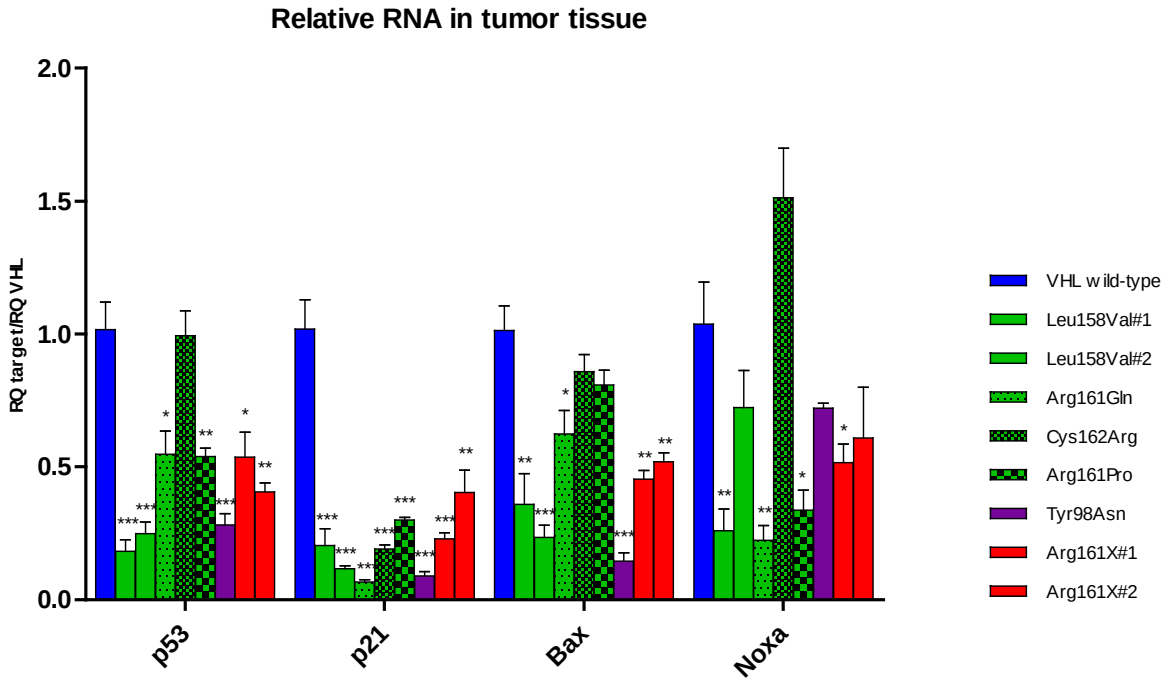

Figure 16: RNA levels of *p53*, *p21*, *Bax*, *Noxa* relative to *VHL* transcription levels in each tumor. No tissue with *VHL* mutation Ser65Trp and Tyr98His was available in our cohort. For each target the RNA level of the *VHL* wild-type tumor is used as reference and compared to the RNA levels of the other tumors. In red, pVHL deficient; in blue, pVHL wild-type; in green, pVHL mutated in p53 binding domain; in purple, pVHL mutated in HIF binding domain. P-value: *<0.05, **<0.01, ***<0.001

Similarly to the established cell lines, wild-type *VHL* tumor showed generally higher relative RNA levels of *p53* and its downstream targets than *VHL* mutated tumors. All except the Cys162Arg mutant displayed significantly lower levels of *p53* RNA. All 8 mutant samples

showed a significant decrease of *p21* RNA levels compared to *VHL* wild-type. In contrast to *VHL* wild-type tumor, significant *Bax* transcription downregulation was seen in all samples except for Cys162Arg and Arg161Pro. All mutants except for Cys162Arg showed lower *Noxa* transcription levels compared to wild-type. We saw that tissues with *VHL* missense mutations located in p53 binding domain were not more affected in p53 signaling than tissues with mutations in HIF binding domain. Additionally, the mutation Arg161Pro which highly destabilize pVHL did not lead to a bigger decrease in *p53* and its downstream targets relative RNA levels than mutations not affecting pVHL stability.

e. Effects of HIF and p53 binding site-specific *VHL* mutations on cell proliferation and apoptosis

The apoptotic behavior of cells expressing different *VHL* missense mutations was evaluated by Caspase 3/7 assay. All pVHL mutants were deficient in apoptosis compared to *VHL* wild type (Figure 17A). By grouping the missense mutations located in the p53 and HIF binding domains, respectively, the HIF binding site-specific *VHL* mutations showed significantly higher apoptotic activity than the cell lines with mutations that affected the p53 binding domain (p-value=0.0088) (Figure 17B). Cell proliferation was not significantly influenced by the different *VHL* mutants, neither by expression of missense mutations located in the p53 nor in the HIF binding domain (Figure 17C-D).

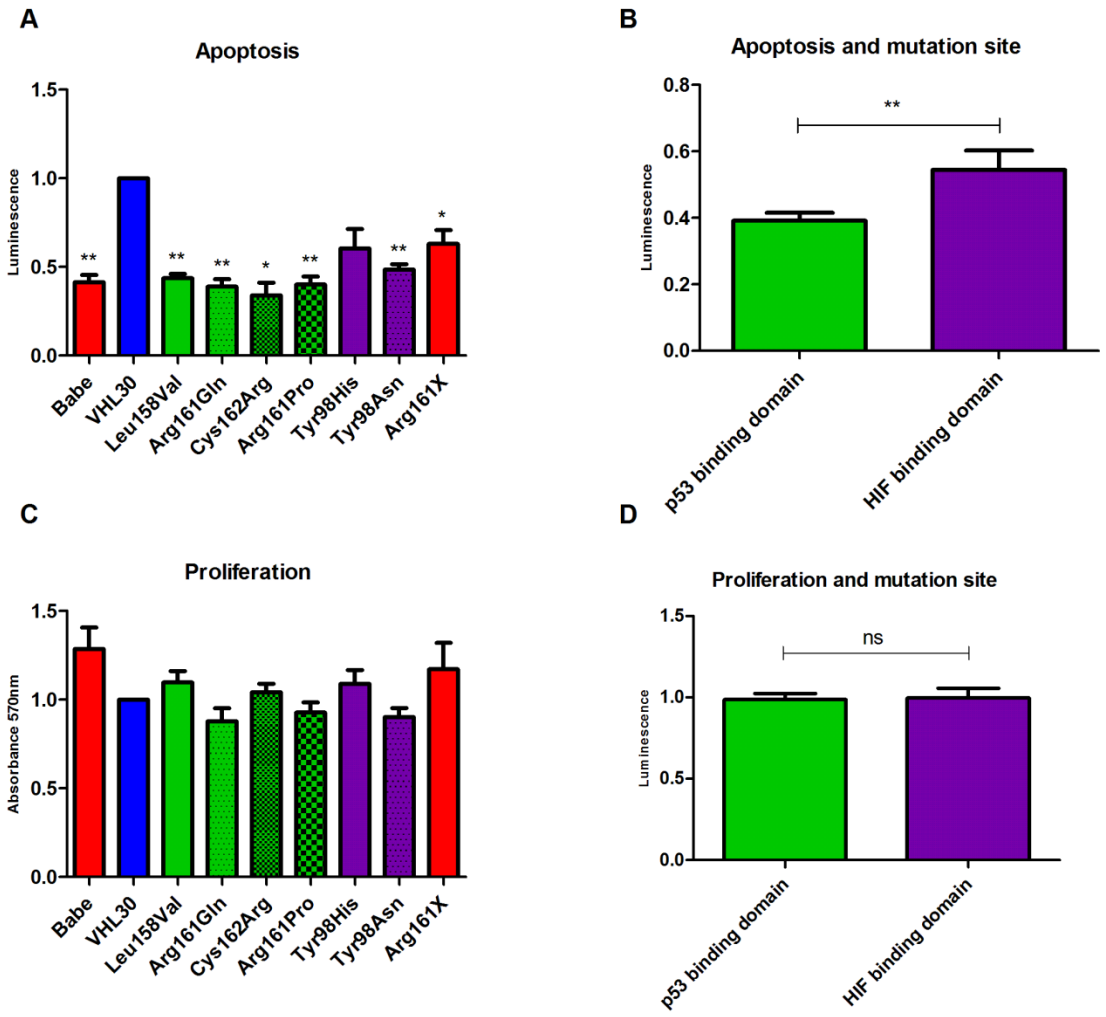

Figure 17: *VHL* mutations and apoptotic behavior of A: all stable cell lines and B: cell lines grouped according to missense mutations in the p53 binding domain and in the HIF binding domain; *VHL* mutations and proliferative behavior of C: all stable cell lines and D: cell lines grouped according to missense mutations in the p53 binding domain and in the HIF binding domain. In red, pVHL deficient; in blue, pVHL wild-type; in green, pVHL mutated in p53 binding domain; in purple, pVHL mutated in HIF binding domain. VHL30 expression was used as reference and compared to the other cell lines. P-value: *<0.05, **<0.01

f. Proliferative and apoptotic behavior of cells upon treatment with camptothecin and/or sunitinib

Camptothecin, which stabilizes and activates p53, was applied to the stable cell lines alone or in combination with Sunitinib. Whereas Sunitinib affects the proliferation pathway, Camptothecin is known to affect both apoptosis and proliferation [92-94]. BrdU and caspase assays were performed with the treated cells and normalized to the number of cells to evaluate the different response to the treatment depending on the *VHL* mutation expressed.

As expected, treatment with Camptothecin alone or in combination with Sunitinib highly increased apoptosis in all cell lines, whereas Sunitinib alone had no effect on apoptosis. Cells with Arg161Gln, Arg161Pro and Tyr98Asn showed the highest response to Camptothecin alone and Arg161Gln and Tyr98Asn seemed to benefit even more from the combined treatment (Figure 18A). All three treatment strategies induced a decrease in cell proliferation except for Arg161X for which the treatment with Sunitinib alone showed only a small decrease in proliferation (Figure 18B). The response to the different treatments seems to be independent of the mutations type, and was similar for cell lines with missense mutation in the p53 binding domain and in the HIF binding domain.

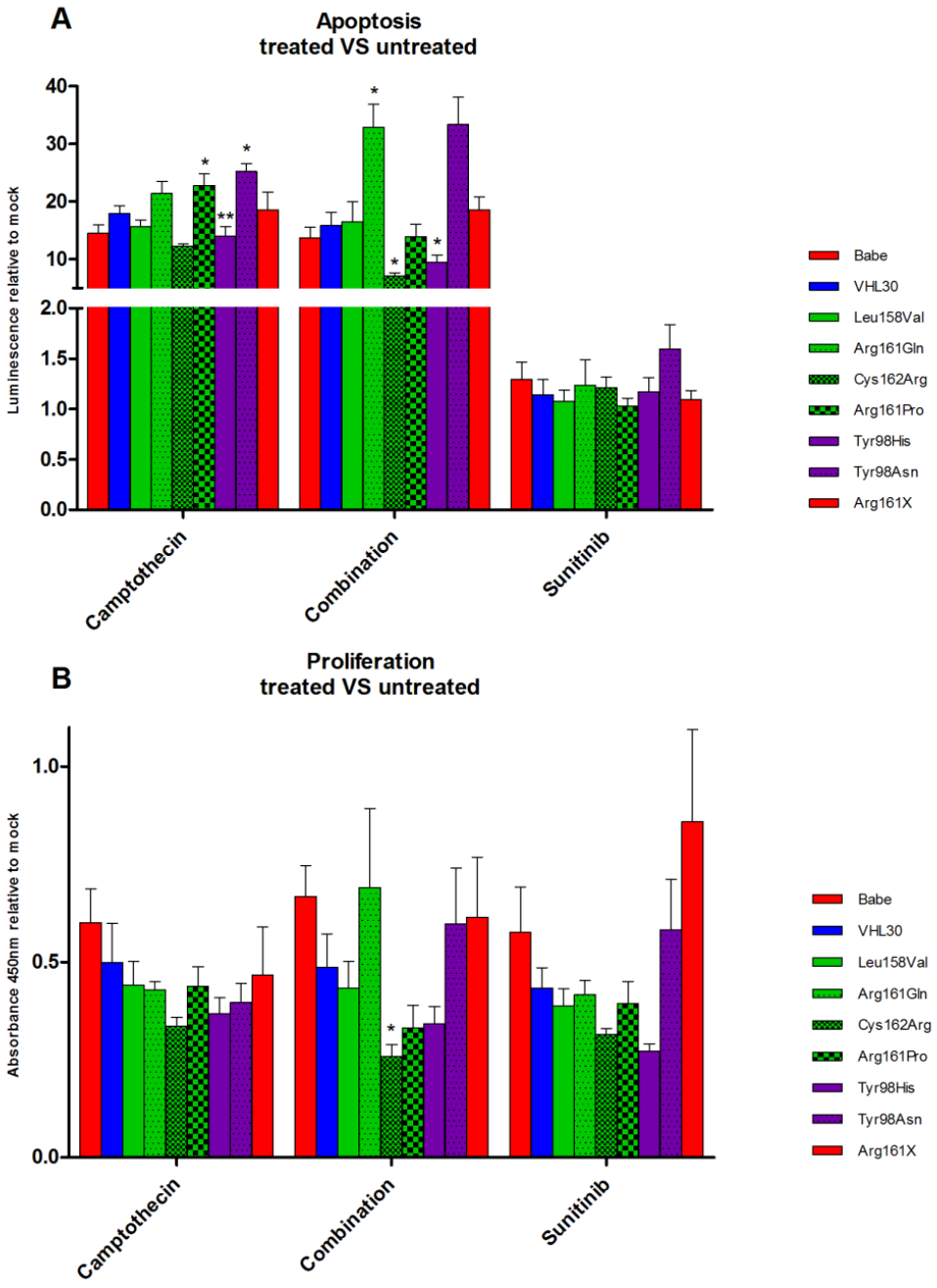

Figure 18: *VHL* mutations and apoptotic and proliferative behavior of the different stable cell lines after treatment with Camptothecin, Sunitinib, alone or in combination A: on apoptotic behavior, B: on proliferative behavior. The signal after treatment of each cell line (treated) is normalized to its own mock signal (untreated). VHL30 is used as reference and is compared to the other cell lines. P-value: *<0.05, **<0.01

The summary of each cell line predicted and observed behavior towards HIF degradation and p53 signaling is shown in Table 9.

Table 9: Comparison of predicted effects of the *VHL* mutations in our stable cell lines and experimental results for HIF degradation and p53 pathways

Cell lines stably expressing	HIF degradation pathway prediction --> Western Blot	p53 pathway prediction --> Caspase & qPCR assay
Babe (Ser65Trp)	strongly altered* --> strongly altered	functional --> strongly altered
VHL30	functional --> functional	functional --> functional
Leu158Val	functional --> functional	strongly altered --> strongly altered
Arg161Gln	functional --> slightly altered	strongly altered --> strongly altered
Cys162Arg	functional --> strongly altered	strongly altered --> strongly altered
Arg161Pro	strongly altered --> strongly altered	strongly altered --> strongly altered
Tyr98His	slightly altered --> slightly altered	functional --> slightly altered
Tyr98Asn	altered --> altered	slightly altered --> altered
Arg161X	strongly altered --> strongly altered	strongly altered --> slightly altered

*known from literature

C. Discussion

In breast, ovarian, bladder and colorectal cancer, p53 accumulation is often due to mutations [125-128], whereas in ccRCC p53 is rarely mutated [79, 80]. By investigating p53 expression in 262 ccRCC cases on our TMA, we saw a relationship between p53 expression and the type of *VHL* mutation: p53 expression decreases with the severity of *VHL* mutation. Among the cases that were p53 negative, 53% had *VHL* LOF mutations, 21% had missense mutations, and 26% were wild-type. For the cases with high p53 expression, 25% were LOF, 29% missense, and 46% wild-type.

Our immunohistochemistry was consistent with other studies showing that p53 expression was significantly lower in ccRCC than in other RCC subtypes [75, 76, 129, 130]. Our result of the correlation between severe *VHL* mutations and negative or low p53 expression suggests that, in contrast to other tumor types, p53's absence may be a consequence of severe *VHL* mutations leading to the incapability of pVHL to bind and stabilize p53 in ccRCC.

As different mutation types in a gene may exert different effects on the function(s) of its protein, we attempted to investigate missense mutations that may specifically affect p53 and its

downstream signaling. Therefore, we selected 4 missense mutations identified in the p53 binding domain, and 2 missense mutations in the HIF binding domain. The missense mutations were predicted to have a range of effects on protein stability, from highly destabilizing to neutral , thus leading to different regulation of the HIF degradation pathway as previously described [43]. As the p53 binding domain is overlapping with the ElonginC binding domain [64], the missense mutations in this region may potentially affect pVHL interactions with one or with both binding partners. We first wanted to verify the HIF degradation pathway of these mutants.

The *VHL* mutations Cys162Arg, Arg161Pro and Arg161X were unable to downregulate HIF1/2α at the protein level. This result was expected for Arg161Pro due to its predicted effect on stability and for the nonsense mutation Arg161X. Interestingly, Cys162Arg which is located in the p53/ElonginC domain and predicted to be neutral was unable to downregulate HIF1/2α. It is therefore possible that mutant Cys162Arg impairs ElonginC binding, thus leading to HIF accumulation. Mutants Arg161 Gln (occurring in p53/EloC binding site), and Tyr98His and Tyr98Asn (HIF binding site) remained only partly functional for HIF degradation which is consistent with the stability prediction and the mutation location. Finally, like VHL30, Leu158Val was able to fully downregulate HIF1/2α. Notably, Arg161Gln and Tyr98His had a milder effect on HIF1α degradation than on HIF2α. Although p53 was demonstrated to be stabilized by wild-type pVHL [64], p53 expression seemed to be unaffected by the *VHL* mutations in our stable cell lines. Only Leu158Val showed an elevated signal for HIF reporter activity while it was efficiently downregulating HIF1/2α at the protein level. In summary, 2 of the missense mutations located in p53/EloC binding domain were still able to downregulate HIF. Since p53 expression appeared unaffected by *VHL* mutations, we hypothesized that those mutations could affect p53 activity rather than stability in our stable cell lines. The detection of phosphorylated forms of p53, representing its activation status, was difficult to assess by Western

Blot. In a previous study it was shown that pVHL wild-type enhances p53 transcriptional activity for its downstream targets p21 and Bax. In addition, pVHL missense mutant Tyr98Asn caused loss of the ability to bind HIF1α, but had no negative effects on p53 binding [64]. Therefore we analyzed *p53* and its downstream targets *p21*, *Bax* and *Noxa* for their transcription levels to have on overview of p53 signaling upon *VHL* mutations in our cell lines.

The RNA levels in the stably transfected cell lines were investigated for p53 and its downstream targets. Indeed, the RNA level of *p53*, *p21* and *Noxa* were lower in all *VHL* mutant cell lines compared to those in RCC4 VHL30. *Bax* RNA levels were hardly affected by the *VHL* mutations. We also analyzed the RNA levels of *p53* and its downstream targets in ccRCC tissue which had the same mutations selected for our stable cell lines with 2 exceptions. None of our tumor tissues had Ser65Trp (to mimic endogenous *VHL* mutation of RCC4) or Tyr98His. *VHL* was transcribed at similar levels in tumor and in normal tissue. p53 signaling was comparable in *VHL* wild-type ccRCC and in normal tissue. In *VHL* mutated tumors RNA levels of *p53*, *p21*, *Bax* and *Noxa* were much lower than in tumors with *VHL* wild-type which was also observed in the cell lines. To investigate the effect of the impaired p53 signaling caused by *VHL* mutations, we investigated the apoptotic and proliferative behavior of our stable cell lines.

All our selected *VHL* mutations led to an attenuated apoptosis compared to *VHL* wild-type, but no significant change in cell proliferation was seen. Given their apoptosis deficiency, *VHL* mutants have a survival advantage compared to *VHL* wild-type. In a previous study, the *VHL* mutants S111R and S111C (part of the HIF binding domain) showed a decrease in apoptosis compared to wild-type via impairment of recruitment of coactivators p300 and Tip60, although p53 binding remained unaffected [65]. The loss of ability to recruit coactivators of p53 could

explain the low apoptotic activity of our cell lines with missense mutations outside the p53 binding domain.

By combining the cell lines in two groups according to their mutation locations, cells with a missense mutation in the p53 binding domain were less apoptotic than cells with missense mutations affecting the HIF binding domain. Hence, cell lines with missense mutations in the p53 binding site had a better survival than the ones that were mutated in the HIF binding domain. Since all pVHL mutants showed attenuated apoptosis compared to wild-type pVHL, we treated the cells with Camptothecin, a chemotherapeutic drug that stabilizes and activates p53 by inducing DNA damage and decreases cell proliferation. Sunitinib, which is the current treatment of choice for ccRCC, is a TKI targeting VEGFR2 and PDGFRβ and also negatively influences cell proliferation. Camptothecin considerably increased apoptosis in all cell lines including *VHL* wild-type, whereas Sunitinib had no apoptotic effect. For cell proliferation, all three treatment modalities (Camptothecin alone, Sunitinib alone or both combined) showed an average of 50% decrease in proliferation. With exception of Arg161X mutant cells which had a lower response (20% decrease in proliferation), all cell lines responded well to Sunitinib alone. Interestingly, cells with *VHL* mutations in the p53 binding domain or with a mutation in HIF binding domain showed the same response to the three treatments.

In summary, Camptothecin was more effective than Sunitinib because not only it decreased proliferation but also increased apoptosis for all the different *VHL* mutated cell lines. Finally, the response to treatment did not seem to depend on the missense mutation location and the binding domain affected. *VHL* mutation status cannot explain (at least alone), the low response response rates observed with TKI treatments in patients.

D. Conclusion

In this study, we showed that p53 expression is inversely correlated to *VHL* mutations severity. We attempted to characterize the effects of missense mutations specifically located in the p53 binding domain of pVHL in terms of HIF degradation, p53 signaling, and their impact on cells behavior and response to treatment. Among the missense mutations selected, we found that 2 out of the 4 mutations occurring in p53 binding domain were still able, at least partially, to downregulate HIF1/2α and therefore their downstream targets CAIX and Glut1, meaning those mutations were still able to bind both HIF and ElonginC. The 2 other missense mutations in this binding site could not downregulate HIF, most probably because of their effect on protein stability (Arg161Pro) and loss of binding to ElonginC (Cys162Arg) since the p53 and ElonginC interaction sites are overlapping. We showed that all *VHL* mutations led to lower RNA levels of *p53* and its downstream targets *p21*, *Bax* and *Noxa* compared to *VHL* wild-type both in our stable cell lines models and in tumors. We next investigated the effects of these mutations on cells behavior and found that all *VHL* mutations showed attenuated apoptosis but had no effect on proliferation. When we focused on the missense mutation location we saw that mutations affecting p53 binding domain were even more deficient in apoptosis than mutations in HIF binding domain, thus providing a growth advantage to cells with *VHL* missense mutations in p53 binding site. We treated cells with Camptothecin or Sunitinib and found that Camptothecin but not Sunitinib was capable of increasing apoptosis, and that both treatment strategies could efficiently diminish proliferation. We saw no benefit in combining both drugs compared to Camptothecin alone in our stable cell lines. The different *VHL* mutations did not seem to have on impact on the treatment response to the different treatment strategies. Finally, Camptothecin was proven more efficient than Sunitinib to lower cell growth, as it is targeting both apoptotic and proliferative pathways. Camptothecin has been investigated in preclinical and initial clinical trials

for ovarian and breast cancer, and is now studied in the context of ccRCC [44-46]. In these studies, the effects of Camptothecin on proliferation and apoptosis have been studied and the drug has been proven more efficient in the presence of pVHL and, contrary to what has been seen in our stable cell lines, it is thought to improve the efficacy of anti-angiogenic drugs. In conclusion, we saw that specific missense mutations of *VHL* lead to specific pathways deregulation, and that the use of a p53-mediated chemotherapy could be useful for ccRCC, independent of *VHL* mutations. The mechanism of chemotherapy resistance in ccRCC does not seem to depend on *VHL* mutations either and need further investigations.

E. Addendum

We attempted to investigate the interaction between pVHL and p53 by different experiments that were inconclusive. In this part are presented the results of these trials.

a. p53 reporter assay

VHL30 showed a higher p53 activity than Arg161Gln, Cys162Arg and Tyr98Asn but a lower activity than the other mutations. None of the mutant pVHLs showed a significant difference compared to pVHL wild-type (Figure 19). The several repeats of this experiments showed that the results were highly variable and hardly reproducible (the mean of 3 repetitions is shown here). To determine the p53 activity induced directly by pVHL, Babe and VHL30 were treated with a *VHL* siRNA and compared to the untreated cells (3 repetitions). Although we see a significant decrease in p53 activity upon *VHL* downregulation (50% decrease for Babe and 60% for VHL30), the global level of p53 activity is higher in Babe than in VHL30, which is not consistent with what is seen in the quantitative PCR experiment, where mutant pVHL showed lower RNA levels of p53 targets than wild-type pVHL.

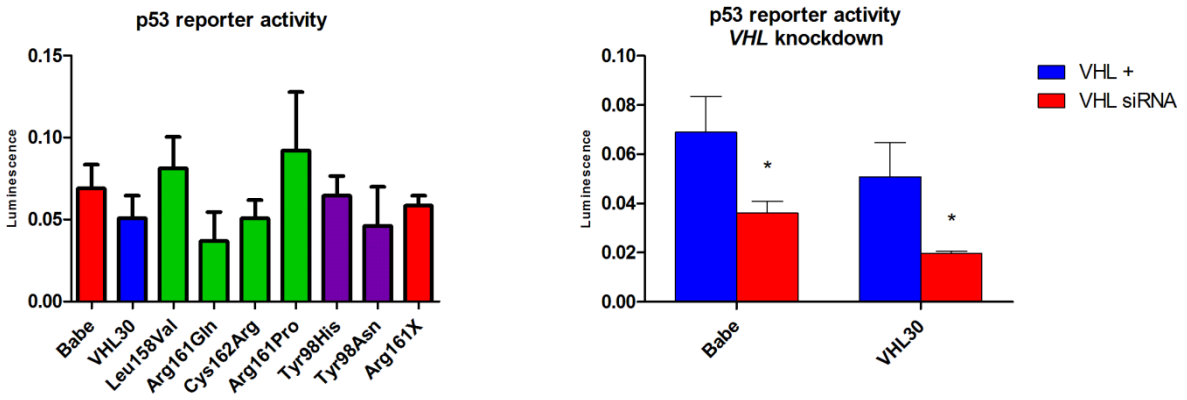

Figure 19: p53 signaling in the established cell lines and in RCC4 Babe and VHL30 upon *VHL* knockdown. P-value: *<0.05

b. pVHL pull-down and co-immunoprecipitation of ElonginC and p53

pVHL is expressed in lysates Leu158Val, Arg161Gln, Cys162Arg, Arg161Pro, Tyr98His, Tyr98Asn and Arg161X in input as well as in IP lanes. Elongin C co-immunoprecipitated with pVHL in lysates Leu158Val, Arg161Gln, Tyr98His, Tyr98Asn and Arg161Gln but not in Cys162Arg and Arg161Pro which is consistent with the level of HIF seen in Western Blot. p53 co-immunoprecipitated in lysates Babe, Leu158Val, Arg161Gln, Cys162Arg, Arg161Pro, Tyr98Asn and Arg161X (Figure 20). Unfortunately, the VHL30 lysate that is supposed to be the positive control of this experiment had lost *VHL* plasmid expression and cannot be used as reference since pVHL is not seen even in VHL30 input, as it has been verified by PCR amplification of the vector (Figure 21).

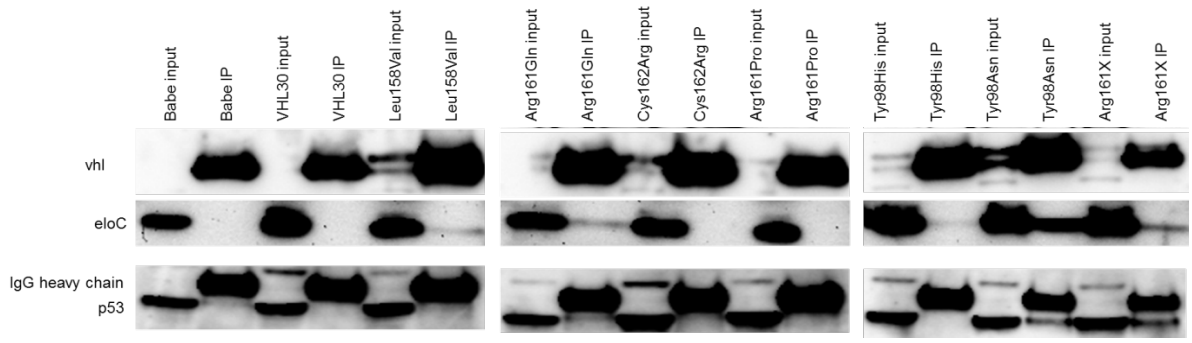

Figure 20: Different pVHL forms binding ability to p53 and EloC

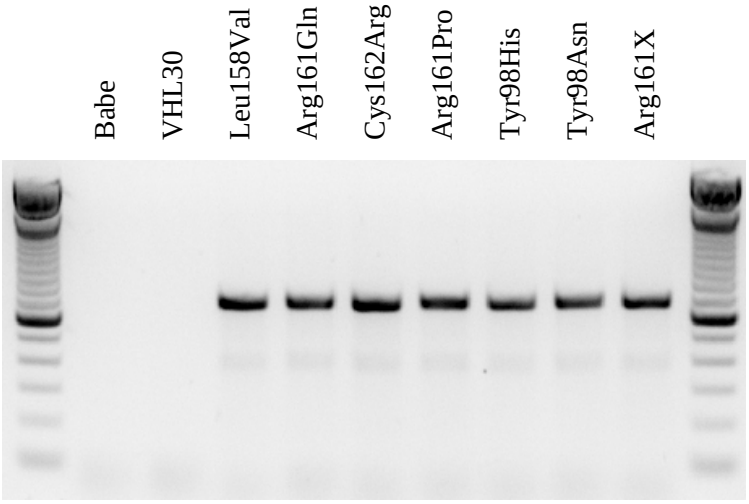

Figure 21: Gel electrophoresis of PCR amplification of stable cell lines DNA using a forward primer in the vector backbone and a reverse primer in *VHL*.

This experiment has been carried out several times with different amounts of total protein for co-immunoprecipitation and with a proper VHL30 lysate but this result could not be exactly reproduced.

c. Surface Plasmon Resonance (SPR)

Preliminary results of the assay showed a binding of 32 Refraction Units (Figure 22) but this result could not be reproduced after several trials and no binding was seen between pVHL and HIF1α. Several artefacts might indicate that the proteins were too fast degraded and that they were not adequately folded.

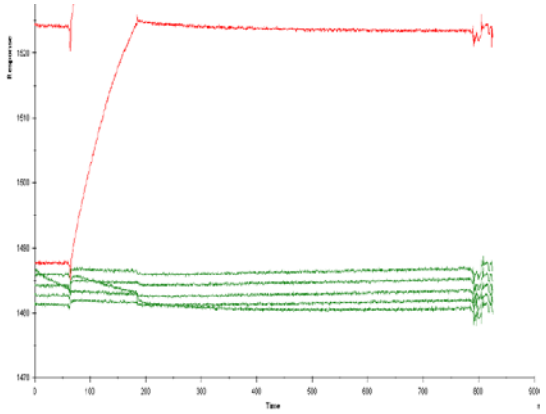

Figure 22: SPR measurement of p53 binding to pVHL. In green: Startup assays, running buffer is injected. In red: 100nM p53 in running buffer is injected. pVHL has been immobilized on the surface (200 RU). P53 binds pVHL WT (32 RU)

d. Mammalian two-hybrid assay

Although the positive control for the assay (mouse-p53 + SV40 T antigen) showed a high increase of the signal, the co-transfection of pVHL and ElonginC or p53 showed no increase in the luciferase activity (Figure 23). Cloning ElonginC and p53 in pCF2 and *VHL* in pCF1 and co-transfecting ElonginB to stabilize pVHL could not solve this issue.

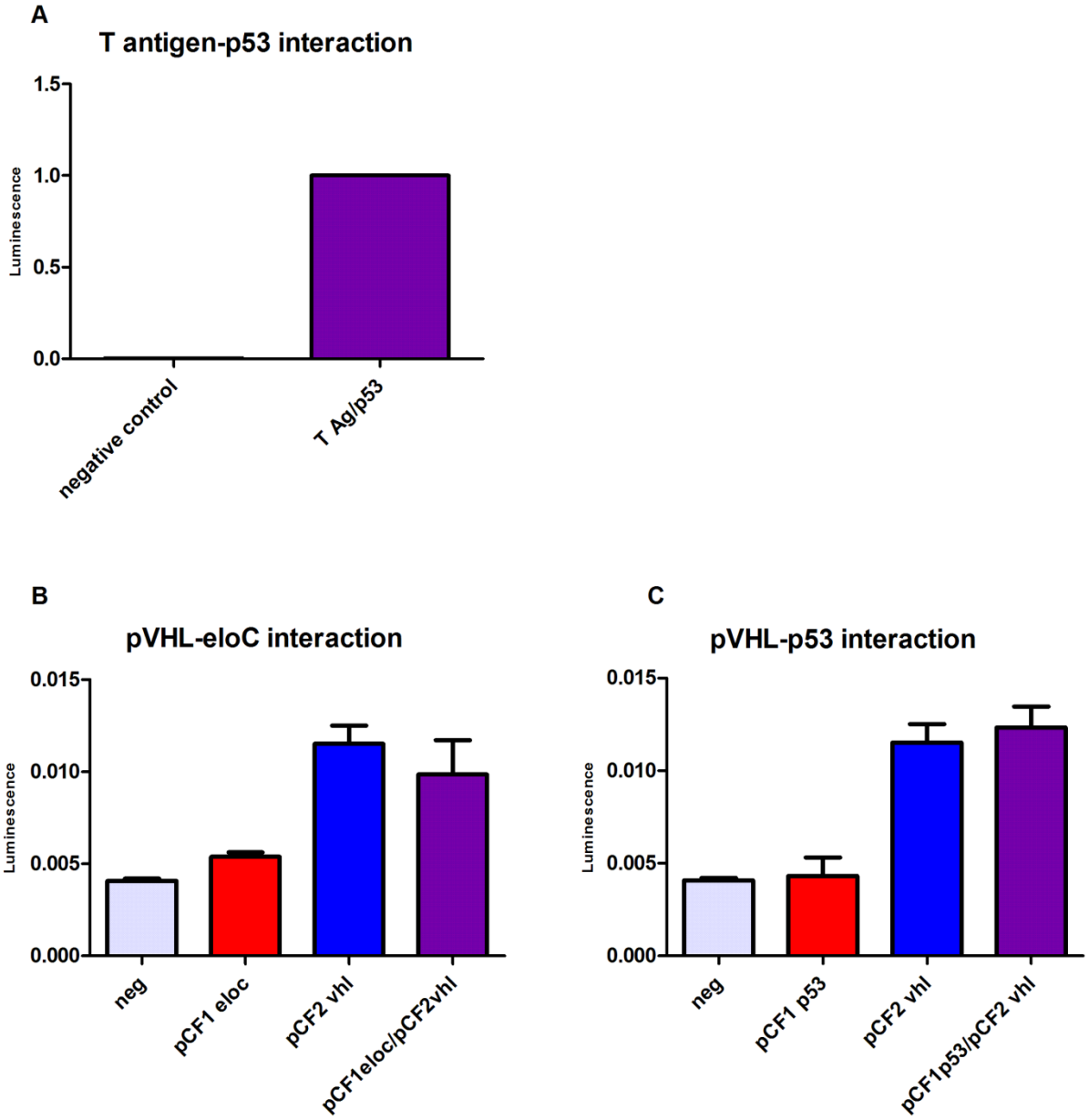

Figure 23: Luminescence signal from mammalian double-hybrid assay for pVHL-p53/EloC interaction

V. Comprehensive investigation of the mutational landscape in clear cell Renal Cell Carcinoma and its correlation to treatment response

Despite the obvious importance of *VHL* alteration in ccRCC development, this gene alone cannot entirely explain tumorigenesis. Several other genes, notably involved in chromatin remodeling, were recently found to be frequently mutated in ccRCC as well. Since *VHL* mutations alone do not clearly correlate with treatment outcome, we used NGS on a cohort of 30 patients treated with anti-angiogenic drugs to search for a possible relation between other genes alterations and therapy response.

A. Abstract

Introduction: Sporadic renal cell carcinoma (RCC) is divided into different subtypes from which clear cell Renal Cell Carcinoma (ccRCC) is the most frequent and aggressive form. Formation of ccRCC is thought to be closely connected to the functional loss of the von Hippel-Lindau (*VHL*) tumor suppressor gene which is mutated in up to 70% of the cases. Data of recent studies indicate that the loss of pVHL function may be not sufficient to cause ccRCC. In addition, several other genes, such as *PBRM1*, *SETD2* and *BAP1*, have recently been found mutated in ccRCC as well. We hypothesized that mutational patterns specific for the clear cell tumor subtype exist, which may have impact on the patients' response to therapy.

Methods: In this study, we used the IonTorrent technology using the Ion Proton instrument and the Ion AmpliSeq™ Comprehensive Cancer Panel. The experiment was conducted on 30 ccRCC samples and focused first on 18 RCC-related genes including *VHL*, *SETD2*, *PBRM1*, *MTOR*, *PDGFRA*, *TSC1*, *PIK3CA*, *BAP1*, *CARD11*, *PDGFRB*, *KDM5C*, *KDM6A*, *EGFR*, *TP53*, *HIF1A*, *NF-κB*, *PTEN*, and *PDGFB*. The ccRCC patients were treated with Tyrosine Kinase Inhibitors,

mTOR inhibitors or immunotherapy after surgery. 18 patients presented with progressive disease, nine had stable disease and six had regressive disease. Sequencing data were analyzed using the Ion Reporter variant caller, CLC genomics workbench and the Integrative Genomics Viewer visualization tool. Total variants found were filtered based on two criteria, a coverage higher than 30 reads and an allele ratio higher than 5%.

Results: All tumors showed at least one variant in one of the selected genes. The genes with the highest mutation rates were *VHL* (83%: 25/30), *PBRM1* and *SETD2* (60%: 18/30), *MTOR* (50%: 15/30) and *PDGFRA* (37%: 11/30). We are currently investigating the impact of the variants on the treatment response and extend the sequence analysis in more detail to all 400 genes with the support of bioinformaticians.

Conclusion: Deciphering individual gene mutation maps may give rise to the pathways being altered in ccRCC, thus revealing new therapeutic options.

B. Results

a. Patients

Sanger sequencing of 30 patietns revealed 5 wild-type and 25 with *VHL* mutations (83%). In-frame, frameshift deletions and insertions were found in 13 patients (43%), nonsense mutations in 4 patients (13%), splice site mutations in 2 patients (7%) and missense mutations in 7 patients (23%). One patient had two mutations, one nonsense and one missense. The details of the clinical data, *VHL* mutation status determined by Sanger sequencing, treatments and responses are shown in Table 10. An overview of the patients' survival, stage and grade of the tumor is presented in Figure 24.

Table 10: Treatment, response, and *VHL* mutation status of the patients treated with anti-angiogenic therapies.

Patient's ID	*VHL* mutation	Mutation consequence	Disease progression status	Treatment	pT stage	Fuhrman grade
75	c.163delG/p.Glu55ArgfsX11	frameshift	PD	Votrient>Afinitor	3	3
42	c172delC/p.Arg58GlyfsX9	frameshift	PD	IFNa>Votrient		
16	c.194C>T/p.Ser65Leu	missense	PD	Sutent		
19	c.240T>A/p.Ser80Arg	missense	PD	IFNa>Sorafenib	1	
40	c. 262T>A/p.Trp88Arg	missense	PD	Sutent	3	3
14	c.268_273del/p.Asn90_Phe91del	in frame	PD	Sutent		3
6	c.IVS1+1G>A (c.340+1G>A)	splice mut	PD	Nexavar>Sutent>Afinitor		
5	c.345_364del/p.Leu116ArgfsX9	frameshift	PD	IFNa>Nexavar		
13	c.349delT/p.Trp117GlyfsX42	frameshift	PD	Sutent	3	3
8	c.484T>C/p.Cys162Arg	missense	PD	Sutent>Nexavar>Afinitor>Votrient	3	3
71	c.497_505del9/p.Arg167ValdelSerLeu	in frame	PD	Sutent	3	3
15	C.580_583delinsAA/p.Val194LysfsX61	frameshift	PD	Sutent>Nexavar		
3	c.586A>T/p.Lys196X	nonsense	PD	Sutent>Nexavar>Afinitor>Everolimus	1	
34		wild-type	PD	Votrient	3	4
61		wild-type	PD	Sutent>Votrient>Nexavar>Afinitor	4	3
69		wild-type	PD	Sutent	2	3
17	c.161_162delTG/p.Met54ArgfsX77	frameshift	SD	Sutent	3	4
74	c.203C>A/p.Ser68X	nonsense	SD	Nexavar/Gemzar/Xeloda>Votrient> Everolimus	3	4
7	c.327insA/p.His110ProfsX22	frameshift	SD	Sutent>Nexavar	1	4
70	c.IVS1+2T>A (c.340+2T>A)	splice mut	SD	Votrient>Axitinib	3	3
48	c.345insC/p.Leu116ProfsX15	frameshift	SD	Avastin>IFNa>Votrient	3	4
35	c. 350delG/p.Trp117CysfsX42	frameshift	SD	IFNa/Avastin	1	3
1	c.481C>T/p.Arg161X	nonsense	SD	Nexavar	2	2
12		wild-type	SD	Sutent>Nexavar>Afinitor		
4	c.167_168delCC/p.Ala56GlyfsX75	frameshift	RD	Nexavar	3	1
72	c.227_229del3/p.Phe76del	in frame	RD	Votrient>Sutent	1	3
39	c.340G>T/p.Gly114Cys	missense	RD	IFNa>Bevacizumab	2	3
76	*c.383T>C/p.Leu128Pro* *	*missense*	*RD*	*Votrient*	*3*	*4*
76	*c.430G>T/p.Gly144X* *	*nonsense*	*RD*	*Votrient*	*3*	*4*
11	c.458T>C/p.Leu153Pro	missense	RD	Sutent	2	3
73		wild-type	RD	Votrient>Afinitor	3	3

PD: progressive disease; SD: Stable disease; RD: Regressive disease

* one patient with two mutations

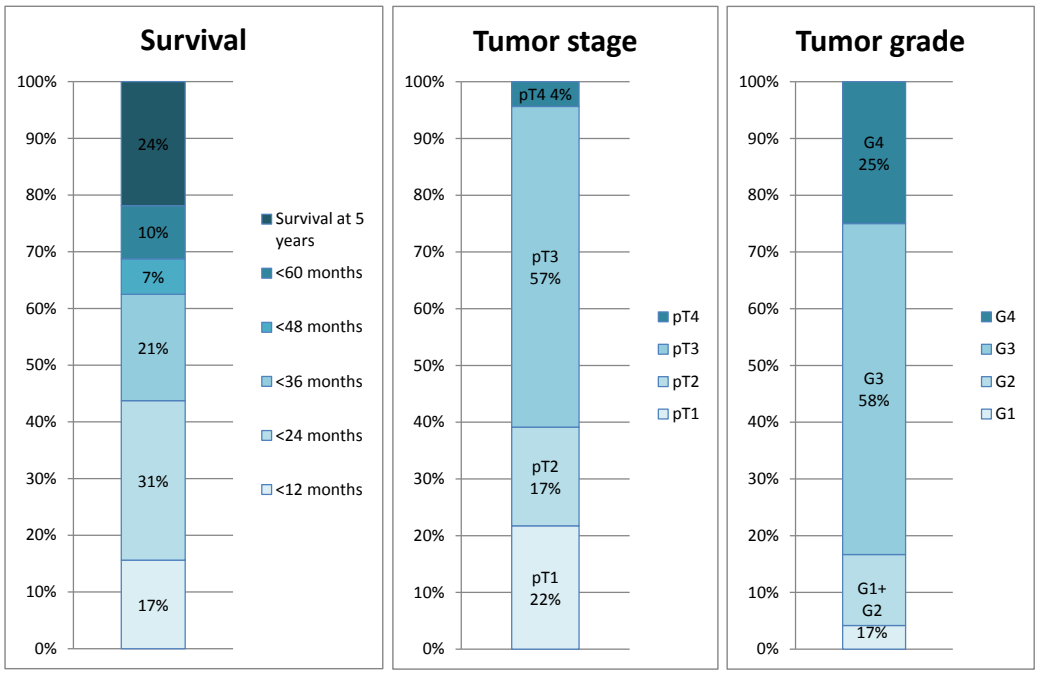

Figure 24: Clinical data overview of the cohort. Survival is unknown for 1 patient; tumor stage/grade is unknown for 7 patients.

b. Libraries

Between 11 and 2384 pM of library DNA was obtained. As an example, the Bioanalyzer results showing the concentration of 4 libraries evaluated by real-time quantitative PCR and the Sanger sequencing result for patient ID #6 are shown in Figure 25.

A

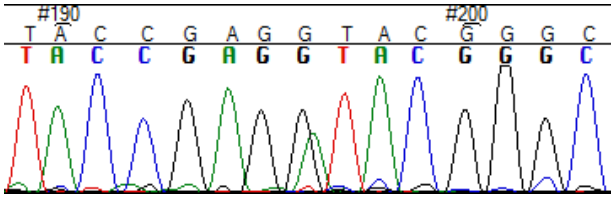

VHL Sanger sequencing:
c.IVS1+1G>A/c.340+1G>A

B

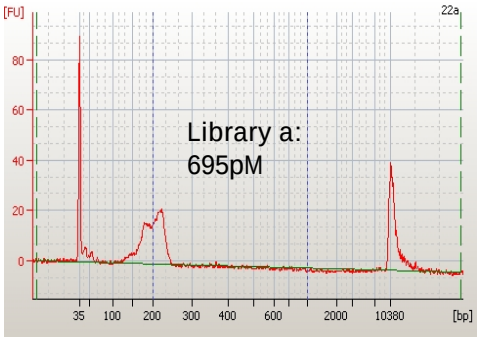

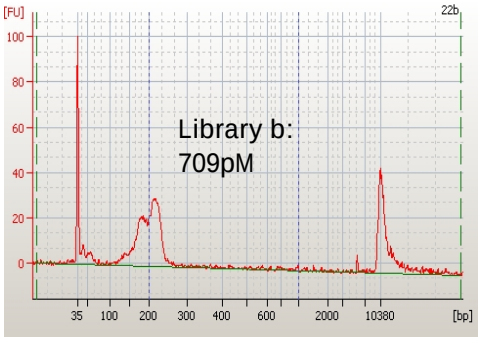

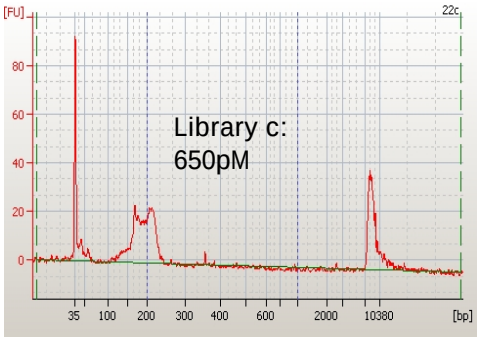

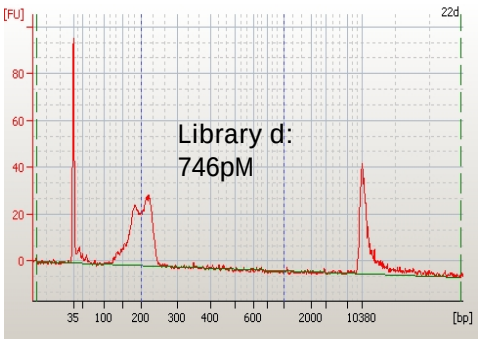

Figure 25: Patient ID #6 example, A: Sanger sequencing mutation analysis, B: Bioanalyzer and qPCR results of the 4 libraries

c. Runs summary

The sequencing of the 30 patients was performed in two runs of 15 patients each.

The two runs produced about 80 million reads, more than 85% of the wells were loaded and in total more than 60% of the reads were usable for analysis. The average “on target” reads was 98% and the average depth was 275 for both runs. The mean reading length of the amplicons was about 110bp. The summary of the runs is shown in Figure 26.

1st run: patients ID #1-19

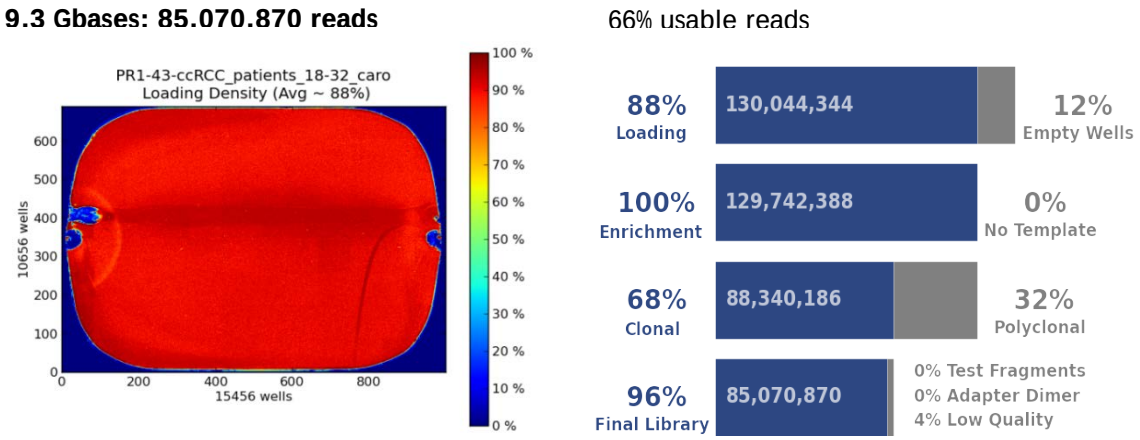

2nd run: patients ID #34-76

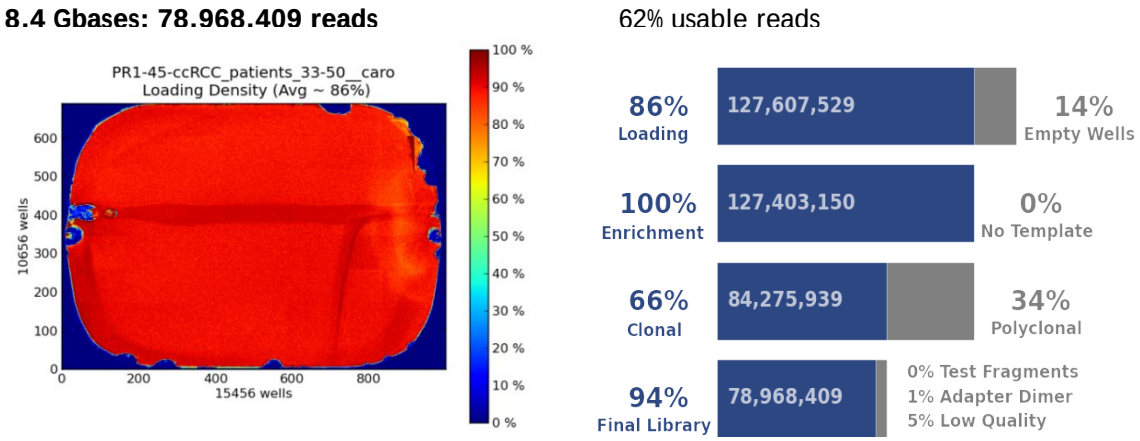

Figure 26: Runs summary

d. Variants in the selected genes

We first focused on a set of 18 genes known to play a critical role in ccRCC and classified regarding their major functions (Table 11). *VHL*, *PBRM1*, *SETD2*, *BAP1*, *TSC1*, *PTEN* and *TP53* are additionally qualified as tumor suppressor genes.

Table 11: Genes selection function/pathway

Genes	**Function/pathway**
VHL and *BAP1*	ubiquitination processes
PBRM1, *SETD2*, *KDM5C*, and *KDM6A*	chromatin remodeling
TSC1, *MTOR*, *EGFR*, *PTEN* and *PIK3CA*	cell growth
TP53, *CARD11* and *NF-κB*	apoptosis
HIF1a, *PDGFRA* and *PDGF(R)B*	angiogenesis

Fifteen of 25 (60%) *VHL* mutations that were identified by Sanger sequencing were also called by Ion Reporter with our filter criteria. After visual inspection of the reads using IGV, additional 6 *VHL* variants were confirmed. Those 6 variants were verified with variant caller CLC Workbench. The mutation sites of the 4 remaining "wild type" samples were not or too low covered by deep sequencing because no or only few reads were available at those positions. In total 21 of 25 (84%) of the *VHL* mutations detected by Sanger sequencing were confirmed by NGS. Patient ID #12 showed a *VHL* missense mutation (c.162G>A/p.Met54Ile) by NGS that was not found by Sanger sequencing. For the analysis, the four *VHL* mutations revealed by Sanger sequencing but not by NGS were included and the additional mutation in patient ID #12 detected only by NGS was neglected. The data of variant calling by Ion reporter and CLC, visual inspection of the reads by IGV and Sanger sequencing is summarized in Table 12.

Table 12: Summary of variant calling by Ion reporter and CLC, visual inspection of the reads by IGV and Sanger sequencing

Barcode	Patient's ID	Ion reporter variant calling	CLC variant calling	IGV visual inspection (allele ratio, total count of reads)	Sanger sequencing	Considered as	Comment	NGS in contradiction with Sanger
18	1	1		1 (0.46)	c.481C>T/p.Arg161X	Mutant		
19	3		1	1 (0.38)	c.586A>T/p.Lys196X	Mutant		
20	4	1		1 (0.06)	c.167_168delCC/p.Ala56GlyfsX75	Mutant		
21	5	1		1 (0.36)	c.345_364del/p.Leu116ArgfsX9	Mutant		
22	6	1		1 (0.34)	c.IVS1+1G>A (c.340+1G>A)	Mutant		
23	7	1		1 (0.31)	c.327insA/p.His110ProfsX22	Mutant		
24	8	1		1 (0.19)	c.484T>C/p.Cys162Arg	Mutant		
25	11	1		1 (0.40)	c.458T>C/p.Leu153Pro	Mutant		
26	12	1	1	1 (0.07, 30 reads) c.162G>A/p.Met54Ile	WT	WT	Low coverage in Sanger	False positive
27	13	1		1 (0.15)	c.349delT/p.Trp117GlyfsX42	Mutant		
28	14	0	0	0 (low coverage, 19 reads)	c.268_273del/p.Asn90_Phe91del	Mutant	Low coverage in NGS	False negative
29	15	0	1	1 (0.34, 341 reads)	c.580_583delinsAA/p.Val194LysfsX61	Mutant	No call by Ion reporter, called by CLC	
30	16	0	1	1 (0.06, 17 reads)	c.194C>T/p.Ser65Leu	Mutant	No call by Ion reporter, called by CLC	
31	17	0	1	1 (0.42, 12 reads)	c.161_162delTG/p.Met54ArgfsX77	Mutant	No call by Ion reporter, called by CLC	
32	19	0	0	0 (not covered)	c.240T>A/p.Ser80Arg	Mutant	No read in NGS	
33	34	0			WT	WT		
34	35	1		1 (0.24)	c. 350delG/p.Trp117CysfsX42	Mutant		
35	39	1		1 (0.40)	c.340G>T/p.Gly114Cys	Mutant		
36	40	0	0	0 (not covered)	c. 262T>A/p.Trp88Arg	Mutant	No read in NGS	
37	42	0	1	1 (0.22, 18 reads)	c172delC/p.Arg58GlyfsX9	Mutant	No call by Ion reporter, called by CLC	
38	48	0	1	1 (0.13, 216 reads)	c.345insC/p.Leu116ProfsX15	Mutant	No call by Ion reporter, called by CLC	
42	61	0			WT	WT		
43	69	0			WT	WT		
44	70	1		1 (0.15)	c.340+2T>A;c.IVS+2T>A/p.?	Mutant		
45	71	1		1 (0.43)	c.497_505del9/p.Arg167ValdelSerLeu	Mutant		
46	72	0	0	0 (low coverage, 1 read)	c.227_229del3/p.Phe76del	Mutant	Low coverage in NGS	False negative
47	73	0			WT	WT		
48	74	1		1 (0.38)	c.203C>A/p.Ser68X	Mutant		
10(#49)	75	0	1	1 (0.68, 22 reads)	c.163delG/p.Glu55ArgfsX11	Mutant	No call by Ion reporter, called by CLC	
11(#50)	76	1		1 (0.04) 1(0.42)	c.383T>C/p.Leu128Pro;c.430G>T/p.Gly144X	Mutant		

1: variant present; 0: no variant reported

The total number of variants obtained from the 30 patients with our filter criteria was 412 among all genes. The number of variants per patient ranged from 171 (patient ID 1#) to 2 (patients ID #12, 16, 40, 61). The number of variants per patient is shown in Figure 27A. The genes with the highest mutation rates were *VHL* (83%: 25/30), *PBRM1* and *SETD2* (60%: 18/30), *MTOR* (50%: 15/30) and *PDGFRA* (37%: 11/30) (Figure 27B).

A

	Progressive disease															Stable disease									Regressive disease					
Patient	69	19	5	13	14	15	6	34	42	71	3	8	75	16	40	61	1	7	35	48	74	17	70	12	4	72	11	76	73	39
Total	16	27	9	4	4	5	4	5	8	4	5	3	3	8	2	3	171	5	6	6	5	5	3	3	64	11	7	7	6	3

B

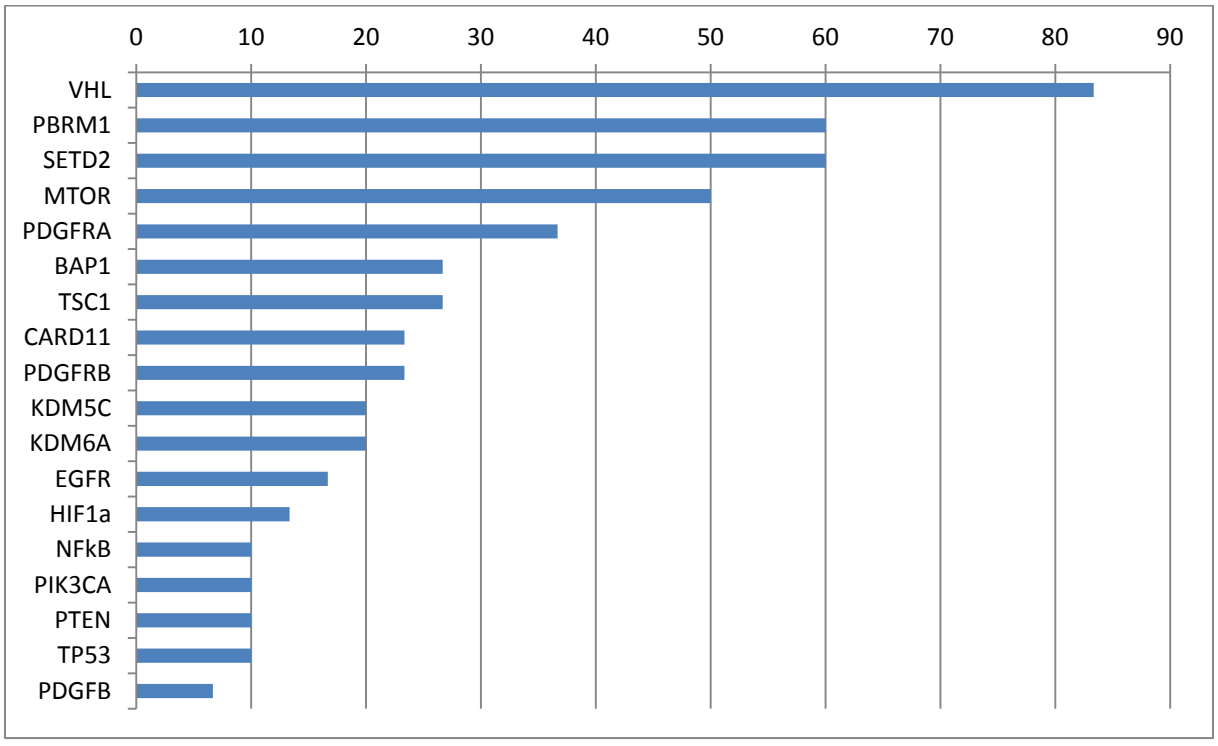

Figure 27: A: Total number of variants per patient in the 409 genes. B: Mutation rate in our selection of 18 genes.

Notably, all patients had a mutation in at least one of the selected genes. Patient ID #6 as an example had a mutation in *VHL* and in *SETD2*, *PBRM1* and *KDM5C*. A heat map showing the strongest impact variants of the 18 selected genes in each patient is shown in Figure 28. A patient with multiple mutations in the same gene will show only the mutation with the worse effect in the heat map. Tumor suppressor genes were mostly affected in 54% of patients showing variants in *VHL*, *BAP1*, *PTEN*, *PBRM1*, *SETD2*, *TSC1* and *TP53*. The mutation types were mainly missense mutations (101, 67.8%) followed by insertion-deletions (23, 15.1%), and nonsense or stop-loss (28, 18.4%) mutations. Notably, 95% (20/21) of the insertion-deletions-splice mutations occurred in the tumor suppressor genes *VHL*, *PBRM1*, *SETD2* and *BAP1*. The other genes were mostly affected by missense mutations.

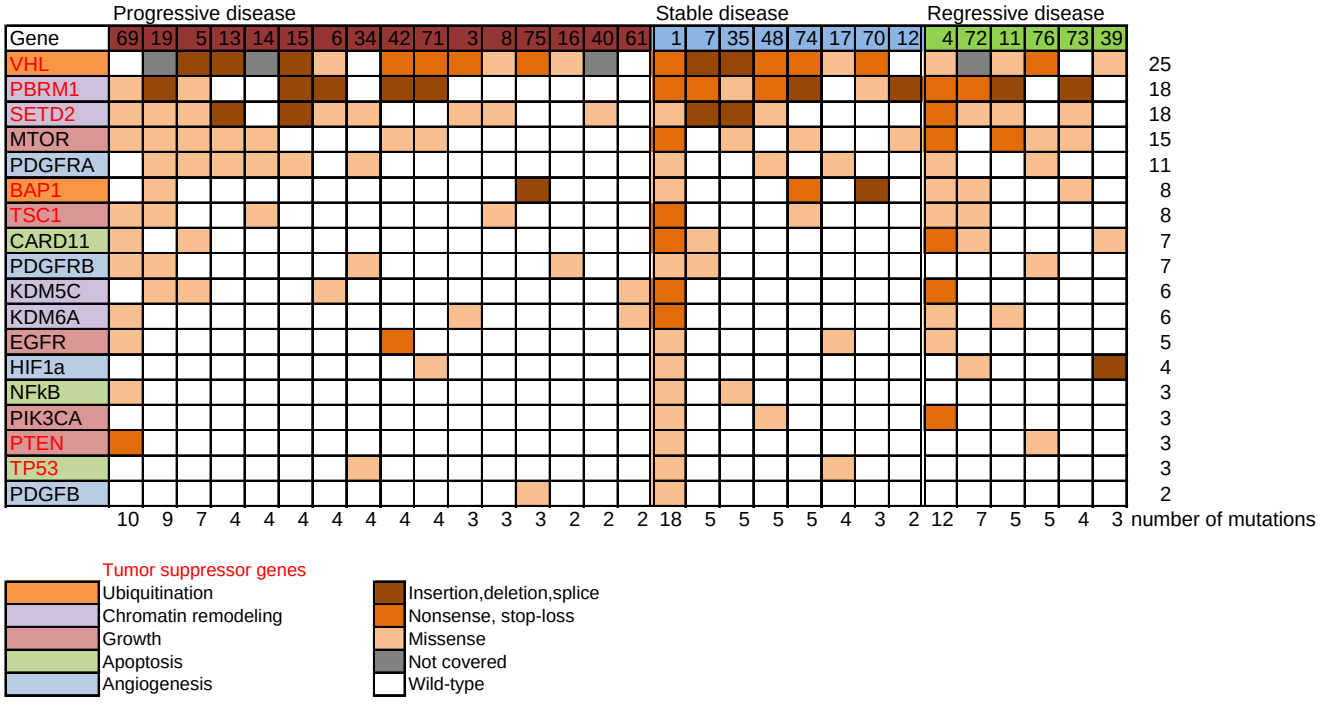

Figure 28: Heat map of the filtered in variants in the 18 selected genes.

The genes involved in chromatin remodeling were mutated in 31.6% of the patients, followed by cell growth regulating genes (22.3%), ubiquitination processes (21.7%), angiogenesis (15.8%) and apoptosis (8.6%). The frequencies of mutations in the genes grouped by the function/pathway are shown in Figure 29.

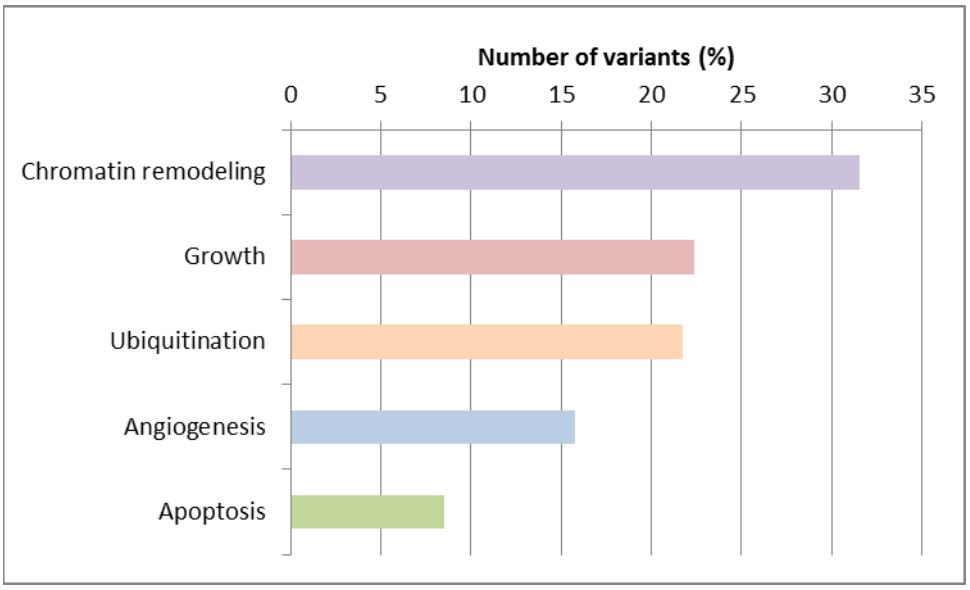

Figure 29: Proportion of variants in the 18 selected genes by their related function or pathway.

e. Mutation spectrum and treatment response

Patients have been classified in two groups, non-responders (progressive disease) and responders (including stable and regressive disease). The proportion of mutant for the combined 18 genes is significantly different in these two groups (p-value=0.0217). Patients with regressive disease had significantly more mutations than patients with progressive disease (Figure 30A). The mutation frequency of each of the selected genes in those two groups is illustrated in Figure 30B. Interestingly, *PBRM1*, *BAP1*, *CARD11* and *HIF1α* were more mutated in the responder group than in patients with progressive disease (79%, 43%, 36%, and 21% of the responder cases versus 44%, 13%, 13%, and 6.3% in the non-responder group). Additionally, *PIK3CA* was found

mutated in 3 stable or regressive tumors but in none of the progressive disease. The proportion of variants in each response group by pathway affected did not show any significant difference between the two groups (Figure 30C).

A

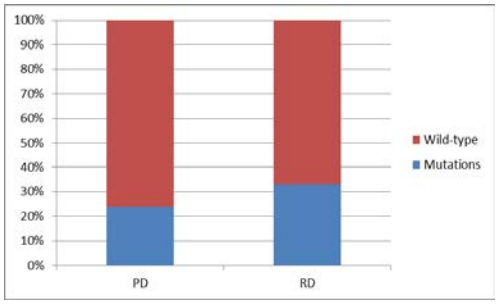

C

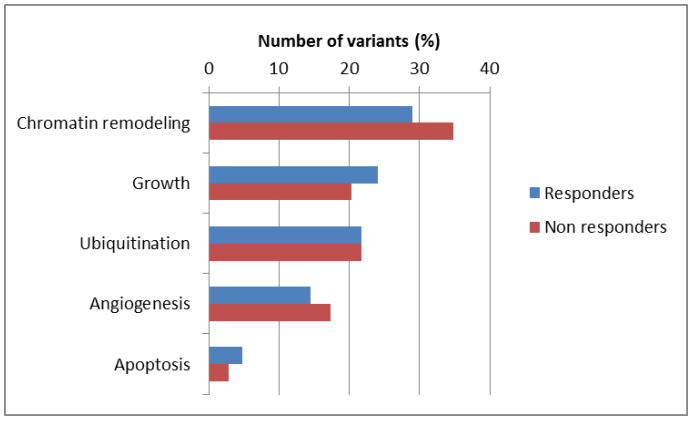

B

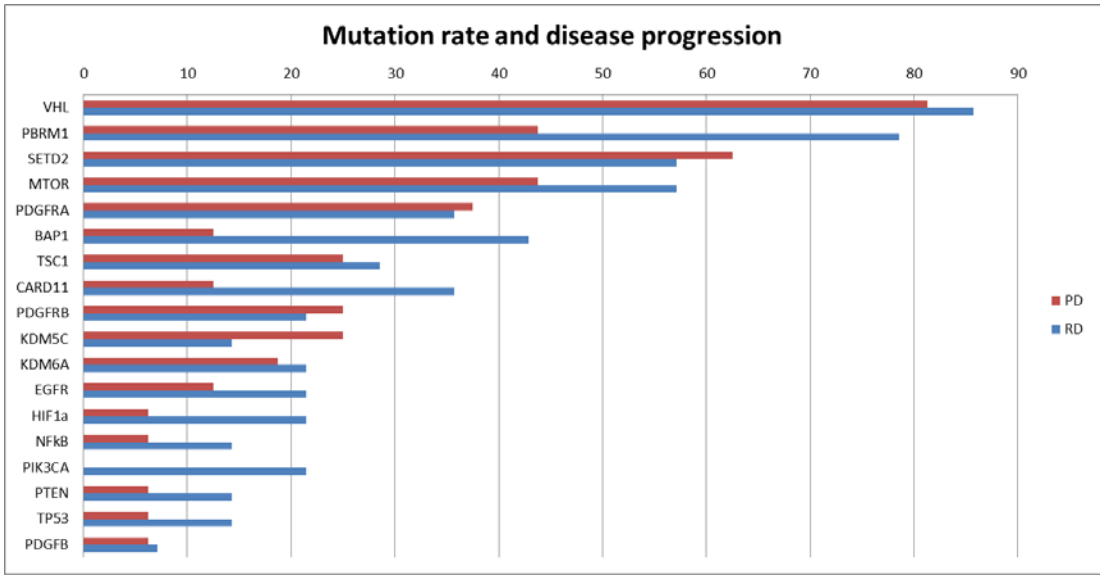

Figure 30: A: Proportion of wild-type and mutations for our selection of genes in the two groups of treatment response. B: Mutation rate for each gene in the two patient outcomes groups. C: Proportion of variants in each response group by pathway affected

C. Discussion

In this study, we investigated more than 400 cancer-related genes using NGS and associated identified gene alterations and variant clusters with targeted treatment outcomes. We found that *VHL*, *PBRM1* and *SETD2* were the most often mutated genes in our mccRCC cohort, and that they also present the vast majority of insertions, deletions and nonsense mutations, thus being the most severely affected genes. We also found that patients responding to anti-angiogenic therapies presented significantly more variants than non-responders, especially in the genes *PBRM1*, *BAP1*, *CARD11* and *HIF1α.*

In total for *VHL* sequencing, we found one false positive (3%), two false negative (7%),two variants were not covered (7%) and 6 variants that were not called by Ion reporter but that were called by CLC (20%). This can be explained by the fact that these two variant callers have their own algorithms and some variants can then be eliminated by one but not by the other along the pipeline, thus not be reported. Altogether, 83% of the Sanger sequencing results matched the NGS results. The systematic use of two different variant callers and the loading of fewer samples per run to increase coverage could improve the global performance of variant calling. Patient #12 presented a *VHL* mutation in NGS which was not found by Sanger sequencing. This could be explained by the low allele ratio (7%) reported by Ion reporter variant caller and the low coverage in our Sanger sequencing mutation analysis. Additionally, the location of this missense mutation close to the annealing site of the Sanger sequencing primer may interfere with the resulting sequence. As Sanger sequencing is still considered as the gold standard for diagnostic mutation analysis, the wild-type sequence has been retained and this mutation has been considered as a false positive.

Each patient presented with at least one variant in one of the 18 selected genes, ranging from 2 to 18 per patient, but the number of mutations alone could not discriminate between the two

response response groups. The highest rates of mutations and the most severe impacts (insertions, nonsense) were observed in *VHL* (83%), *PBRM1* and *SETD2* (each 60%). These results confirm recently published results and support the "river model" (Wei et al. [108]) that describe ccRCC development with *VHL* being the first gene altered in ccRCC initiation, followed by secondary and tertiary events affecting *PBRM1* or *SETD2*. Following their guideline, would then appear a "window of opportunity" for treatment where the hallmarks of cancer are already present and after which additional mutations in others genes could be responsible for resistance. *MTOR* and *PDGFRA* were in the top 5 mutated genes with 50% and 37% respectively. Those genes have already been described as highly mutated in ccRCC although the rates were found higher than in previous studies [97-102, 105, 106]. This discrepancy can be explained by the use of NGS that allows detection of variants between 5% and 15% allele ratio, which is the average detection limit of Sanger sequencing. The total number of variants called by Ion Reporter in our selection of 18 genes was 384 with an allele ratio >5% and 70 with a >15% allele ratio. *BAP1* reached a 25% mutation rate, which is higher than the reported frequency of 15% [97, 103, 104]. Interestingly, the occurrences of variants were very similar to what has been recently reported by Ho et al. in a deep-sequencing study in which also TKI-treated mccRCC were analyzed (i.e. *VHL*: 71% vs 83% in our data set, *PBRM1*: 48.4% vs 60%, *TSC1*: 29% vs 27%, *KDM5C*: 16.1% vs 20%) [131]. More than 85% of the ccRCC cases were mutated in at least one those genes and only 4 patients were wild-type for *PBRM1*, *SETD2*, *MTOR* and *PDGFRA*, which may represent attractive candidates for targeted treatments. The insertions, deletions and nonsense mutations are mostly found in the tumor suppressor genes *VHL*, *PBRM1*, *SETD2* and *BAP1* (95% (20/21)), which could reflect their importance in ccRCC development. Particularly, *PBRM1* and *BAP1* presented a high rate of mutations with severe consequences (50% and 25% of insertions/deletions/splice mutations respectively) which confirmed previous observations where

high frequencies of truncating mutations were reported in those genes [100, 103]. Current therapies repressing VEGF, PDGF and MTOR exist, but treatments tailored to enhance or rescue the tumor suppressor functions of *VHL*, *PBRM1*, *SETD2* and *BAP1* remain challenging to design. A possible therapeutic strategy could be to target directly effector proteins when their genes are altered, and to target the proteins which are in the downstream signaling of affected tumor suppressor genes.

More than half of the mutations affected the tumor suppressor genes *VHL*, *PBRM1*, *SETD2*, *BAP1*, *TSC1*, *PTEN* and *TP53*. Given the potential pleiotropic regulatory effects of tumor suppressors, many different oncogenic processes may be touched by those variants. Regarding the pathways possibly affected and activated by those gene alterations, chromatin remodeling, cell growth and ubiquitination rather than angiogenesis were involved.

In general responders were significantly more frequently mutated than non-responders as a responder shows in average 5,9 mutations and non-responders 4,3 in our selected genes.

Notably, *PBRM1*, *BAP1*, *CARD11* and *HIF1α* were more affected in patients of the responder group. This result confirms recent studies suggesting an association between *PBRM1* mutations and anti-VEGF therapy response, as those alterations were correlating with a longer progression-free survival [132] or a prolonged duration of treatment [131]. Interestingly, mutations in *PIK3CA* were only present in three responder patients but in none of the non-responders. This gene is mutated in 2 to 5% of ccRCC cases [106, 133]. Its alteration is known to be linked to anti-EGFR therapy resistance in breast cancer, but was not found predictive for bevacizumab effect in colorectal cancer [134, 135]. *PIK3CA* implications in ccRCC growth and angiogenesis could be interesting features to study in the context of VEGF-targeted therapies. Indeed, PIK3CA expression has been shown to correlate with the expression of VEGF in ovarian cancer, and its

inhibition led to the downregulation of HIF1α and VEGF [136]. In this context, mutations in *PIK3CA* could attenuate expression of VEGF in ccRCC cells, thus acting synergistically with the anti-angiogenic therapies, leading to a better response.

D. Conclusion

In conclusion, we found that *VHL*, *PBRM1*, *SETD2*, *MTOR* and *PDGFRA* were the most frequently altered genes in our cohort of ccRCC patients. *VHL*, *PBRM1* and *SETD2* were as well the most severely affected in terms of mutation impact on the protein. The pathways that were the most hit by mutations were chromatin remodeling, growth and ubiquitination before angiogenesis that came at the fourth rank but yet is the preferential pathway targeted nowadays in clinics. We also found that responder patients were presenting in general more variants than non-responders and especially for the genes *PBRM1*, *BAP1*, *CARD11* and *HIF1α*.

E. Addendum

Seventeen RCC cell lines were investigated by NGS using the same filter criteria as for the patients. Twelve cell lines are derived from ccRCC, 3 from adenocarcinoma with no other specification, and 2 are derived from normal kidney tissue, adult and embryonic (HK-2 and Hek293 respectively). In total, 63 variants were found among the 18 genes of interest selected. *VHL* mutations known by Sanger sequencing were found for 7 cell lines, 2 mutations were not covered by the NGS, and 2 others were not called by Ion Reporter but found in the reads after visual inspection with IGV and correctly called by CLC with a coverage below 30 but mutations found in all the reads (allele ratio = 1). The 6 wild-type cell lines were assessed correctly by Ion reporter. The top 5 genes mutated in the cell lines were *VHL* (11/17), *SETD2* (7/17), *BAP1*, *PBRM1*and *MTOR* (5/17). The mutation rates for each gene are shown in Figure 31 and the

corresponding heat map in Figure 32. The two normal kidney cell lines reported only one variant each, in *SETD2*.

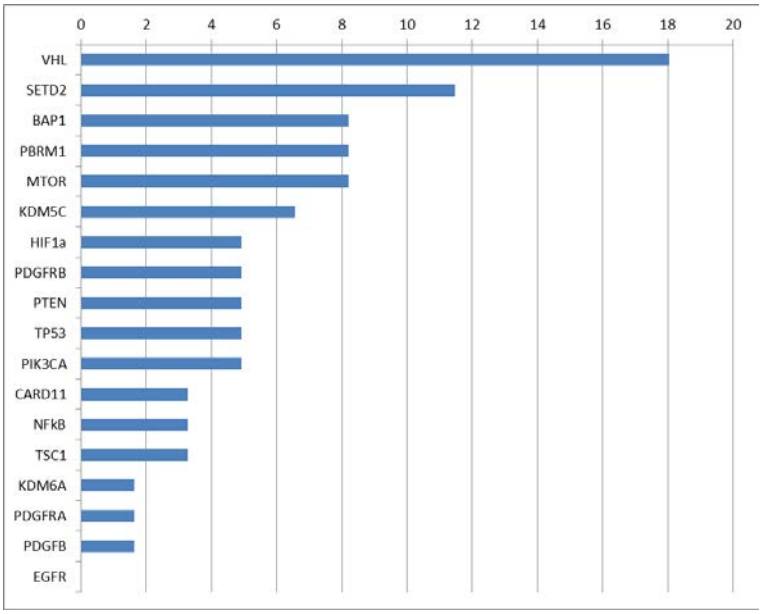

Figure 31: Mutation rates of the selected genes in RCC cell lines

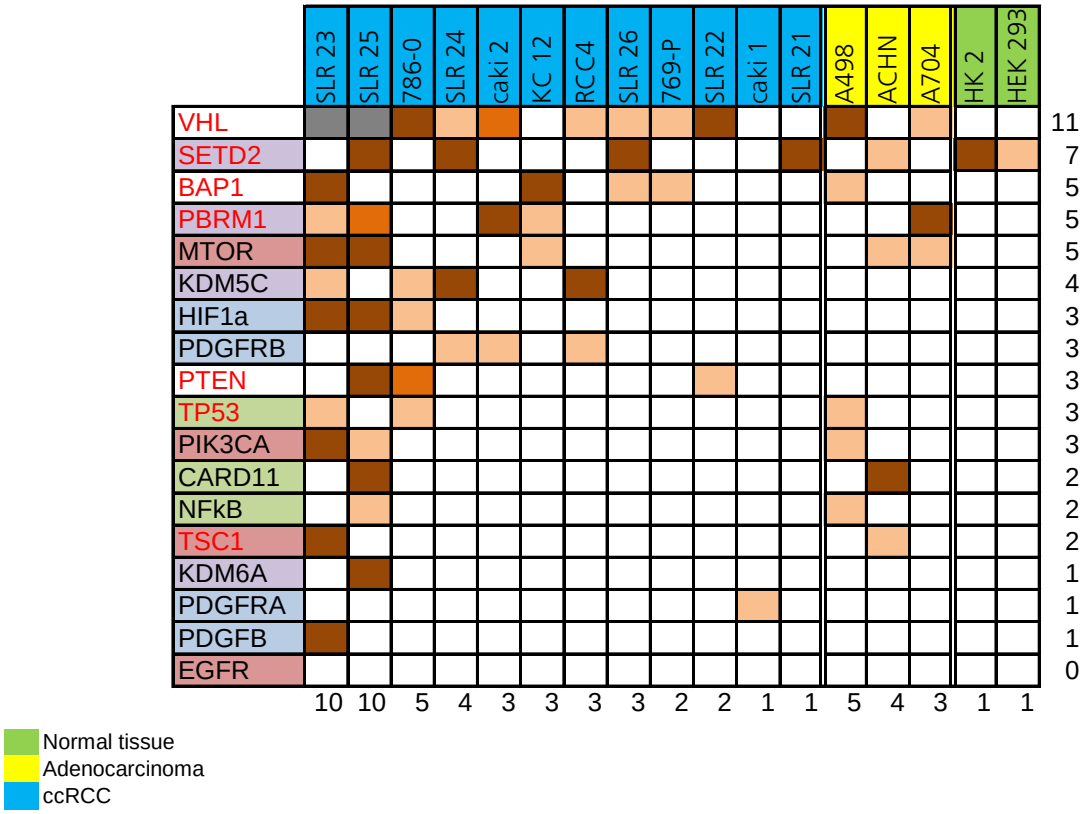

Figure 32: Heat map of the selected genes in RCC cell lines

VI. Conclusion

In this study, we could show that *VHL* missense mutations can specifically affect single binding domains of pVHL, in contrast to *VHL* loss-of-function mutations which highly likely abrogate all multifunctional properties. We observed that especially missense mutations located in the p53 binding domain influence negatively the p53 signaling pathway and attenuate apoptosis. Cell behavior after treatment with Camptothecin or Sunitinib indicates that p53 activator drugs alone or in combination with current anti-proliferative TKIs may optimize ccRCC treatment. As there was no association of *VHL* mutation type and response to treatment in ccRCC patients, the identification and analysis of mutations in additional driver genes, their combinatorial pattern in individual ccRCC and their relation to response/non response is of utmost importance.

VII. Material and Methods

A. Patients and tissue specimens

To a previously described collection of 256 formalin-fixed, paraffin-embedded (FFPE) tissue samples of patients with sporadic ccRCC [43], 90 additional cases from the University Hospital of Zürich and 14 from the Clinical Division of Oncology and Cancer Centre, Medical University of Vienna, Austria, were reviewed by one pathologist (H.M.). The tumors were graded according to the classification of the World Health Organization [12]. The median age of the patients was 64 years. Tumor stage and Fuhrman grade of the tumors were unknown for 14 patients. The cohort consisted of 147 (42.8%) pT1, 31 (9%) pT2, 160 (46.5%) pT3 and 8 (2.3%) pT4 ccRCC. There were 11 (3.2%) grade I, 105 (30.5%) grade II, 144 (41.9%) grade III and 86 (25%) grade IV tumors (Table 4). This study was approved by the cantonal commission of ethics of Zurich (KEK-ZH-nos. 2011-72 and 2013-0629). Areas that contained at least 75% tumor cells were directly marked on the HE section of each tumor and considered for punching.

Thirty patients were treated with at least one of the following anti-angiogenic drugs: Sunitinib, sorafenib, pazopanib and bevacizumab. Tumor response was evaluated according to the RECIST criteria [137] and was classified into three types of response: progressive disease (16 patients), stable disease (8) and regressive disease (6 partial or complete remission) (data provided by Dr. Axel Mischo, Department of Oncology, University Hospital Zürich).The details of the treatments are shown in Table 6. Patients with stable or regressive disease were combined for the analysis in the responder group and patients showing progressive disease in the non-responder group.

B. DNA extraction and *VHL* sequencing

Total DNA was extracted from 3-4 tissue cylinders (diameter 0.6 mm) punched from each FFPE block and processed following the Qiagen DNeasy Blood & Tissue Kit (Qiagen, Germany) or the Maxwell® 16 FFPE Tissue LEV DNA Purification Kit (Promega corporation,USA).

The first 162 base pairs of *VHL* are rarely mutated and were excluded from sequence analysis [33]. The primers used for amplification were 5'-agagtccggcccggaggaact-3' forward, 5'-gaccgtgctatcgtccctgc-3' reverse for exon 1, 5'-accggtgtggctctttaaca-3' forward and 5'-tcctgtacttaccacaacaacctt-3' reverse for exon 2, and 5'-gagaccctagtctgtcactgag-3' forward and 5'-tcatcagtaccatcaaaagctga-3' reverse for exon 3. Sequencing was performed as described previously [43]. The sequences were aligned and compared to the NCBI sequence AF010238 using the informatics tool Sequencher (Sequencher® version 5.3 sequence analysis software, Gene Codes Corporation, Ann Arbor, MI USA, [138]). All *VHL* mutations were validated by a second independent PCR and sequence analysis.

C. *In silico* analysis of *VHL* missense mutants

The effect of missense mutation on the stability of pVHL and its potential association to the disease were predicted *in silico* using the program Site Directed Mutator (SDM) [139]. The crystal structure of pVHL was isolated from VBC complex 1lm8.pdb crystal structure (Piccolo database) and uploaded into the program to calculate the thermodynamic change (ddG) occurring after modification of one amino acid according to the main chain conformation, solvent accessibility and hydrogen bonding class.

The missense mutations were then classified as follows:

- ddG <-2.0: highly destabilizing and disease-associated
- -2.0≤ ddG <-1.0: destabilizing
- -1.0≤ ddG <-0.5: slightly destabilizing
- -0.5≤ ddG ≤0.5: neutral
- 0.5< ddG ≤1: slightly stabilizing
- 1.0 < ddG ≤2: stabilizing
- ddG >2.0: highly stabilizing and disease-associated

The mapping of pVHL's interactors binding domains has been adapted from Leonardi et al. [50].

D. Tissue-Micro-Array (TMA) and immunohistochemistry

A TMA containing 28 normal kidney tissue cores, 93 other subtypes of RCC and 262 ccRCC cores [140] was stained and scored as previously described for nuclear p53 expression in tumor cells using the mouse antibody p53 (clone DO-7, dilution 1:150, Dako A/S) [141].

The scoring was performed as follows:

- No nuclear positivity: 0
- 1-5 nuclei positive: +1
- 6-10 nuclei positive: +2
- >10 nuclei positive: +3

E. *VHL* mutations selection

VHL mutation selection was based on the use of Site Directed Mutator (SDM, http://mordred.bioc.cam.ac.uk/~sdm/links.php) *in silico* tool to select missense mutations out of 360 *VHL* sequences of FFPE samples from patients with ccRCC. We selected 4 mutations that were located in the p53/EloC binding domains of pVHL: 3 were predicted to have no or little

impact on the protein stability (Leu158Val, Arg161Gln, Cys162Arg), 1 predicted to highly destabilize pVHL (Arg161Pro). Controls located in another region of the protein and one nonsense mutation have also been selected (Tyr98His, Tyr98Asn, Arg161X).

F. Establishment of stable cell lines

A pcDNA3.1 vector encoding *VHL* wild-type [43] has been used to generate the selected mutants with the Quick Change Lightning site-directed mutagenesis kit (Agilent technologies, United States). Subsequently, pcDNA3.1 was subcloned into pBabe vectors for transduction in mammalian cells.

pBabe empty vector and vectors containing the *VHL* wild-type or the mutant *VHL* sequences were transfected into Platinum-A Retroviral Packaging Cell Line (Cell Biolabs, United States) for viral pseudo-particles production according to the X-tremeGENE 9 DNA Transfection Reagent 3:1 protocol (Roche Diagnostics, Switzerland). The viral supernatant was collected and applied to RCC4, a pVHL deficient cell line bearing a Ser65Trp missense mutation, for transduction following the manufacturer's recommendations. Polyclonal batches of the transduced RCC4 were then selected with constant concentration of 4ug/mL puromycin for 4 weeks and then maintained at 2ug/mL for cell culture. RCC4 wild-type was kindly provided by W. Krek, ETH Zürich, Switzerland.

G. Western Blot

Cultured cells were lysed using RIPA buffer (Sigma-Aldrich, Switzerland) supplemented with proteinase and phosphatase inhibitors (Roche Diagnostics, Switzerland) for 15 minutes on ice and centrifuged at 6000rpm for 10 minutes at 4°C. Protein concentration has been determined by Protein BCA assay (Thermo Scientific, United States) and 25 or 50 µg of proteins were denatured by boiling 5 minutes at 95°C with β-mercaptoethanol and subsequently loaded on a Bis-Tris

polyacrylamide gel (Life Technologies, United States). After running, the gel was blotted on a PVDF membrane (Bio-Rad, United States) and blocked in 5% non-fat milk TBST 1X solution. Primary antibodies were applied overnight at 4°C and appropriate secondary antibody for 1h at room temperature in 1% milk or 5% BSA TBST 1X solution. The dilutions used for the primary antibodies were 1:1000 for pVHL, HIF1α, HIF2α, CA9, Glut1, EloC, 1:500 for Phospho-p53 and 1:2000 for p53 and actin. Anti-rabbit secondary antibody was diluted 1:1000, anti-mouse 1:2000 and anti-goat 1:5000. Detailed information of the antibodies is listed in the following table (Table 13).

Table 13: Antibodies information

Antigen	Dilution	Name	Provider
pVHL	1:1000	S2-647	BD Biosciences
p53	1:2000	Ab1101	Abcam
HIF1α	1:1000	NB100-479	Novus Biologicals
HIF2α	1:1000	PAB12124	Abnova
CA-IX	1:2000	M75	J. Zavada, Prague, Czech Republic
Glut1	1:1000	07-14-01	Millipore
EloC	1:1000	Sc-1559	Santa Cruz
Actin	1:2000	MAB15-01	Millipore
Rabbit	1:1000	7074	Cell signaling
Mouse	1:2000	Ab672	Abcam
Goat	1:5000	Sc-2020	Santa Cruz

H. RNA extraction and quantitative PCR

RNA was extracted from cultured cells or from two core punches of FFPE samples using Maxwell® 16 LEV simplyRNA and RNA FFPE Purification Kit (Promega corporation,USA). Equal amounts of RNA were reversely transcribed into cDNA using the High-Capacity cDNA Reverse Transcription Kit. RNA levels were determined by quantitative PCR using TaqMan® Gene Expression Assay on the ViiA7 Real-Time PCR System instrument (Applied Biosystems, United States). The probes used were Hs00184451, Hs00153340, Hs00355782, Hs00180269, Hs00736699, Hs00936377 and Hs01026146 for *VHL*, *p53*, *p21*, *Bax*, *Noxa*, *HIF1α* and *HIF2α* respectively and the results were normalized to *PPIA* housekeeping gene (Hs99999904) RNA level in each sample. For the tumor tissue samples, we presented the relative RNA levels of the targets compared to *VHL* transcription levels. The results were displayed as Relative Quantity (RQ).

I. HIF and p53 reporter assays

The transcriptional activity of HIF and p53 were evaluated using Cignal Reporter luciferase Kit (Qiagen, Switzerland) and luciferase activity was measured by Dual-Luciferase® Reporter Assay System (Promega Corporation, United States) according to manufacturers' protocols.

J. Proliferation and Apoptosis assays

To investigate the proliferative and apoptotic behavior of the established cell lines we used a colorimetric Cell Proliferation ELISA BrdU assay (Roche diagnostics, Switzerland) and a Caspase-Glo® 3/7 Assay System (Promega corporation, United States) respectively.

K. Cells counting

To determine the number of cells, MTT assays (Invitrogen, United States) were performed in parallel of each proliferation and apoptosis assays. Cell number was calculated by plating RCC4 Babe cells ranging from 1000 to 8000 cells as a standard curve and MTT signal was correlated to the number of cells. This standard curve was used to assess the number of cells in each well in all experiments for normalization.

L. Drugs treatment

Camptothecin and Sunitinib (Selleck Chemicals, USA) were diluted in DMSO at 0.05uM and 10uM concentration respectively and applied to the cells alone or in combination at a final concentration of 0.3% DMSO for 48h. The vehicle control with 0.3% DMSO was referred to as "mock" and "mock VHL30" was used as a reference.

M. *VHL* knockdown

VHL knockdown was performed for the p53 reporter assay using HP Genome Wide siRNA Hs_VHL_5 and All stars Negative control siRNA at 2pM final concentration following manufacturer's recommendation (Qiagen, Switzerland).

N. Co-immunoprecipitation

In the established stable cell lines, pVHL has been pulled down to verify its ability to co-immunoprecipitate with ElonginC and p53. Cells were lysed in a non-denaturing lysis buffer supplemented with proteinase and phosphatase inhibitors (Complete Mini and PhosSTOP Roche). Co-immunoprecipitation (co-IP) was performed using the protein G immunoprecipitation kit according to the manufacturer's recommendations (Sigma-Aldrich, Switzerland). Per cell line, 7mg of total lysate was used for pVHL pull-down with 2ug of anti-VHL antibody (S2-647, BD

Biosciences). For each cell line, 25ug of input and 2 mg of co-immunoprecipitation lysate have been loaded side by side on a Bis-tris gel for Western Blot. pVHL, ElonginC and p53 expression have been verified as described in the Western Blot section.

O. Surface Plasmon Resonance

SPR was used to measure the binding characteristics of pVHL with HIF1α and p53.

pVHL wild-type, HIF1α wild-type and p53 wild-type have been purchased as >95% pure proteins: Human HIF1α Protein (HIF-1α, N-terminal activation domain NTAD [AA530-698]), Made in E.coli, with His Tag; Human TP53/P53 Protein, Made in E.coli, with GST Tag; Human VHL Protein, Made in Sf21 Insect Cell, with His Tag (SPEED BioSystems, LLC, USA). The ligand, pVHL, has been immobilized on the gold layer surface of a CM5 chip at pH 4.5 and p53 has been injected through the flow-cell and the change in the refracted light on the surface induced by p53 binding to pVHL has been measured on a BIAcore T100 instrument (GE Healthcare, USA).

P. Mammalian double-hybrid assay

Elongin C, p53, *VHL* wild-type and the seven mutants have been cloned into suitable vectors to perform mammalian double hybrid assay. The pCF1 (Gateway compatible) vector contains the herpes simplex virus VP16 activation domain and the pCF2 vector contains the yeast GAL4 DNA-binding domain upstream of a multiple cloning region. The pGRE x5E1bluc contains five GAL4 binding sites upstream of the firefly luciferase gene. The vectors were kindly provided by Prof. Roland Wenger (UZH, Switzerland). *ElonginC* and *p53* have been cloned in the pCF1 vector and *VHL* in the pCF2 vector. pCF1, pCF2 and pGRE x5E1bluc were cotransfected in Hela cells with a vector constitutively expressing the Renilla reniformis luciferase for normalization. The fusion proteins expression has been verified by Western Blot.

Q. Library preparation and deep sequencing

All library preparation steps and sequencing material were used following the manufacturer's recommendations (Life Technologies).

Libraries were generated using Ion AmpliSeq Comprehensive Cancer Panel covering 409 cancer-related genes. 40ng per sample (10ng per pool) were amplified and the primers were partially digested to ensure the production by ligation of barcoded libraries using IonXpress barcoded adapters. The barcoded libraries obtained were then purified and 5 additional cycles of amplification were performed before a final purification. Libraries quality and quantity were assessed using Agilent 2100 Bioanalyzer (Agilent Technologies, USA) and real-time quantitative PCR (Ion Library TaqMan Quantitation Kit, ViiA7 Real-Time PCR System instrument (Applied Biosystems, United States)). The libraries were combined (15x4 libraries per run) at a 10pM final concentration. Templated beads were prepared and enriched using the Ion PI Template OT2 200 Kit v3 on the Ion OneTouch 2 System and were submitted to quality control using Ion Sphere™

Quality Control Kit. The beads were then loaded on an ion semi-conductor chip using the Ion PI Chip Kit v2. The Ion Proton System was used for sequencing and the reads were aligned to hg19 human reference genome by Torrent Suite.

R. NGS variant calling and data analysis

Base calling and variant report were performed with Ion reporter v.4.2 and CLC Genomics Workbench v.8.0.64. Sequencing reads could be visually inspected with Integrative Genomics Viewer (IGV) [142, 143]. A heatmap of the variants was generated by Ion reporter v.4.2 for a selection of 18 genes of interest: *VHL*, *SETD2*, *PBRM1*, *MTOR*, *PDGFRA*, *TSC1*, *PIK3CA*, *BAP1*, *CARD11*, *PDGFRB*, *KDM5C*, *KDM6A*, *EGFR*, *TP53*, *HIF1A*, *NF-κB*, *PTEN*, and *PDGFB*. The filtering criteria used were coverage over 30 reads, and 0.05 allele ratio count for all types of mutations occurring in exonic and splice sites regions of the genes. The small nucleotide variations (SNV) listed in the UCSC genome browser site as "common small nucleotide polymorphism" (SNP) were filtered out [144]. Variants found in more than 90% of the samples (27/30 patients) were considered as false positive and neglected as they were checked in our Sanger sequencing internal database.

S. Statistics

Two-tailed Chi square and Student's t-tests were performed using the program Graphpad prism 5.04 for Windows (GraphPad Software, San Diego California USA, www.graphpad.com). Preferentially mutated codons of *VHL* were determined by calculating observed and expected frequencies of 88 missense mutations.

A two-tailed N-1 Chi-square statistical test was used to evaluate the difference in proportion of mutated cases found by NGS in the two response groups for each of the selected genes.

P-values are represented as follows: *<0.05, **<0.01, ***<0.001

VIII. Annex

Supplementary table 1: List of all *VHL* mutations (exon 1)

256 cases previously described (Rechsteiner et al.)

	nt	AA codon	Mutation	Mutation consequence
Exon 1	161	53	c.161insG/ p.Met54IlefsX78	fs
	167	56	c.167_168delCC/ p.Ala56GlyfsX75	fs
	180	60	c.180_205del/ p. Pro61ArgfsX62	fs
	183	61	c.183delC/ p.Val62CysfsX5	fs
	183	61	c.183C>G/ p.Pro61Pro	silent
	183	61	c.183delC/ p.Val62CysfsX5	fs
	189	63	c.189_190insCT/ p.Arg64CysfsX4	fs
	192	64	c.192_198del/p.Ser65ThrfsX92	fs
	193	65	c.193T>A/p.Ser65Thr	missense
	194	65	c.194C>A/ p.Ser65X	nonsense
	194	65	c.194C>A/ p.Ser65X	nonsense
	194	65	c.194C>T/ p.Ser65Leu	missense
	194	65	c.194C>A/ p.Ser65X	nonsense
	194	65	c.194C>A/ p.Ser65X	nonsense
	194	65	c.194C>A/ p.Ser65X	nonsense
	194	65	c.194C>A/ p.Ser65X	nonsense
	194	65	c.194C>A/ p.Ser65X	nonsense
	196	66	c.196_204del/ p.Val66_Ser68	in frame
	199	67	c.199insG/ p.Asn67GlufsX65	fs
	202	68	c.202T>A/p.Ser68Thr	missense
	203	68	c.203C>A/ p.Ser68X	nonsense
	203	68	c.203C>A/ p.Ser68X	nonsense
	209	70	c.209_226del18/ p.Glu70_Phe73delinsVal	in frame
	214	72	c.214T>C/p.Ser72Pro	missense
	214	72	c.214_216delTCC/ p.Ser72del	in frame
	215	72	c.215_216delCCinsA/ p. Ser72ThyfsX87	fs
	217	73	c.217C>T/ p.Gln73X	nonsense
	221	74	c.221T>A/p.Val74Asp	missense
	224	75	c.224delT/ p.Ile75ThrfsX84	fs
	224	75	c.224delT/ p.Ile75ThrfsX84	fs
	225	75	c.225_251del27/ p.Ile75_Val84delinsMet	in frame
	227	76	c.227delT/ p.Phe76SerfsX83	fs
	227	76	c.227_229delTCT/ p.Phe76_Phe76del	in frame
	227	76	c.227_229delTCT/ p.Phe76_Phe76del	in frame
	227	76	c.227delT/ p.Phe76SerfsX83	fs
	227	76	c.227insG/ p.Phe76CysfsX56	fs
	227	76	c.227_229delTCT/ p.Phe76_Phe76del	in frame
	231	77	c.231C>A/p.Cys77X	nonsense
	231	77	c.231C>A/p.Cys77X	nonsense
	232	78	c.232A>T/ p.Asn78Tyr	missense
	233	78	c.233A>G/ p.Asn78Ser	missense
	234	78	c.234T>A/p.Asn78Lys	missense
	234	78	c.234T>A/p.Asn78Lys	missense
	234	78	c.234T>G/p.Asn78Lys	missense
	234	78	c.234insA/ p.Asn78LysfsX54	fs
	238	80	c.238_239delAG/ p.Pro81AlafsX50	fs
	239	80	c.239G>A/ p.Ser80Asn	missense
	240	80	c.240T>A/ p.Ser80Arg	missense
	240	80	c.240T>A/ p.Ser80Arg	missense
	245	82	c.245G>C/ p.Arg82Pro	missense
	251	84	c.251T>A/p.Val84Glu	missense
	256	*86*	*c.256C>A/ p.Pro86Thr*	*missense*
	257	86	c.257C>A/ p.Pro86His	missense
	261	87	c.261insT/ p. Trp88MetfsX44	fs
	262	*88*	*c.262T>C/ p.Trp88Arg*	*missense*
	264	88	c.264G>T/ p.Trp88Cys	missense
	266	89	c.266T>A/ p.Leu89His	missense
	266	89	c.266T>C/ p.Leu89Pro	missense
	266	89	c.266T>G/ p.Leu89Arg	missense
	267	89	c.267_271del/ p. Asn90ArgfsX40	fs
	272	*91*	*c.272insCAACT / p.Phe91SerfsX3*	*fs*
	273	*91*	*c.273G>A / p.Phe91Leu*	*missense*
	272	91	c.272_280del9/ p.Phe91X	in frame
	273	91	c.273insT/ p.Asp92ArgfsX40	fs
	275	92	c.275_285del11/ p.Asp92AlafsX36	fs
	276	92	c.276_279delCGGC/ p.Asp92GlufsX66	fs
	278	*93*	*c.278G>A / p.Gly93Asp*	*missense*
	278	*93*	*c.279C>G / p.Gly93Glu*	*missense*
	280	94	c.280G>T/ p.Glu94X	nonsense
	288	96	c.288delG/ p.Gln96HisfsX63	fs
	292	98	c.292T>A/ p.Tyr98Asn	missense
	294	98	c.294delC/ p.Pro99GlnfsX60	fs
	294	98	c.294C>G/p.Tyr98X	nonsense
	296	99	c.296delC / p.Pro99GlnfsX60	fs
	299	100	c.299delC/ p.Thr100SerfsX59	fs
	302	101	c.302T>C/p.Leu101Pro	missense
	316	106	c.316_317delGG/ p.Gly106ProfsX25	fs
	319	107	c.319_340del22/ p.Arg107ValfsX45	fs
	323	108	c.323insC/ p.Arg108ProfsX24	fs
	330	110	c.330insTCCA/ p. Ser111ProfsX22	fs
	333	111	c.333C>A/ p.Ser111Arg	missense
	334	112	c.334T>G/p.Tyr112Asp	missense
	340	114	c.340G>C/ p.Gly114Arg	missense
	340+1		c.IVS1+1G>T (c.340+1G>T)	splice mut
	340+1		c.IVS1+1G>A (c.340+1G>A)	splice mut
	340+2		c.IVS+2T>G (c.340+2T>G)	splice mut

Supplementary table 1: List of all *VHL* mutations (exon 2)

Exon 2	*341*	*114*	*c.341G>A/ p.Gly114Asp*	*missense*
	341-1	114	IVS1-1_342delGGT (c.[341-1]_342delGGT)	splice mut
	341-1	*114*	*c.IVS1-1G>A (c.341-1G>A)*	*splice mut*
	342	115	c.342insG/ p.His115SerfsX17	fs
	343	115	c.343C>A/p.His115Asn	missense
	343	115	c.343C>T/ p.His115Tyr	missense
	343	115	c.343_344delCA/ p.His115ProfsX16	fs
	344	115	c.344A>T/p.His115Leu	missense
	349	117	c.349T>C/ p.Trp117Arg	missense
	350	117	c.350G>T/p.Trp117Leu	missense
	350	117	c.350G>C/p.Trp117Ser	missense
	350	117	c.350insT/ p.Trp117LeufsX15	fs
	351	117	c.351G>T/ p.Trp117Cys	missense
	353	118	c.353T>C/ p.Leu118Pro	missense
	357	119	c.357C>A/p.Phe119Leu	missense
	361	121	c.361_363delGAT/ p.Asp121del	in frame
	361	121	c.361G>T/p.Asp121Tyr	missense
	362	121	c.362A>G/ p.Asp121Gly	missense
	367	123	c.367delG/ p.Thr124HisfsX35	fs
	370	*124*	*c.370A>G/ p.Thr124Ala*	*missense*
	370	124	c.370delA/ p. Thr124HisfsX35	fs
	371	*124*	*c.371_378del/ p.Thr124ArgfsX5*	*fs*
	374	125	c.374_380del/ p.His125ArgfsX32	fs
	375	125	c.375insA/ p.His125fsX7	fs
	383	128	c.383T>A/p.Leu128His	missense
	388	130	c.388G>T/p.Val130Phe	missense
	389	130	c.389T>A/p.Val130Asp	missense
	393	131	c.393insA/ p.Asn131LysfsX4	fs
	394	132	c.394delC/ p.Gln132LysfsX27	fs
	395	132	c.395A>C/p.Gln132Pro	missense
	397	133	c.397delA/ p.Thr133LeufsX26	fs
	398	133	c.398delC/ p.Thr133MetfsX26	fs
	400	134	c.400_403delGAAT/ p.Glu134TyrfsX24	fs
	402	134	c.402delA/ p.Glu134AspfsX25	fs
	403	135	c.403insA/ p.Leu135IlefsX9	fs
	404	135	c.404delT/ p.Leu135TyrfsX24	fs
	404	135	c.404T>A/ p.Leu135X	nonsense
	405	135	c.405_406insTT/ p.Leu135fsPheX25	fs
	405	135	c.405insT/ p.Leu135PhefsX9	fs
	406	136	c.406insATTA/ p.Phe136IlefsX9	fs
	407	136	c.407ins9/ p.Phe136TyrfsX82	in frame
	407	136	c.407insATAT/ p.Phe136TyrfsX9	fs
	409	137	c.409delG/ p.Val137CysfsX22	fs
	420	140	c.420ins44/ p.Asn141ArgfsX4	fs
	421	141	c.421delA/ p.Asn141MetfsX18	fs
	424	142	c.424_439del/ p.Val142PhefsX12	fs
	426	143	c.426delT/ p. Asp143ThrfsX16	fs
	426	143	c.426delT/ p.Asp143ThrfsX16; 432: sequence repeat from 377	fs
	433	145	c.433C>T/ p.Gln145X	nonsense
	444	148	c.444delT/ p.Phe148 LeufsX11	fs
	444	148	c.444delT/ p.Phe148 LeufsX11	fs
	445	149	c.445insT/ p.Ala149CysfsX25	fs
	452	151	c.452T>G/ p.Ile151Ser	missense
	452	151	c.452T>C/ p.Ile151Thr	missense
	456	152	c.456insC/ p. Leu153ThrfsX21	fs
	458	153	c.458T>C/ p.Leu153Pro	missense
	462	155	c.462delA/ p.Val155CysfsX4	fs
	341-1		c.IVS1-1G>A (c.341-1G>A)	splice mut
	341-2		c.IVS1-2A>T (c.341-2A>T)	splice mut
	341-2		c.IVS1-2 A>G (c.341-2 A>G)	splice mut
	341-2		IVS1-2 A>G (c.341-2 A>G)	splice mut
	463+1		c.IVS2+1G>A (c.463+1G>A)	splice mut
	463+1		IVS2+1delG (c.463+1delG)	splice mut

Supplementary table 1: List of all *VHL* mutations (exon 3)

Exon 3	468	157	c.468_470delTAC/ p.Thr157_ Thr157del	in frame
	472	158	c.472C>G/ p.Leu158Val	missense
	472	158	c.472C>G/ p.Leu158Val	missense
	477	159	c.477A>T/p.Lys159Asn	missense
	481	161	c.481C>T/ p.Arg161X	nonsense
	481	161	c.481C>T/ p.Arg161X	nonsense
	481	161	c.481C>T/ p.Arg161X	nonsense
	481	161	c.481insAG/ p.Arg161SerfsX10	fs
	482	161	c.482G>C/p.Arg161Pro	missense
	482	161	c.482G>A/p.Arg161Gln	missense
	491	164	c.491_494delAGGT/ p.Gln164LeufsX5	fs
	499	167	c.499_510del12/ p.Arg167_Val170del	in frame
	501	167	c.501delG/ p.Ser168AlafsX2	fs
	506	169	c.506T>C/ p.Leu169Pro	missense
	506	169	c.506T>C/ p.Leu169Pro	missense
	507	169	c.507_508delAG/ p. Val170 GlnfsX3	fs
	509	170	c.509T>A/ p.Val170Asp	missense
	517	173	c.517G>T/p.Glu173X	nonsense
	520	174	c.520delA/ p.Asn174IlefsX28	fs
	522	174	c.522_523delTT/ p.Asn174LysfsX81	fs
	523	175	c.523delT/ p.Tyr175ThrfsX27	fs
	531	177	c.531delA/ p.Arg177fsX25	fs
	531	177	c.531delA/ p.Arg177SerfsX25	fs
	538	180	c.538A>G/ p.Ile180Val	missense
	540	180	c.540_564del25/ p.Val181LysfsX14	fs
	551	184	c.551T>C/ p.Leu184Pro	missense
	551	184	c.551T>C/ p.Leu184Pro	missense
	551	184	c.551T>C/ p.Leu184Pro	missense
	551	*184*	*c.551T>C / p.Leu184Pro*	*missense*
	551	*184*	*c.552C>T/ p.Leu184Pro*	*missense*
	557	186	c.557_561delAAGAT/ p.Glu186AlafsX68	fs
	565	189	c.565G>T/p.Glu189X	nonsense
	586	196	c.586A>T/p.Lys196X	nonsense
	612	205	c.612insA/ p.Arg205AlafsX51	fs
	619	207	c.619insT/ p.Ala207CysfsX49	fs
	642	214	c.642 A>C/ p.X214Cys	missense
	464-1		c.IVS2-1G>A (c.464-1G>A)	splice mut
	464-2		c.IVS2-2A>T (c.464-2A>T)	splice mut

Supplementary table 1: List of all *VHL* mutations (additional 104 cases all exons)

Additional 104 cases

	nt	AA codon	Mutation	Mutation consequence
Exon 1	161	54	c.161_162delTG/p.Met54ArgfsX77	fs
	163	55	c. 163insA/p.Glu55ArgfsX77	splice mut
	163	55	c.163delG/p.Glu55ArgfsX11	fs
	167	56	c.167_168delCC/p.Ala56GlyfsX75	fs
	172	58	c172delC/p.Arg58GlyfsX9	fs
	193	65	c.193T>A/p.Ser65Thr	missense
	194	65	c.194C>T/p.Ser65Leu	missense
	194	65	c. 194C>A/p.Ser65X	nonsense
	194	65	c.194C>T/p.Ser65Leu	missense
	194	65	c.194C>T/p.Ser65Leu	missense
	203	68	c.203C>A/p.Ser68X	nonsense
	226	76	c.226_236del10/p.Phe76AlafsX79	fs
	227	76	c.227_229del3/p.Phe76del	in frame
	233	78	c. 233A>G/p.Asn78Ser	missense
	238	80	c.238A>C/p.Ser80Arg	missense
	238	80	c.238A>C/p.Ser80Arg	missense
	240	80	c.240T>A/p.Ser80Arg	missense
	254	85	c. 254_262del9/p.Leu85_Trp88delinsArg	in frame
	254	85	c. 254_262del9/p.Leu85_Trp88delinsArg	in frame
	262	88	c. 262T>G/p.Trp88Gly	missense
	262	88	c. 262T>A/p.Trp88Arg	missense
	268	90	c.268_273del/p.Asn90_Phe91del	in frame
	314	105	c. 314insA/p.Thr105AsnfsX27	fs
	315	106	c.315_318del4/p.Gly106AlafsX51	fs
	327	110	c.327insA/p.His110ProfsX22	fs
	335	112	c.335_340+1del7/p.Tyr112PhefsX45	splice mut
	340	114	c.340G>T/p.Gly114Cys	missense
	340+1		c.IVS1+1G>A (c.340+1G>A)	splice mut
	340+2		c.IVS1+2T>A (c.340+2T>A)	splice mut
	340+1		c.IVS1+1G>A (c.340+1G>A)	splice mut
Exon 2	345	116	c.345_364del/p.Leu116ArgfsX9	fs
	345	116	c.345insC/p.Leu116ProfsX15	fs
	345	115	c.345C>G/p.His115Gln	missense
	349	117	c.349delT/p.Trp117GlyfsX42	fs
	349	117	c.349T>C/p.Trp117Arg	missense
	350	117	c. 350delG/p.Trp117CysfsX42	fs
	351	117	c. 351G>A/p.Trp117X	nonsense
	376	126	c.376insG/p.Asp126GlyfsX5	fs
	383	*128*	*c.383T>C/p.Leu128Pro*	*missense*
	385	135	c.385_404dup/Leu135PhefsX31	fs
	397	133	c.397delA/p.Thr133LeuFsX26	fs
	405	135	c. 405-406delAT/p.Leu135PhefsX7	fs
	407	136	c.407T>C/p.Phe136Ser	missense
	423	141	c.423insA/p.Asn141LysfsX2	fs
	430	*144*	*c.430G>T/p.Gly144X*	*nonsense*
	435	*145*	*c.435delG/p.Gln145HisfsX13*	*fs*
	437	*146*	*c.437C>T/p.Pro146Leu*	*missense*
	444	148	c.444delT/p.Phe148LeufsX10	fs
	458	153	c.458T>C/p.Leu153Pro	missense
	458	153	c. 458T>C/p.Leu153Pro	missense
Exon 3	fs exon 3		frameshift	fs
	473	158	c.493T>A/p.Leu158Gln	missense
	481	161	c.481C>T/p.Arg161X	nonsense
	484	162	c.484T>C/p.Cys162Arg	missense
	484	162	c.484T>C/p.Cys162Arg	missense
	493	165	c.493_503del/p.Val165ProfsX5	fs
	497	167	c.497_505del9/p.Arg167ValdelSerLeu	in frame
	509	170	c.509_512del4/p.Val170GlyfsX31	fs
	515	172	c.515delC/p.Pro172LeufsX29	fs
	524	175	c. 524insA/p.Tyr175X	nonsense
	533	178	c. 533T>C/p.Leu178Pro	missense
	546	183	c.546insG/p.Ser183ValfsX32	fs
	548	183	c.548C>T/p.Ser183Leu*	missense
	555	185	c.555C>A/p.Tyr185X	nonsense
	580	194	C.580_583delinsAA/p.Val194LysfsX61	fs
	586	196	c.586A>T/p.Lys196X	nonsense
	598	200	c.598C>T/p.Arg200Trp*	missense

Supplementary S1: Information on pVHL's binding partners

Preferentially altered binding domains

HIF1αN (alias FIH1) is an inhibitor of the α subunit of HIF1 that interacts with pVHL and HIF1α to mediate repression of HIF1 transcriptional activity [145] by preventing HIF-1α from binding to p300/CBP [146].

BCL2L11 is an apoptosis facilitator leading to the expression of BIM(EL) protein which can be stabilized by *VHL* wild-type protein [147].

HIF1α is the alpha subunit of transcription factor hypoxia-inducible factor-1, which is formed by the association of an alpha and a beta subunit. HIF-1 is a regulator of cellular response to hypoxia that activates transcription of many genes for metabolism, angiogenesis and apoptosis for adaptation to hypoxia. One of pVHL major role is to facilitate the oxygen-dependent ubiquitination of HIF1 for proteasomal degradation, leading to downregulation of HIF target genes [148].

HIF2α is the alpha subunit of hypoxia-inducible factor-2, a transcription factor responding to hypoxia and involved in the induction of genes regulated by oxygen. As HIF1α, its ubiquitination is mediated by pVHL which acts as a downregulator of HIF2α [149].

RPB1 is the largest subunit of the RNA polymerase II complex that can be ubiquitinated by pVHL thus regulating its expression in RCC cells [150]. Levels of Rpb1 are significantly higher in RCC tumors compared with normal kidneys and RCC tumors with pVHL wild-type show higher levels of Rpb1 than tumors with *VHL* mutations [46].

PRKCZ is a serine/threonine kinase which is recruited by pVHL causing ubiquitination and degradation thus influencing cell polarity [151, 152].

aPKC-λ/ι is a tyrosine kinase member of the protein kinase C family and aPKC isotypes are involved in the regulation of cell growth and apoptosis and interact directly with the β-domain of pVHL [153].

EEF1α1 encodes the alpha subunit of the elongation factor-1 complex, which is responsible for the enzymatic delivery of aminoacyl tRNAs to the ribosome. This translation factor interacts specifically with the transcription-dependent nuclear export motif of *VHL*, mediating the nuclear export of pVHL [48].

CCT-ζ-2 is a molecular chaperone protein, member of the chaperonin containing TCP1 complex (CCT). CCT-ζ-2 mediates the proper folding and assembly of the VCB complex and some *VHL* mutations have been demonstrated to impair this interaction [49, 115].

Cullin2 is a negative regulator of cell cycle and associates with pVHL in the VBC complex [154, 155].

Spared binding domains

Nur77 is a nuclear transcription factor that promotes cancer cell growth when located in the nucleus or induces apoptosis when translocated to mitochondria. Nur77 indirectly stabilizes HIF-α by binding to pVHL, thus increasing HIF1α transcriptional activity [156].

VBP1 interacts with pVHL to form an intracellular complex. VBP1 is a chaperone protein, and pVHL plays a role in its transport from the perinuclear granules to the nucleus or cytoplasm but VBP1 implication in ccRCC remains unknown [116].

Other interactors

NEDD8 is an ubiquitin-like protein playing an important role in cell cycle control. NEDD8 association with pVHL prevents the formation of the VCB complex [157].

VDU1 is able to be ubiquitinated via a pVHL-dependent pathway for proteasomal degradation, and *VHL* mutations that disrupt the interaction between VDU1 and pVHL abrogate the ubiquitination of VDU1 [47, 158].

VDU2 can also be ubiquitinated and degraded in a pVHL-dependent manner, preventing it from rescuing HIF1α degradation by deubiquitination [158].

PRKCD is a serine/threonine kinase involved in diverse cellular signaling pathways such as growth, apoptosis, and differentiation. pVHL blocks the interaction of PRKCD with IGF1R to decrease tumor progression [159].

p53 is a tumor suppressor protein responding to diverse cellular stresses such as DNA damage and hypoxia to regulate expression of target genes leading to cell cycle arrest, apoptosis, senescence, DNA repair, or changes in metabolism. Recently p53 has been shown to interact with pVHL. This interaction prevents p53 ubiquitination by the Mdm2 protein, therefore leading to p53 stabilization and transactivation of p53 target genes for apoptosis and cell cycle arrest [64, 65, 67, 78].

VHLAK, also known as zinc finger protein 197, is a regulatory and transcription factor involved in transcriptional regulation that acts as a negative regulator of HIF-1αlpha transactivation. *VHL* protein recruits VHLAK to repress HIF-1αlpha transcriptional activity and HIF-1αlpha-induced VEGF expression [160].

RPB7 is the seventh largest subunit of the RNA polymerase II complex. VHL protein facilitates its ubiquitination and proteasomal degradation and decreases its nuclear accumulation. pVHL can also suppress hsRPB7-induced VEGF promoter transactivation, mRNA expression and VEGF protein secretion [161].

SP1 is implicated in regulation of genes that control multiple cellular processes, including cell cycle, apoptosis, and DNA damage. pVHL inhibits sp1 interaction with PKC zeta and Sp1-dependent transcriptional regulation of VEGF expression and thus tumor angiogenesis [162].

HuR is a RNA binding protein regulating gene expression that is highly expressed in many cancers including ccRCC where it is activated in the early tumor stages. HuR induces VEGF and IGF1R mRNA stabilization and pVHL interaction with HuR has been demonstrated to antagonize these effects [163-165].

TUBA4A is a member of the tubulin superfamily and one of the major components of microtubules. pVHL binds α-tubulin and stabilizes it, stabilizing microtubules [166-168].

KIF3A is a member of the kinesin protein family mediating pVHL's interaction with microtubules [167].

JADE1 is involved in apoptosis and differentiation in epithelia and ubiquitinates βcatenin for degradation. This protein is stabilized by interaction with pVHL and this stabilization is VHL mutation-dependent [45, 169, 170].

CARD9 is an activator of BCL10 leading to NFKB activation and also acts as a positive regulator of apoptosis. VHL protein associates with CARD9 and promotes its phosphorylation by CK2, thus inhibiting its activation of NFkB [171].

EloC is a subunit of the transcription factor B composed of elongins A/A2, B and C and activating elongation by RNA polymerase II. EloC is also one component of the VCB complex for negative regulation of HIFs [172].

TBP1 is a regulator of proteasome, ATPase subunit contributing to the E3 ubiquitin ligase function of the VHL protein. TBP-1 has been show to interact with the β-domain of pVHL and to form a complex with pVHL and HIF1α to promote HIF1α degradation [173].

CK1 is a serine/threonine kinase involved in the regulation of the G1-checkpoint. CK1 phosphorylates pVHL at Ser72 which is a priming event to phosphorylation of pVHL's Ser68 by GSK3 [174].

GSK3 is a glycogen synthase kinase that phosphorylates pVHL at position Ser68 thus negatively regulating microtubule stabilization by pVHL [174].

CK2 is a protein involved in regulation of cell growth that phosphorylates the acidic domain of pVHL to stabilize its interaction with fibronectin [175].

Supplementary table 2: List of missense mutations, stability and disease association prediction

Stability and disease prediction	ddG	nt	AA codon	Mutation	Interacting partners
highly destabilizing	-5.07	221	74	c.221T>A/p.Val74Asp	HIF1αN/VDU1/USP33/VDU2/USP20/RPB7/VHLAK/BCL2L11/HIF1α/EPAS1/RPB1
cause protein malfunction and disease	-3.53	245	82	c.245G>C/ p.Arg82Pro	HIF1αN/VDU1/USP33/VDU2/USP20/RPB7/VHLAK/BCL2L11/HIF1α/EPAS1/RPB1
	-3.8	251	84	c.251T>A/p.Val84Glu	HIF1αN/RPB7/VHLAK/BCL2L11/HIF1α/EPAS1/RPB1
	-2.86	262	88	c. 262T>G/p.Trp88Gly	HIF1αN/RPB7/VHLAK/BCL2L11/HIF1α/EPAS1/RPB1/PRKCZ
	-2.46	262	88	*c.262T>C/ p.Trp88Arg*	HIF1αN/RPB7/VHLAK/BCL2L11/HIF1α/EPAS1/RPB1/PRKCZ
	-2.46	262	88	c. 262T>A/p.Trp88Arg	HIF1αN/RPB7/VHLAK/BCL2L11/HIF1α/EPAS1/RPB1/PRKCZ
	-4.04	266	89	c.266T>C/ p.Leu89Pro	HIF1αN/RPB7/VHLAK/BCL2L11/HIF1α/EPAS1/RPB1/PRKCZ
	-3.19	266	89	c.266T>A/ p.Leu89His	HIF1αN/RPB7/VHLAK/BCL2L11/HIF1α/EPAS1/RPB1/PRKCZ
	-3.12	266	89	c.266T>G/ p.Leu89Arg	HIF1αN/RPB7/VHLAK/BCL2L11/HIF1α/EPAS1/RPB1/PRKCZ
	-3.36	278	93	*c.279C>G / p.Gly93Glu*	HIF1αN/RPB7/VHLAK/BCL2L11/HIF1α/EPAS1/RPB1/PRKCZ/CARD9
	-6.48	302	101	c.302T>C/p.Leu101Pro	HIF1αN/RPB7/VHLAK/BCL2L11/HIF1α/EPAS1/RPB1/PRKCZ/CARD9/TUBA4A/KIF3A/SP1/JADE1
	-2.99	334	112	c.334T>G/p.Tyr112Asp	HIF1αN/RPB7/VHLAK/BCL2L11/HIF1α/EPAS1/RPB1/PRKCZ/CARD9/TUBA4A/KIF3A/SP1/JADE1
	-2.53	341	114	*c.341G>A/ p.Gly114Asp*	HIF1αN/VHLAK/BCL2L11/HIF1α/EPAS1/RPB1/PRKCZ/CARD9/TUBA4A/KIF3A/SP1/JADE1/PRKCD/aPKC-λ/ι/EEF1A1
	-3.1	343	115	c.343C>A/p.His115Asn	HIF1αN/VHLAK/BCL2L11/HIF1α/EPAS1/RPB1/PRKCZ/CARD9/TUBA4A/KIF3A/SP1/JADE1/PRKCD/aPKC-λ/ι/EEF1A1
	-2.15	345	115	c.345C>G/p.His115Gln	F1αN/VHLAK/BCL2L11/HIF1α/EPAS1/RPB1/PRKCZ/CARD9/TUBA4A/KIF3A/SP1/JADE1/PRKCD/aPKC-λ/ι/EEF1A1/CCT-ζ
	-2.14	349	117	c.349T>C/ p.Trp117Arg	F1αN/VHLAK/BCL2L11/HIF1α/EPAS1/RPB1/PRKCZ/CARD9/TUBA4A/KIF3A/SP1/JADE1/PRKCD/aPKC-λ/ι/EEF1A1/CCT-ζ
	-2.14	349	117	c.349T>C/p.Trp117Arg	F1αN/VHLAK/BCL2L11/HIF1α/EPAS1/RPB1/PRKCZ/CARD9/TUBA4A/KIF3A/SP1/JADE1/PRKCD/aPKC-λ/ι/EEF1A1/CCT-ζ
	-2.52	350	117	c.350G>C/p.Trp117Ser	F1αN/VHLAK/BCL2L11/HIF1α/EPAS1/RPB1/PRKCZ/CARD9/TUBA4A/KIF3A/SP1/JADE1/PRKCD/aPKC-λ/ι/EEF1A1/CCT-ζ
	-4.04	353	118	c.353T>C/ p.Leu118Pro	HIF1αN/VHLAK/BCL2L11/RPB1/PRKCZ/CARD9/TUBA4A/KIF3A/SP1/JADE1/PRKCD/aPKC-λ/ι/EEF1A1/CCT-ζ-2
	-6.48	383	128	*c.383T>C/p.Leu128Pro*	HIF1αN/VHLAK/BCL2L11/EEF1A1
	-2.43	383	128	c.383T>A/p.Leu128His	HIF1αN/VHLAK/BCL2L11/EEF1A1
	-5.07	389	130	c.389T>A/p.Val130Asp	HIF1αN/VHLAK/BCL2L11/PRKCD/EEF1A1
	-8.69	395	132	c.395A>C/p.Gln132Pro	HIF1αN/VHLAK/BCL2L11/PRKCD/EEF1A1
	-4.9	407	136	c.407T>C/p.Phe136Ser	HIF1αN/VHLAK/BCL2L11/PRKCD/EEF1A1/TBP1
	-4.99	452	151	c.452T>G/ p.Ile151Ser	HIF1αN/VHLAK/PRKCD/CCT-ζ-2/TBP1
	-4.34	452	151	c.452T>C/ p.Ile151Thr	HIF1αN/VHLAK/PRKCD/CCT-ζ-2/TBP1
	-2.28	482	161	c.482G>C/p.Arg161Pro	NEDD8/VHLAK/p53/Nur77/EloC/HuR
	-2.05	509	170	c.509T>A/ p.Val170Asp	VHLAK/Nur77/EloC/HuR/EloB
	-3.7	551	184	c.551T>C/ p.Leu184Pro	VHLAK/Nur77/HuR/Cullin2
	-3.7	551	184	c.551T>C/ p.Leu184Pro	VHLAK/Nur77/HuR/Cullin2
	-3.7	551	184	c.551T>C/ p.Leu184Pro	VHLAK/Nur77/HuR/Cullin2
	-3.7	551	184	*c.551T>C / p.Leu184Pro*	VHLAK/Nur77/HuR/Cullin2
	-3.7	551	184	*c.552C>T/ p.Leu184Pro*	VHLAK/Nur77/HuR/Cullin2
destabilizing	-1.41	214	72	c.214T>C/p.Ser72Pro	CK1/HIF1αN/VDU1/USP33/VDU2/USP20/RPB7/VHLAK/BCL2L11/HIF1α/EPAS1/RPB1
non-disease-associated	-1.31	234	78	c.234T>A/p.Asn78Lys	HIF1αN/VDU1/USP33/VDU2/USP20/RPB7/VHLAK/BCL2L11/HIF1α/EPAS1/RPB1
	-1.31	234	78	c.234T>A/p.Asn78Lys	HIF1αN/VDU1/USP33/VDU2/USP20/RPB7/VHLAK/BCL2L11/HIF1α/EPAS1/RPB1
	-1.31	234	78	c.234T>G/p.Asn78Lys	HIF1αN/VDU1/USP33/VDU2/USP20/RPB7/VHLAK/BCL2L11/HIF1α/EPAS1/RPB1
	-1.92	238	80	c.238A>C/p.Ser80Arg	HIF1αN/VDU1/USP33/VDU2/USP20/RPB7/VHLAK/BCL2L11/HIF1α/EPAS1/RPB1
	-1.92	238	80	c.238A>C/p.Ser80Arg	HIF1αN/VDU1/USP33/VDU2/USP20/RPB7/VHLAK/BCL2L11/HIF1α/EPAS1/RPB1
	-1.92	240	80	c.240T>A/ p.Ser80Arg	HIF1αN/VDU1/USP33/VDU2/USP20/RPB7/VHLAK/BCL2L11/HIF1α/EPAS1/RPB1
	-1.92	240	80	c.240T>A/ p.Ser80Arg	HIF1αN/VDU1/USP33/VDU2/USP20/RPB7/VHLAK/BCL2L11/HIF1α/EPAS1/RPB1
	-1.92	240	80	c.240T>A/p.Ser80Arg	HIF1αN/VDU1/USP33/VDU2/USP20/RPB7/VHLAK/BCL2L11/HIF1α/EPAS1/RPB1
	-1.95	278	93	*c.278G>A / p.Gly93Asp*	HIF1αN/RPB7/VHLAK/BCL2L11/HIF1α/EPAS1/RPB1/PRKCZ/CARD9
	-1.35	292	98	c.292T>A/ p.Tyr98Asn	HIF1αN/RPB7/VHLAK/BCL2L11/HIF1α/EPAS1/RPB1/PRKCZ/CARD9/TUBA4A/KIF3A/SP1/JADE1
	-1.86	350	117	c.350G>T/p.Trp117Leu	F1αN/VHLAK/BCL2L11/HIF1α/EPAS1/RPB1/PRKCZ/CARD9/TUBA4A/KIF3A/SP1/JADE1/PRKCD/aPKC-λ/ι/EEF1A1/CCT-ζ
	-1.05	388	130	c.388G>T/p.Val130Phe	HIF1αN/VHLAK/BCL2L11/PRKCD/EEF1A1
	-1.6	477	159	c.477A>T/p.Lys159Asn	NEDD8/VHLAK/p53/Nur77/EloC/HuR
	-1.87	506	169	c.506T>C/ p.Leu169Pro	VHLAK/Nur77/EloC/HuR
	-1.87	506	169	c.506T>C/ p.Leu169Pro	VHLAK/Nur77/EloC/HuR
slightly destabilizing	-0.94	193	65	c.193T>A/p.Ser65Thr	HIF1αN/VDU1/USP33/VDU2/USP20/RPB7/VHLAK/BCL2L11/RPB1
non-disease-associated	-0.94	193	65	c.193T>A/p.Ser65Thr	HIF1αN/VDU1/USP33/VDU2/USP20/RPB7/VHLAK/BCL2L11/RPB1
	-0.86	239	80	c.239G>A/ p.Ser80Asn	HIF1αN/VDU1/USP33/VDU2/USP20/RPB7/VHLAK/BCL2L11/HIF1α/EPAS1/RPB1
	-0.52	333	111	c.333C>A/ p.Ser111Arg	HIF1αN/RPB7/VHLAK/BCL2L11/HIF1α/EPAS1/RPB1/PRKCZ/CARD9/TUBA4A/KIF3A/SP1/JADE1
	-0.55	357	119	c.357C>A/p.Phe119Leu	HIF1αN/VHLAK/BCL2L11/RPB1/PRKCZ/CARD9/TUBA4A/KIF3A/SP1/JADE1/PRKCD/aPKC-λ/ι/EEF1A1/CCT-ζ-2
	-0.8	458	153	c.458T>C/ p.Leu153Pro	HIF1αN/VHLAK/PRKCD/CCT-ζ-2/TBP1
	-0.8	458	153	c.458T>C/p.Leu153Pro	HIF1αN/VHLAK/PRKCD/CCT-ζ-2/TBP1
	-0.8	458	153	c. 458T>C/p.Leu153Pro	HIF1αN/VHLAK/PRKCD/CCT-ζ-2/TBP1
	-0.63	472	158	c.472C>G/ p.Leu158Val	VHLAK/p53/Nur77/EloC/HuR
	-0.63	472	158	c.472C>G/ p.Leu158Val	VHLAK/p53/Nur77/EloC/HuR
	-0.8	533	178	c. 533T>C/p.Leu178Pro	VHLAK/Nur77/HuR
neutral	-0.41	202	68	c.202T>A/p.Ser68Thr	GSK3/HIF1αN/VDU1/USP33/VDU2/USP20/RPB7/VHLAK/BCL2L11/HIF1α/EPAS1/RPB1
non-disease-associated	-0.21	233	78	c.233A>G/ p.Asn78Ser	HIF1αN/VDU1/USP33/VDU2/USP20/RPB7/VHLAK/BCL2L11/HIF1α/EPAS1/RPB1
	-0.21	233	78	c. 233A>G/p.Asn78Ser	HIF1αN/VDU1/USP33/VDU2/USP20/RPB7/VHLAK/BCL2L11/HIF1α/EPAS1/RPB1
	0.05	340	114	c.340G>T/p.Gly114Cys	HIF1αN/VHLAK/BCL2L11/HIF1α/EPAS1/RPB1/PRKCZ/CARD9/TUBA4A/KIF3A/SP1/JADE1/PRKCD/aPKC-λ/ι/EEF1A1
	0.44	362	121	c.362A>G/ p.Asp121Gly	HIF1αN/VHLAK/BCL2L11/PRKCZ/CARD9/TUBA4A/KIF3A/SP1/JADE1/PRKCD/aPKC-λ/ι/EEF1A1
	-0.14	370	124	*c.370A>G/ p.Thr124Ala*	HIF1αN/VHLAK/BCL2L11/EEF1A1
	0.11	473	158	c.493T>A/p.Leu158Gln	VHLAK/p53/Nur77/EloC/HuR
	-0.19	482	161	c.482G>A/p.Arg161Gln	NEDD8/VHLAK/p53/Nur77/EloC/HuR
	0.37	484	162	c.484T>C/p.Cys162Arg	VHLAK/p53/Nur77/EloC/HuR
	0.37	484	162	c.484T>C/p.Cys162Arg	VHLAK/p53/Nur77/EloC/HuR
	-0.01	538	180	c.538A>G/ p.Ile180Val	VHLAK/Nur77/HuR
slightly stabilizing	0.68	232	78	c.232A>T/ p.Asn78Tyr	HIF1αN/VDU1/USP33/VDU2/USP20/RPB7/VHLAK/BCL2L11/HIF1α/EPAS1/RPB1
non-disease-associated	0.79	256	86	*c.256C>A/ p.Pro86Thr*	HIF1αN/RPB7/VHLAK/BCL2L11/HIF1α/EPAS1/RPB1
	0.7	273	91	*c.273G>A / p.Phe91Leu*	HIF1αN/RPB7/VHLAK/BCL2L11/HIF1α/EPAS1/RPB1/PRKCZ
	0.81	437	146	*c.437C>T/p.Pro146Leu*	HIF1αN/VHLAK/PRKCD/TBP1
stabilizing	1.57	194	65	c.194C>T/ p.Ser65Leu	HIF1αN/VDU1/USP33/VDU2/USP20/RPB7/VHLAK/BCL2L11/RPB1
non-disease-associated	1.57	194	65	c.194C>T/p.Ser65Leu	HIF1αN/VDU1/USP33/VDU2/USP20/RPB7/VHLAK/BCL2L11/RPB1
	1.57	194	65	c.194C>T/p.Ser65Leu	HIF1αN/VDU1/USP33/VDU2/USP20/RPB7/VHLAK/BCL2L11/RPB1
	1.57	194	65	c.194C>T/p.Ser65Leu	HIF1αN/VDU1/USP33/VDU2/USP20/RPB7/VHLAK/BCL2L11/RPB1
	1.36	257	86	c.257C>A/ p.Pro86His	HIF1αN/RPB7/VHLAK/BCL2L11/HIF1α/EPAS1/RPB1
	1.22	340	114	c.340G>C/ p.Gly114Arg	HIF1αN/VHLAK/BCL2L11/HIF1α/EPAS1/RPB1/PRKCZ/CARD9/TUBA4A/KIF3A/SP1/JADE1/PRKCD/aPKC-λ/ι/EEF1A1
	1.36	343	115	c.343C>T/ p.His115Tyr	HIF1αN/VHLAK/BCL2L11/HIF1α/EPAS1/RPB1/PRKCZ/CARD9/TUBA4A/KIF3A/SP1/JADE1/PRKCD/aPKC-λ/ι/EEF1A1
	1.2	351	117	c.351G>T/ p.Trp117Cys	F1αN/VHLAK/BCL2L11/HIF1α/EPAS1/RPB1/PRKCZ/CARD9/TUBA4A/KIF3A/SP1/JADE1/PRKCD/aPKC-λ/ι/EEF1A1/CCT-ζ
	1.49	361	121	c.361G>T/p.Asp121Tyr	HIF1αN/VHLAK/BCL2L11/PRKCZ/CARD9/TUBA4A/KIF3A/SP1/JADE1/PRKCD/aPKC-λ/ι/EEF1A1
	1.02	548	183	c.548C>T/p.Ser183Leu	VHLAK/Nur77/HuR/Cullin2
	1.64	598	200	c.598C>T/p.Arg200Trp	VHLAK/Nur77/VBP1
highly stabilizing	3.41	264	88	c.264G>T/ p.Trp88Cys	HIF1αN/RPB7/VHLAK/BCL2L11/HIF1α/EPAS1/RPB1/PRKCZ
cause protein malfunction and disease	2.24	344	115	c.344A>T/p.His115Leu	HIF1αN/VHLAK/BCL2L11/HIF1α/EPAS1/RPB1/PRKCZ/CARD9/TUBA4A/KIF3A/SP1/JADE1/PRKCD/aPKC-λ/ι/EEF1A1

In italic: two mutations in the same tumor

IX. References

1. Znaor, A., et al., *International Variations and Trends in Renal Cell Carcinoma Incidence and Mortality.* European Urology, 2015. **67**(3): p. 519-530.
2. *National Cancer Institute, http://seer.cancer.gov/*.
3. *World Cancer reports, International Agency for Research on Cancer, http://www.iarc.fr/*.
4. *National Cancer Institute, Surveillance, epidemiology and end results program, http://seer.cancer.gov/*.
5. Levy, D.A., et al., *Stage specific guidelines for surveillance after radical nephrectomy for local renal cell carcinoma.* J Urol, 1998. **159**(4): p. 1163-7.
6. Pantuck, A.J., A. Zisman, and A.S. Belldegrun, *The changing natural history of renal cell carcinoma.* J Urol, 2001. **166**(5): p. 1611-23.
7. *TNM Classification Help Manual for Cancer Staging, http://cancerstaging.blogspot.ch/*.
8. Moch, H., et al., *Reassessing the current UICC/AJCC TNM staging for renal cell carcinoma.* Eur Urol, 2009. **56**(4): p. 636-43.
9. Fuhrman, S.A., L.C. Lasky, and C. Limas, *Prognostic significance of morphologic parameters in renal cell carcinoma.* Am J Surg Pathol, 1982. **6**(7): p. 655-63.
10. Sun, M., et al., *Reply from Authors re: Vincenzo Ficarra, Giacomo Novara, Guido Martignoni. The Use of Simplified Versions of the Fuhrman Nuclear Grading System in Clinical Practice Requires the Agreement of a Multidisciplinary Panel of Experts. Eur Urol 2009;56:782–4.* European Urology, 2009. **56**(5): p. 784-785.
11. subtypes, R., et al., *Prognostic and therapeutic impact of the histopathologic definition of parenchymal epithelial renal tumors.* Eur Urol, 2010. **58**(5): p. 655-68.
12. *The World Health Organization, http://www.who/*.
13. Pavlovich, C.P. and L.S. Schmidt, *Searching for the hereditary causes of renal-cell carcinoma.* Nat Rev Cancer, 2004. **4**(5): p. 381-93.
14. *NCBI, http://www.ncbi.nlm.nih.gov/*
15. Gossage, L., T. Eisen, and E.R. Maher, *VHL, the story of a tumour suppressor gene.* Nat Rev Cancer, 2015. **15**(1): p. 55-64.
16. Kamura, T., et al., *Rbx1, a Component of the VHL Tumor Suppressor Complex and SCF Ubiquitin Ligase.* Science, 1999. **284**(5414): p. 657-661.
17. Iwai, K., et al., *Identification of the von Hippel-lindau tumor-suppressor protein as part of an active E3 ubiquitin ligase complex.* Proc Natl Acad Sci U S A, 1999. **96**(22): p. 12436-41.
18. Shen, C. and W.G. Kaelin Jr, *The VHL/HIF axis in clear cell renal carcinoma.* Seminars in Cancer Biology, 2013. **23**(1): p. 18-25.
19. Struckmann, K., et al., *pVHL co-ordinately regulates CXCR4/CXCL12 and MMP2/MMP9 expression in human clear-cell renal cell carcinoma.* J Pathol, 2008. **214**(4): p. 464-71.
20. Schödel, J., et al., *Hypoxia, Hypoxia-inducible Transcription Factors, and Renal Cancer.* European Urology.
21. Warburg, O., *On the origin of cancer cells.* Science, 1956. **123**(3191): p. 309-14.
22. Kroeger, N., et al., *Deletions of chromosomes 3p and 14q molecularly subclassify clear cell renal cell carcinoma.* Cancer, 2013. **119**(8): p. 1547-54.
23. Shen, C., et al., *Genetic and Functional Studies Implicate HIF1α as a 14q Kidney Cancer Suppressor Gene.* Cancer Discovery, 2011. **1**(3): p. 222-235.
24. Raval, R.R., et al., *Contrasting Properties of Hypoxia-Inducible Factor 1 (HIF-1) and HIF-2 in von Hippel-Lindau-Associated Renal Cell Carcinoma.* Molecular and Cellular Biology, 2005. **25**(13): p. 5675-5686.
25. Cowey, C.L. and W.K. Rathmell, *VHL gene mutations in renal cell carcinoma: Role as a biomarker of disease outcome and drug efficacy.* Current Oncology Reports, 2009. **11**(2): p. 94-101.
26. Schraml, P., et al., *VHL mutations and their correlation with tumour cell proliferation, microvessel density, and patient prognosis in clear cell renal cell carcinoma.* J Pathol, 2002. **196**(2): p. 186-93.
27. Song, Y., et al., *Analyses of Potential Predictive Markers and Response to Targeted Therapy in Patients with Advanced Clear-cell Renal Cell Carcinoma.* Chin Med J (Engl), 2015. **128**(15): p. 2026-2033.

28. Gad, S., et al., *Somatic von Hippel-Lindau (VHL) gene analysis and clinical outcome under antiangiogenic treatment in metastatic renal cell carcinoma: preliminary results.* Targeted Oncology, 2006. **2**(1): p. 3-6.
29. Gossage, L. and T. Eisen, *Alterations in VHL as potential biomarkers in renal-cell carcinoma.* Nat Rev Clin Oncol, 2010. **7**(5): p. 277-88.
30. Choueiri, T.K., et al., *von Hippel-Lindau gene status and response to vascular endothelial growth factor targeted therapy for metastatic clear cell renal cell carcinoma.* J Urol, 2008. **180**(3): p. 860-5; discussion 865-6.
31. Yao, M., et al., *VHL Tumor Suppressor Gene Alterations Associated With Good Prognosis in Sporadic Clear-Cell Renal Carcinoma.* Journal of the National Cancer Institute, 2002. **94**(20): p. 1569-1575.
32. Young, A.C., et al., *Analysis of VHL Gene Alterations and their Relationship to Clinical Parameters in Sporadic Conventional Renal Cell Carcinoma.* Clin Cancer Res, 2009. **15**(24): p. 7582-7592.
33. Banks, R.E., et al., *Genetic and epigenetic analysis of von Hippel-Lindau (VHL) gene alterations and relationship with clinical variables in sporadic renal cancer.* Cancer Res, 2006. **66**(4): p. 2000-11.
34. Nickerson, M.L., et al., *Improved identification of von Hippel-Lindau gene alterations in clear cell renal tumors.* Clin Cancer Res, 2008. **14**(15): p. 4726-34.
35. Kondo, K., et al., *Comprehensive mutational analysis of the VHL gene in sporadic renal cell carcinoma: relationship to clinicopathological parameters.* Genes Chromosomes Cancer, 2002. **34**(1): p. 58-68.
36. Kaelin, W.G., Jr., *Molecular basis of the VHL hereditary cancer syndrome.* Nat Rev Cancer, 2002. **2**(9): p. 673-82.
37. Ong, K.R., et al., *Genotype-phenotype correlations in von Hippel-Lindau disease.* Hum Mutat, 2007. **28**(2): p. 143-9.
38. von Teichman, A., et al., *Whole genome and transcriptome amplification: practicable tools for sustainable tissue biobanking?* Virchows Arch, 2012. **461**(5): p. 571-80.
39. Taylor, C., et al., *Determination of the consequences of VHL mutations on VHL transcripts in renal cell carcinoma.* Int J Oncol, 2012. **41**(4): p. 1229-40.
40. Schraml, P., et al., *Relevance of nuclear and cytoplasmic von hippel lindau protein expression for renal carcinoma progression.* Am J Pathol, 2003. **163**(3): p. 1013-20.
41. Alves, M., et al., *Mutational status of VHL gene and its clinical importance in renal clear cell carcinoma.* Virchows Archiv, 2014. **465**(3): p. 321-330.
42. Yang, C., et al., *Proteostasis modulators prolong missense VHL protein activity and halt tumor progression.* Cell Rep, 2013. **3**(1): p. 52-9.
43. Rechsteiner, M.P., et al., *VHL gene mutations and their effects on hypoxia inducible factor HIFalpha: identification of potential driver and passenger mutations.* Cancer Res, 2011. **71**(16): p. 5500-11.
44. Hoffman, M.A., et al., *von Hippel-Lindau protein mutants linked to type 2C VHL disease preserve the ability to downregulate HIF.* Human Molecular Genetics, 2001. **10**(10): p. 1019-1027.
45. Zhou, M.I., et al., *Tumor Suppressor von Hippel-Lindau (VHL) Stabilization of Jade-1 Protein Occurs through Plant Homeodomains and Is VHL Mutation Dependent.* Cancer Research, 2004. **64**(4): p. 1278-1286.
46. Yi, Y., et al., *von Hippel-Lindau–Dependent Patterns of RNA Polymerase II Hydroxylation in Human Renal Clear Cell Carcinomas.* Clinical Cancer Research, 2010. **16**(21): p. 5142-5152.
47. Li, Z., et al., *Ubiquitination of a Novel Deubiquitinating Enzyme Requires Direct Binding to von Hippel-Lindau Tumor Suppressor Protein.* Journal of Biological Chemistry, 2002. **277**(7): p. 4656-4662.
48. Khacho, M., et al., *eEF1A Is a Novel Component of the Mammalian Nuclear Protein Export Machinery.* Molecular Biology of the Cell, 2008. **19**(12): p. 5296-5308.
49. Feldman, D.E., et al., *Tumorigenic Mutations in VHL Disrupt Folding In Vivo by Interfering with Chaperonin Binding.* Molecular Cell, 2003. **12**(5): p. 1213-1224.
50. Leonardi, E., A. Murgia, and S.C. Tosatto, *Adding structural information to the von Hippel-Lindau (VHL) tumor suppressor interaction network.* FEBS Lett, 2009. **583**(22): p. 3704-10.
51. Barry, R.E. and W. Krek, *The von Hippel-Lindau tumour suppressor: a multi-faceted inhibitor of tumourigenesis.* Trends Mol Med, 2004. **10**(9): p. 466-72.

52. Frew, I.J. and W. Krek, *pVHL: a multipurpose adaptor protein.* Sci Signal, 2008. **1**(24): p. pe30.
53. Robinson, C.M. and M. Ohh, *The multifaceted von Hippel-Lindau tumour suppressor protein.* FEBS Lett, 2014. **588**(16): p. 2704-11.
54. Frew, I.J. and H. Moch, *A clearer view of the molecular complexity of clear cell renal cell carcinoma.* Annu Rev Pathol, 2015. **10**: p. 263-89.
55. Richards, F.M., *Molecular pathology of von Hippel–Lindau disease and the VHL tumour suppressor gene.* Expert Reviews in Molecular Medicine, 2001. **3**(08): p. 1-27.
56. Linehan, W.M., R. Srinivasan, and L.S. Schmidt, *The genetic basis of kidney cancer: a metabolic disease.* Nat Rev Urol, 2010. **7**(5): p. 277-85.
57. Lavin, M.F. and N. Gueven, *The complexity of p53 stabilization and activation.* Cell Death Differ, 2006. **13**(6): p. 941-950.
58. *The p53 web site, http://p53.free.fr/*.
59. Olivier, M., et al., *The IARC TP53 database: new online mutation analysis and recommendations to users.* Hum Mutat, 2002. **19**(6): p. 607-14.
60. Levine, A.J. and M. Oren, *The first 30 years of p53: growing ever more complex.* Nat Rev Cancer, 2009. **9**(10): p. 749-58.
61. Hollstein, M., et al., *p53 mutations in human cancers.* Science, 1991. **253**(5015): p. 49-53.
62. Brown, C.J., et al., *Awakening guardian angels: drugging the p53 pathway.* Nat Rev Cancer, 2009. **9**(12): p. 862-873.
63. Stickle, N.H., et al., *Expression of p53 in renal carcinoma cells is independent of pVHL.* Mutat Res, 2005. **578**(1-2): p. 23-32.
64. Roe, J.S., et al., *p53 stabilization and transactivation by a von Hippel-Lindau protein.* Mol Cell, 2006. **22**(3): p. 395-405.
65. Roe, J.S., et al., *Phosphorylation of von Hippel-Lindau protein by checkpoint kinase 2 regulates p53 transactivation.* Cell Cycle, 2011. **10**(22): p. 3920-8.
66. Galban, S., et al., *Influence of the RNA-binding protein HuR in pVHL-regulated p53 expression in renal carcinoma cells.* Mol Cell Biol, 2003. **23**(20): p. 7083-95.
67. Roe, J.S. and H.D. Youn, *The positive regulation of p53 by the tumor suppressor VHL.* Cell Cycle, 2006. **5**(18): p. 2054-6.
68. Jung, Y.S., et al., *Loss of VHL promotes progerin expression, leading to impaired p14/ARF function and suppression of p53 activity.* Cell Cycle, 2013. **12**(14): p. 2277-90.
69. Sánchez-Puig, N., D.B. Veprintsev, and A.R. Fersht, *Binding of Natively Unfolded HIF-1α ODD Domain to p53.* Molecular Cell, 2005. **17**(1): p. 11-21.
70. Sermeus, A. and C. Michiels, *Reciprocal influence of the p53 and the hypoxic pathways.* Cell Death Dis, 2011. **2**: p. e164.
71. Timani, K.A., et al., *Tip110 regulates the cross-talk between p53 and HIF-1α under hypoxia and promotes survival of cancer cells.* Molecular and Cellular Biology, 2015.
72. Fels, D.R. and C. Koumenis, *HIF-1alpha and p53: the ODD couple?* Trends Biochem Sci, 2005. **30**(8): p. 426-9.
73. Roberts, A.M., et al., *Suppression of Hypoxia-Inducible Factor 2α Restores p53 Activity via Hdm2 and Reverses Chemoresistance of Renal Carcinoma Cells.* Cancer Research, 2009. **69**(23): p. 9056-9064.
74. Bertout, J.A., et al., *HIF2α inhibition promotes p53 pathway activity, tumor cell death, and radiation responses.* Proceedings of the National Academy of Sciences, 2009. **106**(34): p. 14391-14396.
75. Hodorova, I., et al., *Investigation of tumour supressor protein p53 in renal cell carcinoma patients.* Biomed Pap Med Fac Univ Palacky Olomouc Czech Repub, 2014. **158**(1): p. 44-9.
76. Zigeuner, R., et al., *Value of p53 as a prognostic marker in histologic subtypes of renal cell carcinoma: a systematic analysis of primary and metastatic tumor tissue.* Urology, 2004. **63**(4): p. 651-5.
77. Moch, H., et al., *p53 protein expression but not mdm-2 protein expression is associated with rapid tumor cell proliferation and prognosis in renal cell carcinoma.* Urol Res, 1997. **25 Suppl 1**: p. S25-30.
78. Semenza, G.L., *VHL and p53: tumor suppressors team up to prevent cancer.* Mol Cell, 2006. **22**(4): p. 437-9.

79. Tomasino, R.M., et al., *p53 expression in human renal cell carcinoma: an immunohistochemical study and a literature outline of the cytogenetic characterization.* Pathologica, 1994. **86**(3): p. 227-33.
80. Vasavada, S.P., A.C. Novick, and B.R. Williams, *P53, bcl-2, and Bax expression in renal cell carcinoma.* Urology, 1998. **51**(6): p. 1057-61.
81. *COSMIC database, http://cancer.sanger.ac.uk/cosmic*.
82. Wallace-Brodeur, R.R. and S.W. Lowe, *Clinical implications of p53 mutations.* Cell Mol Life Sci, 1999. **55**(1): p. 64-75.
83. Gurova, K.V., et al., *p53 pathway in renal cell carcinoma is repressed by a dominant mechanism.* Cancer Res, 2004. **64**(6): p. 1951-8.
84. Gurova, K.V., et al., *Small molecules that reactivate p53 in renal cell carcinoma reveal a NF-kappaB-dependent mechanism of p53 suppression in tumors.* Proc Natl Acad Sci U S A, 2005. **102**(48): p. 17448-53.
85. Ma, J., et al., *Ubiquitin E3 ligase UHRF1 regulates p53 ubiquitination and p53-dependent cell apoptosis in clear cell Renal Cell Carcinoma.* Biochem Biophys Res Commun, 2015. **464**(1): p. 147-53.
86. Caratozzolo, M.F., et al., *TRIM8 anti-proliferative action against chemo-resistant renal cell carcinoma*. 2014. 2014.
87. Weiss, R.H., et al., *p21 is a prognostic marker for renal cell carcinoma: implications for novel therapeutic approaches.* J Urol, 2007. **177**(1): p. 63-8; discussion 68-9.
88. Weber, T., et al., *Stage-dependent prognostic impact of molecular signatures in clear cell renal cell carcinoma.* Onco Targets Ther, 2014. **7**: p. 645-54.
89. van der Mijn, J.C., et al., *Predictive biomarkers in renal cell cancer: Insights in drug resistance mechanisms.* Drug Resistance Updates, 2014. **17**(4–6): p. 77-88.
90. Zhu, Y., et al., *Sunitinib induces cellular senescence via p53/Dec1 activation in renal cell carcinoma cells.* Cancer Science, 2013. **104**(8): p. 1052-1061.
91. Yu, J.L., et al., *Effect of p53 Status on Tumor Response to Antiangiogenic Therapy.* Science, 2002. **295**(5559): p. 1526-1528.
92. Conley, S., et al., *CRLX101, an investigational camptothecin-containing nanoparticle-drug conjugate, targets cancer stem cells and impedes resistance to antiangiogenic therapy in mouse models of breast cancer.* Breast Cancer Research and Treatment, 2015. **150**(3): p. 559-567.
93. Pham, E., et al., *Translational Impact of Nanoparticle–Drug Conjugate CRLX101 with or without Bevacizumab in Advanced Ovarian Cancer.* Clinical Cancer Research, 2015. **21**(4): p. 808-818.
94. Selvarajah, J., et al., *Chemotherapy-mediated p53-dependent DNA damage response in clear cell renal cell carcinoma: role of the mTORC1/2 and hypoxia-inducible factor pathways.* Cell Death Dis, 2013. **4**: p. e865.
95. Mandriota, S.J., et al., *HIF activation identifies early lesions in VHL kidneys: evidence for site-specific tumor suppressor function in the nephron.* Cancer Cell, 2002. **1**(5): p. 459-68.
96. Rankin, E.B., J.E. Tomaszewski, and V.H. Haase, *Renal cyst development in mice with conditional inactivation of the von Hippel-Lindau tumor suppressor.* Cancer Res, 2006. **66**(5): p. 2576-83.
97. Brugarolas, J., *PBRM1 and BAP1 as novel targets for renal cell carcinoma.* Cancer J, 2013. **19**(4): p. 324-32.
98. Piva, F., et al., *BAP1, PBRM1 and SETD2 in clear-cell renal cell carcinoma: molecular diagnostics and possible targets for personalized therapies.* Expert Review of Molecular Diagnostics. **0**(0): p. 1-10.
99. Macher-Goeppinger, S., et al., *PBRM1 (BAF180) protein is functionally regulated by p53-induced protein degradation in renal cell carcinomas.* J Pathol, 2015.
100. Varela, I., et al., *Exome sequencing identifies frequent mutation of the SWI/SNF complex gene PBRM1 in renal carcinoma.* Nature, 2011. **469**(7331): p. 539-42.
101. Carvalho, S., et al., *SETD2 is required for DNA double-strand break repair and activation of the p53-mediated checkpoint.* Elife, 2014. **3**: p. e02482.
102. Dalgliesh, G.L., et al., *Systematic sequencing of renal carcinoma reveals inactivation of histone modifying genes.* Nature, 2010. **463**(7279): p. 360-3.
103. Pena-Llopis, S., et al., *BAP1 loss defines a new class of renal cell carcinoma.* Nat Genet, 2012. **44**(7): p. 751-9.

104. Guo, G., et al., *Frequent mutations of genes encoding ubiquitin-mediated proteolysis pathway components in clear cell renal cell carcinoma.* Nat Genet, 2012. **44**(1): p. 17-9.
105. Sato, Y., et al., *Integrated molecular analysis of clear-cell renal cell carcinoma.* Nat Genet, 2013. **45**(8): p. 860-867.
106. Cancer Genome Atlas Research, N., *Comprehensive molecular characterization of clear cell renal cell carcinoma.* Nature, 2013. **499**(7456): p. 43-9.
107. Gerlinger, M., et al., *Intratumor heterogeneity and branched evolution revealed by multiregion sequencing.* N Engl J Med, 2012. **366**(10): p. 883-92.
108. Wei, E.Y. and J.J. Hsieh, *A river model to map convergent cancer evolution and guide therapy in RCC.* Nat Rev Urol, 2015.
109. Banks, R.E., et al., *Genetic and Epigenetic Analysis of von Hippel-Lindau (VHL) Gene Alterations and Relationship with Clinical Variables in Sporadic Renal Cancer.* Cancer Research, 2006. **66**(4): p. 2000-2011.
110. Gallou, C., et al., *Mutations of the VHL gene in sporadic renal cell carcinoma: Definition of a risk factor for VHL patients to develop an RCC.* Human Mutation, 1999. **13**(6): p. 464-475.
111. *VHL mutations database-UMD, http://www.umd.be/VHL/*.
112. DeSimone, M.C., W.K. Rathmell, and D.W. Threadgill, *Pleiotropic Effects of the Trichloroethylene-Associated P81S VHL Mutation on Metabolism, Apoptosis, and ATM-Mediated DNA Damage Response.* Journal of the National Cancer Institute, 2013. **105**(18): p. 1355-1364.
113. Kanno, T., et al., *JunB promotes cell invasion and angiogenesis in VHL-defective renal cell carcinoma.* Oncogene, 2012. **31**(25): p. 3098-3110.
114. Lee, S., et al., *Neuronal apoptosis linked to EglN3 prolyl hydroxylase and familial pheochromocytoma genes: Developmental culling and cancer.* Cancer Cell, 2005. **8**(2): p. 155-167.
115. Feldman, D.E., et al., *Formation of the VHL–Elongin BC Tumor Suppressor Complex Is Mediated by the Chaperonin TRiC.* Molecular Cell, 1999. **4**(6): p. 1051-1061.
116. Tsuchiya, H., T. Iseda, and O. Hino, *Identification of a Novel Protein (VBP-1) Binding to the von Hippel-Lindau (VHL) Tumor Suppressor Gene Product.* Cancer Research, 1996. **56**(13): p. 2881-2885.
117. Gossage, L., et al., *An integrated computational approach can classify VHL missense mutations according to risk of clear cell renal carcinoma.* Hum Mol Genet, 2014. **23**(22): p. 5976-88.
118. Kaelin, W.G., Jr., *The von Hippel-Lindau tumor suppressor gene and kidney cancer.* Clin Cancer Res, 2004. **10**(18 Pt 2): p. 6290S-5S.
119. Beuselinck, B., et al., *MOLECULAR SUBTYPES OF CLEAR CELL RENAL CELL CARCINOMA ARE ASSOCIATED TO SUNITINIB RESPONSE IN THE METASTATIC SETTING.* Clinical Cancer Research, 2015.
120. Gossage, L., et al., *Clinical and pathological impact of VHL, PBRM1, BAP1, SETD2, KDM6A, and JARID1c in clear cell renal cell carcinoma.* Genes Chromosomes Cancer, 2014. **53**(1): p. 38-51.
121. Hakimi, A.A., et al., *Adverse outcomes in clear cell renal cell carcinoma with mutations of 3p21 epigenetic regulators BAP1 and SETD2: a report by MSKCC and the KIRC TCGA research network.* Clin Cancer Res, 2013. **19**(12): p. 3259-67.
122. Ibragimova, I., et al., *Aberrant promoter hypermethylation of PBRM1, BAP1, SETD2, KDM6A and other chromatin-modifying genes is absent or rare in clear cell RCC.* Epigenetics, 2013. **8**(5): p. 486-93.
123. Kapur, P., et al., *Effects on survival of BAP1 and PBRM1 mutations in sporadic clear-cell renal-cell carcinoma: a retrospective analysis with independent validation.* The Lancet Oncology, 2013. **14**(2): p. 159-167.
124. Liao, L., J.R. Testa, and H. Yang, *The roles of chromatin-remodelers and epigenetic modifiers in kidney cancer.* Cancer Genetics, (0).
125. Esrig, D., et al., *p53 nuclear protein accumulation correlates with mutations in the p53 gene, tumor grade, and stage in bladder cancer.* Am J Pathol, 1993. **143**(5): p. 1389-97.
126. Kupryjanczyk, J., et al., *p53 gene mutations and protein accumulation in human ovarian cancer.* Proc Natl Acad Sci U S A, 1993. **90**(11): p. 4961-5.
127. López, I., et al., *Different mutation profiles associated to P53 accumulation in colorectal cancer.* Gene, 2012. **499**(1): p. 81-87.

128. Alsner, J., et al., *A comparison between p53 accumulation determined by immunohistochemistry and TP53 mutations as prognostic variables in tumours from breast cancer patients.* Acta Oncologica, 2008. **47**(4): p. 600-607.
129. Mombini, H., M. Givi, and I. Rashidi, *Relationship between expression of p53 protein and tumor subtype and grade in renal cell carcinoma.* Urol J, 2006. **3**(2): p. 79-81.
130. Noroozinia, F., et al., *Expression of CD44 and P53 in renal cell carcinoma: association with tumor subtypes.* Saudi J Kidney Dis Transpl, 2014. **25**(1): p. 79-84.
131. Ho, T.H., et al., *Correlation Between Molecular Subclassifications of Clear Cell Renal Cell Carcinoma and Targeted Therapy Response.* European Urology Focus, 2015.
132. Hsieh, J.D.C., Patricia Wang, Yingbei Chen, Almedina Redzematovic, Mahtab Marker, Parul Patel, Michael Chevinsky, Umeshkumar Bhanot, Patrizia Pinciroli, Nancy Bouvier, Kety H. Huberman, Michael F. Berger, Nicholas D. Socci, Emily Cheng, William Lee, Jennifer J. Knox, Martin Henner Voss, Maurizio Voi, Robert Motzer; , *Identification of efficacy biomarkers in a large metastatic renal cell carcinoma (mRCC) cohort through next generation sequencing (NGS): Results from RECORD-3.* J Clin Oncol., 2015. **33**((suppl; abstr 4509)).
133. Sato, Y., et al., *Integrated molecular analysis of clear-cell renal cell carcinoma.* Nat Genet, 2013. **45**(8): p. 860-7.
134. Majewski, I.J., et al., *PIK3CA Mutations Are Associated With Decreased Benefit to Neoadjuvant Human Epidermal Growth Factor Receptor 2–Targeted Therapies in Breast Cancer.* Journal of Clinical Oncology, 2015.
135. Price, T.J., et al., *Correlation of extended RAS and PIK3CA gene mutation status with outcomes from the phase III AGITG MAX STUDY involving capecitabine alone or in combination with bevacizumab plus or minus mitomycin C in advanced colorectal cancer.* Br J Cancer, 2015. **112**(6): p. 963-970.
136. Zhang, L., et al., *The oncogene phosphatidylinositol 3'-kinase catalytic subunit alpha promotes angiogenesis via vascular endothelial growth factor in ovarian carcinoma.* Cancer Res, 2003. **63**(14): p. 4225-31.
137. Eisenhauer, E.A., et al., *New response evaluation criteria in solid tumours: revised RECIST guideline (version 1.1).* Eur J Cancer, 2009. **45**(2): p. 228-47.
138. *Sequencher® version 5.3 sequence analysis software, Gene Codes Corporation, Ann Arbor, MI USA, http://www.genecodes.com*.
139. *Site Directed Mutator, http://mordred.bioc.cam.ac.uk/~sdm/links.php*.
140. Mertz, K.D., et al., *Automated immunofluorescence analysis defines microvessel area as a prognostic parameter in clear cell renal cell cancer.* Human Pathology, 2007. **38**(10): p. 1454-1462.
141. Dahinden, C., et al., *Mining Tissue Microarray Data to Uncover Combinations of Biomarker Expression Patterns that Improve Intermediate Staging and Grading of Clear Cell Renal Cell Cancer.* Clinical Cancer Research, 2010. **16**(1): p. 88-98.
142. Robinson, J.T., et al., *Integrative genomics viewer.* Nat Biotech, 2011. **29**(1): p. 24-26.
143. Thorvaldsdóttir, H., J.T. Robinson, and J.P. Mesirov, *Integrative Genomics Viewer (IGV): high-performance genomics data visualization and exploration.* Briefings in Bioinformatics, 2013. **14**(2): p. 178-192.
144. *UCSC Genome Browser site, https://genome.ucsc.edu/*.
145. Mahon, P.C., K. Hirota, and G.L. Semenza, *FIH-1: a novel protein that interacts with HIF-1α and VHL to mediate repression of HIF-1 transcriptional activity.* Genes & Development, 2001. **15**(20): p. 2675-2686.
146. Sirin, Y. and H. Pavenstadt, *FIH1 (factor inhibiting HIF-1) in the kidney: more than an oxygen sensor[quest].* Kidney Int, 2010. **78**(9): p. 836-837.
147. Guo, Y., M.C. Schoell, and R.S. Freeman, *The von Hippel-Lindau protein sensitizes renal carcinoma cells to apoptotic stimuli through stabilization of BIM(EL).* Oncogene, 2009. **28**(16): p. 1864-74.
148. Keefe, S.M., K.L. Nathanson, and W. Kimryn Rathmell, *The Molecular Biology of Renal Cell Carcinoma.* Seminars in Oncology, 2013. **40**(4): p. 421-428.
149. Kaelin, W.G., Jr., *The von Hippel-Lindau tumour suppressor protein: O2 sensing and cancer.* Nat Rev Cancer, 2008. **8**(11): p. 865-73.

150. Mikhaylova, O., et al., *The von Hippel-Lindau Tumor Suppressor Protein and Egl-9-Type Proline Hydroxylases Regulate the Large Subunit of RNA Polymerase II in Response to Oxidative Stress.* Molecular and Cellular Biology, 2008. **28**(8): p. 2701-2717.
151. Iturrioz, X., et al., *The von Hippel-Lindau tumour-suppressor protein interaction with protein kinase Cdelta.* Biochem J, 2006. **397**(1): p. 109-20.
152. Iturrioz, X. and P.J. Parker, *PKCζII is a target for degradation through the tumour suppressor protein pVHL.* FEBS Letters, 2007. **581**(7): p. 1397-1402.
153. Okuda, H., et al., *Direct Interaction of the β-Domain of VHL Tumor Suppressor Protein with the Regulatory Domain of Atypical PKC Isotypes.* Biochemical and Biophysical Research Communications, 1999. **263**(2): p. 491-497.
154. Kinoshita, K., et al., *Ternary complex formation of pVHL, elongin B and elongin C visualized in living cells by a fluorescence resonance energy transfer-fluorescence lifetime imaging microscopy technique.* FEBS J, 2007. **274**(21): p. 5567-75.
155. Kamura, T., et al., *VHL-box and SOCS-box domains determine binding specificity for Cul2-Rbx1 and Cul5-Rbx2 modules of ubiquitin ligases.* Genes & Development, 2004. **18**(24): p. 3055-3065.
156. Kim, B.-Y., et al., *Nur77 upregulates HIF-[alpha] by inhibiting pVHL-mediated degradation.* Exp Mol Med, 2008. **40**: p. 71-83.
157. Russell, R.C. and M. Ohh, *NEDD8 acts as a 'molecular switch' defining the functional selectivity of VHL*. Vol. 9. 2008. 486-491.
158. Li, Z., et al., *Identification of a deubiquitinating enzyme subfamily as substrates of the von Hippel–Lindau tumor suppressor.* Biochemical and Biophysical Research Communications, 2002. **294**(3): p. 700-709.
159. Datta, K., et al., *Inhibition of Insulin-like Growth Factor-I-mediated Cell Signaling by the von Hippel-Lindau Gene Product in Renal Cancer.* Journal of Biological Chemistry, 2000. **275**(27): p. 20700-20706.
160. Li, Z., et al., *The VHL protein recruits a novel KRAB-A domain protein to repress HIF-1α transcriptional activity*. Vol. 22. 2003. 1857-1867.
161. Na, X., et al., *Identification of the RNA polymerase II subunit hsRPB7 as a novel target of the von Hippel—Lindau protein*. Vol. 22. 2003. 4249-4259.
162. Pal, S., et al., *Activation of Sp1-mediated Vascular Permeability Factor/Vascular Endothelial Growth Factor Transcription Requires Specific Interaction with Protein Kinase C ζ.* Journal of Biological Chemistry, 1998. **273**(41): p. 26277-26280.
163. Danilin, S., et al., *Role of the RNA-binding protein HuR in human renal cell carcinoma.* Carcinogenesis, 2010. **31**(6): p. 1018-1026.
164. Datta, K., et al., *Role of elongin-binding domain of von hippel lindau gene product on HuR-mediated VPF//VEGF mRNA stability in renal cell carcinoma.* Oncogene, 2005. **24**(53): p. 7850-7858.
165. Yuen, J.S.P., et al., *The VHL tumor suppressor inhibits expression of the IGF1R and its loss induces IGF1R upregulation in human clear cell renal carcinoma.* Oncogene, 2007. **26**(45): p. 6499-6508.
166. Hergovich, A., et al., *Regulation of microtubule stability by the von Hippel-Lindau tumour suppressor protein pVHL.* Nat Cell Biol, 2003. **5**(1): p. 64-70.
167. Lolkema, M.P., et al., *The von Hippel–Lindau tumour suppressor interacts with microtubules through kinesin-2.* FEBS Letters, 2007. **581**(24): p. 4571-4576.
168. Lolkema, M.P., et al., *The von Hippel–Lindau tumor suppressor protein influences microtubule dynamics at the cell periphery.* Experimental Cell Research, 2004. **301**(2): p. 139-146.
169. Zhou, M.I., et al., *The von Hippel-Lindau Tumor Suppressor Stabilizes Novel Plant Homeodomain Protein Jade-1.* Journal of Biological Chemistry, 2002. **277**(42): p. 39887-39898.
170. Berndt, J.D., R.T. Moon, and M.B. Major, *β-catenin gets jaded and von Hippel-Lindau is to blame.* Trends in Biochemical Sciences, 2009. **34**(3): p. 101-104.
171. Yang, H., et al., *pVHL Acts as an Adaptor to Promote the Inhibitory Phosphorylation of the NF-κB Agonist Card9 by CK2.* Molecular Cell, 2007. **28**(1): p. 15-27.
172. Tyers, M. and R. Rottapel, *VHL: A very hip ligase.* Proceedings of the National Academy of Sciences, 1999. **96**(22): p. 12230-12232.
173. Corn, P.G., et al., *Tat-binding protein-1, a component of the 26S proteasome, contributes to the E3 ubiquitin ligase function of the von Hippel-Lindau protein.* Nat Genet, 2003. **35**(3): p. 229-237.

174. Hergovich, A., et al., *Priming-Dependent Phosphorylation and Regulation of the Tumor Suppressor pVHL by Glycogen Synthase Kinase 3.* Molecular and Cellular Biology, 2006. **26**(15): p. 5784-5796.
175. Lolkema, M.P., et al., *Tumor Suppression by the von Hippel-Lindau Protein Requires Phosphorylation of the Acidic Domain.* Journal of Biological Chemistry, 2005. **280**(23): p. 22205-22211.

X. Curriculum Vitae

Caroline Razafinjatovo
14.05.1985
Fronwaldstrasse 21
8046 Zürich
Nationality: french

Education and research experience

10.2011 - 04.2016 PhD thesis at University Hospital Zurich, Institute of Surgical Pathology, Zurich Switzerland
- Cancer Biology PhD Program, Life Science Graduate School Zurich
- University Zurich, University Hospital Zurich
- "Molecular Profiling of Clear Cell Renal Cell Carcinoma and Targeted Therapy Response" with Holger Moch (MD)

09.2007 - 07.2009 Master Degree in Molecular and Cellular Physiopathology with honors, Medical Faculty, University of Strasbourg, France
- Human genetics, Immunology, Human reproduction biology and Virology "Molecular approach of the impact of HCV E1/E2 envelope glycoproteins on response to antiviral treatment by pegylated-IFNα/Ribavirin"

09.2004 - 07.2007 Licence Degree in Life Sciences, Cellular Biology and Physiology, Natural Sciences Faculty, Louis Pasteur University, Strasbourg, France

09.2002 - 07.2004 1st year of medical studies, Medical Faculty, Louis Pasteur University, Strasbourg, France

09.2001 - 07.2002 Scientific A-levels with honors, Specialty Biology, Condorcet High school, Belfort, France

Work experience

10.2011 - 04.2016 Research assistant, Institute of Surgical Pathology, University Hospital Zurich, Switzerland PhD research project "Molecular Profiling of Clear Cell Renal Cell Carcinoma and Targeted Therapy Response"
- Collection and interpretation of medical data
- Design and performance of molecular biological experiments and results analysis
- Collection and biobanking renal cell carcinoma patients' blood, Urology Department
- Coordination of lab meetings

09.2012 - 12.2012 Teaching assistant in Practical Class of Basic Chemistry, University of Zürich, Switzerland (1 semester).
- Personal preparation, attendance at assistant's meetings
- Review students' laboratory notebooks, feedback, grading students' works
- Independent supervision of 20-25 students for theoretical and practical work

01.2009 – 07.2009 Internship INSERM Unity U 748, Strasbourg, France (6 months)
- "Multicentric study of envelop glycoproteins E1 and E2 from the Hepatitis C Virus and their implication in the antiviral treatment response"

09.2009 - 10.2009 Biology teacher, Professionnal Highschool, Erstein, France (1 month)

09.2008 - 07.2009 Internships Nouvel Hôpital Civil, Strasbourg, France, IGBMC, Illkirch-Graffenstaden, France, Hôpital de Hautepierre, Strasbourg, France, IGBMC, Illkirch-Graffenstaden, France (5 weeks)
- "Anti-native DNA antibodies: Detection techniques and applications in medicine"
- "Mental syndrome with fragile X chromosome and protein FMRP function"
- "Study of the *Tex 19.1* gene expression"
- "MLS syndrome in cytogenetic"

Competences and skills

Laboratory	Cell culture, transient and stable transfections, treatment with different compounds, hypoxia, gene reporter assays, proliferative, metabolic and apoptotic assays, PCR, RT-qPCR, DNA/RNA/protein isolation, Sanger and Next-Generation Sequencing, mutation analysis, Western Blotting, IFC, fluorescence microscopy, FACS, Immunoprecipitation, Surface Plasmon Resonance, Mammalian Two-Hybrid assay, bacteria cloning
Languages	Native French, Fluent English, Intermediate German and Italian
Informatics	MS Office, Endnote, Graph Pad Prism, Inkscape, Sequencher, Ion reporter, CLC Genomics workbench, Integrative Genomics Viewer
Personal interests	Movies, Reading, Hiking, Skiing, Tennis

Publications

February 2016	*"Characterization of VHL missense mutations in sporadic clear cell renal cell carcinoma hotspots, affected binding domains, functional impact on pVHL and therapeutic relevance"* Caroline Fanja Razafinjatovo, Svenja Bihr, Axel Mischo, Ursula Vogl, Manuela Schmidinger, Holger Moch, Peter Schraml, under revision in "BMC Cancer"
April 2010	*"Tropisme leucocytaire du virus de l'hépatite C – Intérêt de l'analyse des séquences des gènes des glycoprotéines d'enveloppe virales E1 et E2"* Rémy Moenne-Loccoz, Caroline Razafinjatovo, François Habersetzer, Ahmed Ananna, Michel Doffoel, Philippe Wolf, Jean-Pierre Gut, Thomas Baumert, Françoise Stoll-Keller, Evelyne Schvoerer, "Pathologie Biologie"

Scholarships

March 2015	Zurich Hartmann Müller Stiftung Travel Grant (1000 CHF) for *Keystone Symposium* May 2015, Dublin, Ireland "Hypoxia From Basic Mechanisms to Therapeutics"
December 2013	Zurich Hartmann Müller Stiftung Travel Grant (1000 CHF) for *Keystone Symposium* January 2014, Breckenridge, Colorado, USA "Sensing and Signaling of Hypoxia Interfaces with Biology and Medicine"

Attendance to conferences

May 2015	CO *Keystone Symposium*, Dublin, Ireland Hypoxia From Basic Mechanisms to Therapeutics,
April 2015	*14th Day of Clinical Research*, Zürich, Switzerland Center for Clinical Research (CCR)/Clinical Trials Center (CTC)
January 2015	*12th Charles Rodolphe Brupbacher Symposium* , Zürich, Switzerland Breakthroughs in Cancer Research and Therapy
January 2014	CO *Keystone Symposium*, Breckenridge, Colorado, USA Hypoxia Sensing and Signaling
January 2013	*11th Charles Rodolphe Brupbacher Symposium*, Zürich, Switzerland Breakthroughs in Cancer Research and Therapy
June 2012	*3rd Symposium Clinical Trial Organization*, Zürich, Switzerland "Personnalized medicine in clinical research"
February 2012	*4th interdisciplinary uro-oncology symposium*, Zürich, Switzerland "Theme Renal cell carcinoma"

Acknowledgements

First of all, I would like to thank Prof. Holger Moch for giving me the opportunity to work in his research group on this very exciting and challenging project.

My thanks also go to the other members of my thesis committee, Prof. Ulrich Hübscher, Prof. Roland Wenger, Prof. Niko Beerenwinkel and Dr. Peter Schraml, for supervising this work and for their helpful comments throughout these years. Sincere thanks to Peter who has read and corrected all my first drafts.

Particularly, I want to acknowledge Dr. Markus Rechsteiner who initiated this project and gave me valuable advice and assistance for both theory and technical issues.

In addition, I would like to thank Christiane Mittmann, Dinh-Van Vuong, Adriana von Teichmann, Annette Bohnert, Martina Storz, André Wethmar, Norbert Wey and Susanne Dettwiller for their technical help and for their work in the lab.

For the nice working atmosphere, my thanks go to the former and current lab members of the Institute, namely Dorothee Pflüger, Magda Lukamowics-Rajska, Marion Bawohl, Yannick Böge, Mohsen Malehmir, Renaud Maire, Alex Soltermann, Peter Wild, Kathrin Oehl, Elisa Bellini, Christine Fritz, Ed Fritz, Qing Zhong and Uli Wagner. I make a point in thanking Anna Nowicka, Melanie Ruf, Claudia Corrò, Nadejda Valtcheva and Ruben Casanova, who made everyday lab life easy and entertaining. Both their friendship and kindness have been key elements to help me to go through this challenging and rewarding experience.

Finally, my deepest thanks go to my parents for their unconditional love and support throughout all my studies and particularly during my PhD, and for always putting their children first. Last but not least, I thank Pierre for his love and care, for always being there for me, and for sharing my life. For this and much more I dedicate my thesis to my Family, and to my uncle Richard who died from cancer during this work.